Reconstruction of a High-Rise Fire Using Experimental and Computational Techniques

Major Qualifying Project

Submitted to:
The Faculty of Worcester Polytechnic Institute
in partial fulfillment of the requirements for the
Degree of Bachelor of Science in Mechanical Engineering

Project Advisors: Professor Milosh Puchovsky and Dr. Kevin McGrattan (NIST)

Submitted by:
Abigail Benoit
Grace Cummings
Matthew Guarneri
Peter Guertin

Date Submitted: 27 April 2023

Table of Contents

Executive Summary

Introduction

Reconstructing building fires at full-scale for research is impractical, therefore computational models and sometimes scaled physical models are utilized to study fire events. The confidence level with computational and scaled models accurately approximating the broad range of conditions during a building fire can vary. This project examined the degree to which the computational model - Consolidated Fire and Smoke Transport (CFAST), developed and maintained by the National Institute of Standards and Technology (NIST), approximated and calculated certain fire conditions that were also measured during physical fire testing of a scaled model of an actual fire event. Both the physical and numerical models were utilized to evaluate different scenarios that could have occurred during the actual fire event potentially providing more insight about outcomes of smoke spread.

In January of 2022, a fire originating on the lower floor of a two-story dwelling unit of a 19-story high-rise building claimed the lives of 17 people. The loss of life was largely due to smoke spread from apartment 3N to the 3rd floor hallway and up through the structure to the 15th and 19th floor. Critical aspects of the building and fire were physically reconstructed at a reduced scale in WPI's Fire Laboratory. The scaled building and fire were also simulated using CFAST. A range of scenarios with varying door positions throughout the structure were physically tested and numerically simulated as ventilation openings play a key role in the propagation of fire effects. Temperature, velocity, and smoke spread were measured and calculated in key areas. The results of the scaled model and numerical simulation were evaluated.

The challenges of this project consisted of scaling fire behavior and physical building characteristics to match the actual fire event, and aligning the scaled model and test measurement locations with CFAST calculations. Other significant challenges pertained to recreating the degree of door openings, how these were approximated in CFAST, and how and where physical measurements should best be taken during testing. Recommendations were made on how future fire tests could be conducted to better correlate with the CFAST calculations. The long-term goal of this project is to advance work on the application of reduced-scale fire testing and how such testing can be used in the development and implementation of computer fire models.

Methodology

The following tasks were conducted to achieve our project goals:

- Research Bronx Fire Case Study
- Identify Key Areas for Replication
- Formulate Building Details
- Calculate Reduced-Scale Model Dimensions
- Design and Construct the Test Apparatus
- Configure the Scaled Building in CFAST
- Develop Fire Size and Growth Parameters
- Conduct Preliminary Bench Tests
- Develop Data Acquisition Software and Program Codes
- Install and Test the Instrumentation on the Scaled Physical Model
- Develop the Testing Procedure
- Run Fire Tests and Computer Simulations
- Evaluate the Experimental and CFAST Results

Building dimensions were estimated from the New York Times (Singhvi, et al., 2022) article, "The Chain of Failures That Left 17 Dead in a Bronx Apartment Fire", and the model used within the article created by researchers at WPI. We determined that a 1:12 scale would fit best under the large-scale calorimeter and would be feasible to reconstruct in the laboratory. Approximated fire growth of the Bronx Event was scaled using Froude equations. Key aspects of the building that were affected by smoke spread were reconstructed. These consisted of apartment 3N, the centrally located scissor stairwell, the 3rd, 15th, and 19th floor hallways, and the penthouse roof. The NYT reported that after the fire started in apartment 3N, these specific locations were predominately affected by smoke accumulation. In the fire laboratory, our model was constructed at a total height of 15 feet and the hallways spanned 10 feet. These key locations were concurrently simulated via CFAST with certain assumptions made as discussed further in this paper.

To develop a realistic reduced-scaled fire, the physical construction of the scaled model and lab instrumentation were critical considerations. The parameters of the fire that were addressed were flame height, heat release rate, smoke production, and repeatability. We considered hot and cold smoke generation techniques with various configurations of gas and fuel sources. A pipe burner connected to a mass rotameter flowing propylene was determined to best replicate the fire scenario for our purposes. Iterations of pipe length and hole sizes were analyzed to achieve the desired flame height and heat release rate for our fire scenarios. In CFAST, we utilized a fire source with a specified steady-state heat release rate and size to obtain similar fire and smoke sources with the fire tests.

Instrumentation devices and locations had to be determined for key aspects of the fire scenarios within the scale model so appropriate measurements could be made. We determined that

temperature, gas flow, and smoke movement measurements could best be compared with CFAST results. Instrumentation in the laboratory included bi-directional probes (BDP), thermocouples, and cameras. This instrumentation also had to be configured with thermocouple extensions (snakes), and probe tubing connected to Raspberry Pis and a DAQ system. Data collection programs were written with the assistance of lab personnel in order to correctly register and record data. CFAST calculations for temperature and mass flow were exported into spreadsheets. Smokeview files were used for the visualization of smoke movement though spaces as a function of time and space.

A procedure was developed for the fire testing within the scaled model. The fire tests were characterized into three scenarios where door position was the varying parameter, and each scenario consisted of a steady-state 2.3 kW fire. The three door positions were fully-open, 45 degrees open, and 20 degrees open. In CFAST, this was approximated as 100% open, 77% open, and 33% vent opening fractions.

Three trials of each fire test were conducted within our two-week testing period. To post-process the data, the camera footage was exported and filtered. Thermocouple data conveying temperatures was also filtered. The bi-directional probe output pressure differential readings were recorded and correlated with temperatures to calculate flow velocity. The CFAST results and lab test results were evaluated at key locations throughout the scaled model. Output data was graphically presented to illustrate trends of temperature change and velocity. Camera footage was compared to Smokeview files to evaluate smoke movement.

Findings

Our findings are as follows:

1. **The calculated and measured temperature rise within the scaled model qualitatively agree in trends.**

CFAST predicts average upper- and lower-layer temperatures within a compartment, whereas in the lab tests, measurements were made at a few select locations. A reasonable degree of consistency trends were observed for gas temperatures between the fire test measurements and the CFAST calculations. Compartment gas leakage within our lab tests could prompt a decrease in temperature which was unaccounted for in CFAST.

2. **A greater degree of variability was observed for gas velocities between the fire test measurements and the CFAST calculations.**

Velocity measurements were made at select locations. Those measurements not recorded within a door or window opening could not be directly compared to CFAST. Of those measurements made within doorways or windows, the most significant was that at the penthouse window where testing and computer simulation had a difference of 102% for Test 1, 110% for Test 2, and 124% for Test 3. Additionally due to the relatively low gas flows, the uncertainty of the bi-directional probe's accuracy was increased. This was evident in the graph fluctuations within our experimental data, which made it difficult to extrapolate and create a clear trend. While there was a clear difference in results with varying door configurations, no clear conclusions could be drawn.

3. **The calculated and measured travel time had a difference of 43% for Test 1, 27% for Test 2, 7% for Test 3.**

We were able to compare the time for the smoke to reach the penthouse in the lab tests and CFAST simulations and compare those results to that reported for the Bronx Fire. The main contributor of these differences can be found within the different methods of modeling the stairs. In the lab, we utilized ramps to model stairs, and in CFAST we utilized vents at stair landings, this can affect the path of smoke spread and impact the travel time. Other differences can be attributed to the methodology used to determine the time at which smoke reached the penthouse. Smokeview and cameras were employed. The results indicated approximately a one-minute difference between the open-door lab fire and 100% open CFAST trials. As door openings decreased in our experiments, the difference between our CFAST and fire tests decreased. However, we are unable to effectively quantify the differences within our results. To determine the time to reach the penthouse in our lab experiments, we reviewed the camera footage, and marked the time where we saw the smoke. However, there may have been smoke leaking out of the penthouse that was unable to captured by the cameras. For the CFAST model, we used Smokeview and paused the simulation when the smoke layer reached the penthouse level. Our basis of time for the fire event was from the emergency calls from occupants in the building reporting smoke.

4. **The smoke dispersed through the building, rather than forming distinct layers. A distinct layering of smoke could only be observed within the 3N compartment and adjacent hallway.**

Upon ignition, there was significant smoke generated from the burner with high temperatures that formed an upper smoke layer in the burn room. As smoke flowed out of the third-floor compartment and into the hall, the smoke began to decrease in temperature. As smoke was forced through the space and eventually up the building, the flow became less buoyancy driven. As the smoke moved up the building, it dispersed throughout the space, appearing as a dark mass and significantly reduced the vision from the windows. Within the stairwell, the smoke mixed with ambient air and cooled. Thus, there was no stratification of smoke evident on the higher floors. Visually, the smoke movement was very difficult to compare between tests as the locations of the cameras, insufficient lighting, and smoke dispersion as opposed to defined layer resulted in imperceptible views.

5. **The door positions in the fire tests and CFAST simulations influenced the results.**

A difference in temperature rise can be seen between each test for both CFAST and fire tests, although in CFAST these differences were less prominent. As the doors closed, the delay of smoke exhausting from the penthouse window increased in the experimental trials. This influence of the doors closing also resulted in higher temperatures near the immediate fire area (lower level of apartment 3N), and slightly slower velocities throughout the building. The rest of the building generally experienced lower temperatures as the doors closed, due to the reduction in gas flows. In the upper level of the third-floor apartment, the highest temperatures were recorded within Test 1, which correlates with CFAST, however, we struggled to interpret the data gathered, and further investigation is suggested to gain a better understanding of the results. In CFAST, the temperature results between door positions also correlate with the results of our lab experiments.

Recommendations for Future Testing

Our recommendations include refined testing strategies for future laboratory work and improved correlation with computer modeling output.

Refined Testing Strategies

In the future, to conduct these experiments with increased accuracy and frequency for data collection we recommend constructing the test apparatus in a way that ensures easy access to the interior compartments. This would allow for the compartments to be cleaned and ensure repeatability within each test. To reduce the leakage within the test apparatus, we suggest the application of fire caulking, silicon, and foil tape. We were able to use these methods to prevent smoke leakage and fire spread, and they were also used to secure our instrumentation. To adequately assess the leakage throughout the building, once testing is ready, a calibrated fan is recommended. This device compares the mass flow input at one end and the output at another and determines the difference. This is helpful to quantify any discrepancies within the data collection due to leakage. To optimally observe the movement of smoke throughout the test apparatus, plexiglass should be in place of plywood on one side of the stairwell shaft. This will aid in better assessment of smoke leakage and movement. These methods are best utilized for better observation and measurement of smoke movement throughout a testing apparatus.

To best assess the velocity, we recommend positioning the bi-directional probes in the cross-sectional area of any vents or doorways, parallel to the flow. While this may not be as important for solely laboratory fire testing, it is essential when comparing these values to computational zone models such as CFAST. CFAST computes the flow rate normal to the plane of the door or window vent measured in (kg/s).

We also recommend using cameras that can sync with one another and be controlled with a remote to start a test at the same time stamp. We were unable to access a remote and spent approximately four minutes every test just starting the go-pros. Following these tests, we had to go back and edit to start them all at the same time to cross-compare the recordings. To prevent this time-consuming process, a remote is advised to sync the time stamps.

Methods to Better Correlate CFAST Experiments with Fire Tests

We are proposing methods to better ensure the experiments in the computational model and the lab can be compared. Before the lab tests are constructed, it would be beneficial to first create the CFAST model and run a simulation to determine potential fire behavior and design limitations. We also recommend utilizing measurement inputs which can be directly replicated in the laboratory. To improve CFAST tests, the simulations should be run with different zone types defined in the compartment geometry. This is better to gauge the sensitivity of different zone configurations and effects it has on the calculations to better align with the fire tests. CFAST can better expand its computational analysis by adding a stair geometry option during the compartment input phase of modeling, but this is not possible within the context of a two-zone model.

Future Testing Possibilities

In the future, we hope this study can lead to further developments in reduced-scale high-rise fire tests. Some ideas for future work include the variation of the heat release rates, alternative burner techniques, different and more accurate instrumentation, a variation of the scale and a wider arrangement of door configurations. Ideally, future testing will also include scaling of more than just the heat release rate. These ideas can lead to feasible and reliable alternatives to full-scale tests, and may also lead to the use of reduced-scale fire tests to validate computational fire models.

Abstract

In January 2022, a fire originating in a second-floor apartment of a 19-story high-rise in New York City claimed the lives of 17 people. The loss of life was largely due to smoke spread. Physical reconstruction of full-scale fire events are impractical, and therefore computational and reduced-scale models are utilized. The project focused on constructing, evaluating and comparing the critical aspects of a physical model to the computational zone model, CFAST (Consolidated Fire and Smoke Transport) at a reduced-scale. A series of fire tests with varying door positions were conducted in the lab and simulated in CFAST. Temperature, velocity, and smoke spread were measured in key areas. Analysis concluded that CFAST approximated the general trends of the fire test data with reasonable agreement for temperatures, but a wider range of variability for smoke spread and flows. Both the physical and numerical model demonstrated how quickly smoke can spread through this type of building and the importance of door positions.

Acknowledgments

The success of our project was dependent on the contributions of many individuals over the past ten months. We would like to thank all who have helped and supported us in this process.

First, we would like to thank Dr. Kevin McGrattan of NIST for his expertise in the field of fire research and computer fire modeling. He was invaluable in guiding us throughout our project. Dr. McGrattan helped create the fire modeling program CFAST, and without his weekly feedback and troubleshooting, we would not have been able to complete our complex simulations.

Next, we would like to thank Fritz Brokaw the WPI Fire Lab Manager. He aided us nearly every day during our construction progress and we would not have been able to conduct our fire tests without him. We would also like to thank Diane Poirier, the Administrative Assistant of the WPI Fire Protection Department. Diane is the heart of the WPI Fire Protection Department, and without her help and care this project would not have been successful.

Additionally, we would like to the Dr. Muthu Selvaraj and Abhinandan Singh. Muthu had recently worked with the New York Times on the Bronx Apartment Fire, and he had modeled the building in FDS. Muthu was able to provide our team important information regarding the fire scenario and the building schematics which allowed us to design our testing apparatus upon this case study. Abhinandan, a PhD student in the fire lab, provided us with the MATLAB and Python code along with explanations for our instrumentation and helped post-process our data. Without Muthu and Abhinandan, our data would not have been to the standard that we held ourselves accountable for.

Finally, we would like to thank our advisor from Worcester Polytechnic Institute, Professor Milosh Puchovsky, who introduced us to this project and Dr. McGrattan. Professor Puchovsky provided us with weekly guidance and support. He spent countless hours dedicated to editing and advising to help refine our project and bring it to its greatest potential.

Authorship Table

The team proofread and edited every section of the report.

Section Title	**Primary Author(s)**
Executive Summary	Abigail
Abstract	All
Acknowledgements	Matt, Abigail
1 Introduction	Abigail
2 Background	All
2.1 Case Study: The Bronx Apartment Fire	Abigail
2.2 Consolidated Fire and Smoke Transport (CFAST)	Peter
2.2.1 Zone Model	Peter
2.2.1 Inputs and Outputs	Grace
2.2.2 Limitations of CFAST	Matt
2.3 Key Factors in Compartment Fires	Abigail, Grace
2.3.1 Smoke Generation Techniques	Abigail
2.3.2 Fire Dynamic Principles	Abigail, Peter
2.3.3 Scale Modeling Principles	Abigail, Grace
3.0 Project Scope and Goals	Abigail, Grace
3.1 Mission Statement	Abigail
3.2 Objectives	Abigail
4.0 Fire Testing	Grace, Abigail, Peter
4.1 Objectives	All
4.2 Experimental Model Design	Grace, Abigail, Peter
4.2.1 Scale-Model Dimensions	Grace
4.2.2 Physical Construction	Abigail
4.2.3 Design Fire & Burner Configuration	Grace
4.3. Measurement Devices	Peter, Abigail, Grace
4.3.1. Rotameter	Abigail
4.3.2 Thermocouples	Peter, Grace
4.3.3 Bi-Directional Probes	Abigail, Grace

4.3.4 Camera	Grace
4.4.1 Trial Configurations	Grace
4.4.2 Experimental Setup	Matt
4.4.2 Experimental Overview	Abigail
5 CFAST Model	Matt
5.1 Objectives	Abigail
5.2 Model Configuration	Matt
5.2.1 Model Assumptions	Matt
5.2.2 Model geometry	Matt
5.2.3 Design fire	Matt
5.2.4 Instrumentation	Grace
5.3.1 Gas Temperature	Grace
5.3.2 Vent Mass Flow	Grace
6 Results	Peter, Abigail
6.1 Temperature Results	Peter
6.2 Velocity Results	Abigail
6.3 Smoke Visualization Results	Grace
7.0 Conclusions	Abigail, Peter
8.0 Recommendations	Abigail, Peter
Appendix A	Abigail
Appendix B	Abigail, Grace
Appendix C	Peter
Appendix D	Peter, Grace
Appendix E	Grace, All
Appendix F	External Source
Appendix G	Peter
Appendix H	Abigail
Appendix I	Grace
Appendix J	Abigail
Appendix K	Grace
Appendix L	Grace

Appendix M	External Source
Appendix N	Matt
Appendix O	Peter
Appendix P	Peter

List of Figures

List of Tables

Abbreviations

BDP	Bi-Directional Probe
CFAST	Consolidated Fire and Smoke Transport
DAQ	Data Acquisition Device
HRR	Heat Release Rate
FDS	Fire Dynamics Simulator
FPH	Fire Protection Handbook
NIST	National Institute of Standards and Technology
NYT	New York Times
SFPE	Society of Fire Protection Engineers Handbook
TC	Thermocouple

Nomenclature

A	Cross-Sectional Area [m^2]
dp_{eff}	Effective Bi-Directional Pressure [Pa]
D	Diameter of tube [m]
ε	Efficiency
Fr	Froude number
g	Gravitational acceleration [m/s^2]
H_C	Heat of Combustion [kJ/kg]
L	Length of Hose [m]
l	Characteristic Length (non-dimensional)
$\dot{m}$	Mass Flow Rate [kg/s]
m_c	Mass Flow Constant (BDP constant)
η	Viscosity of Air
ρ	Density [kg/m^3]
ΔP	Differential Pressure [Pa]
P	Pressure [Pa]
Δp_c	BDP Sensor Pressure Constant [Pa]
Q	Heat Release Rate [kW]
t	Time [s]
T	Temperature [C]
V	Velocity [m/s]

1. Introduction

Currently, there is limited research available on reduced-scale buildings for computational fire modeling software. This is important, as it allows fire protection engineers to run fire simulations in buildings to design fire protection systems to ensure life safety and property protection. On a large scale, these models are commonly used, but not commonly tested in a laboratory setting, due to size and economic feasibilities. This can result in uncertainties within simulations, if models cannot be constructed and cross-compared with simulations, in other words, validated. Our team's focus is on reconstructing a high-rise fire at a reduced-scale, in Worcester Polytechnic Institute's Fire Laboratory, and comparing the results with that of Consolidated Fire and Smoke Transport (CFAST) computer model. The case study we will be basing our fire design upon is the January 2022 Bronx Apartment Fire which was analyzed in the New York Times. This fire originated in the lower floor of a two-story dwelling unit, and smoke was able to spread through the building up to the roof, claiming multiple lives. The complexities of this project will consist of scaling the fire dynamic properties to match the actual fire event and to work within the limitations of CFAST. Throughout these fire tests, we will be varying the door positions to study the impact of door openings on smoke spread. The goal of this project is to determine the degree to which the physical construction and the CFAST compare, and to obtain experience in the process of reconstructing and testing complex fire scenarios of a scaled high-rise building. In the future, we hope this study can lead to further developments in reduced-scale high-rise fire tests, to be used as a feasible and reliable alternative to full-scale tests. These developments may also lead to the use of reduced-scale fire tests to validate computational fire models.

2. Background

2.1. Case Study: The Bronx Apartment Fire

The information included within this section is based upon the article published in the New York Times (Singhvi, et al., 2022). On January 9th, 2022, 17 people died from a fire at the Twin Parks North West, Site 4, high-rise apartment building in the Bronx, New York City. This 19-story residential high rise was built in 1972 and contained 120 apartment units, as shown in Figure 1. The building was not sprinklered and the only means of egress from the floors above ground level was the centrally located scissor stairwell. The fire started in the lower floor of a two-story dwelling unit which was only accessible via the third floor. The cause of this fire was investigated to be the result of space heater that ran continuously for a prolonged time and ignited an adjacent mattress. The residents evacuated through the upper floor of their apartment and left their door open, which resulted in smoke rapidly spreading throughout the building. Investigators concluded the self-closing mechanisms within the corridor doors connecting to stairwell A and B on the 3rd floor and the door to stairwell B in the 15th and 19th floors, which contributed to the rapidly accelerating heavy smoke spread throughout the rest of the building. Victims of this event did not die from the fire itself, but rather the smoke inhalation which was abundant in the egress routes. Of the 17 people who died, 14 had been on the 15th, 18th and 19th floors.

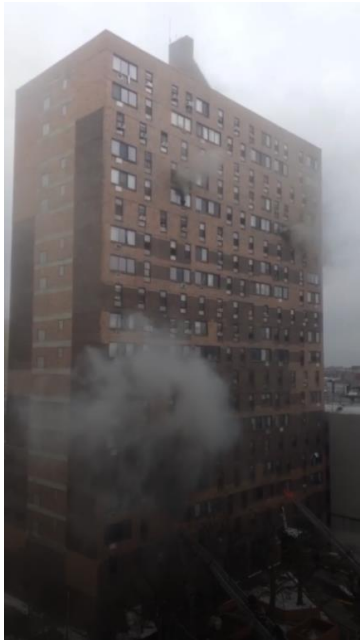

Figure 1: Bronx Apartment Fire (NYT)

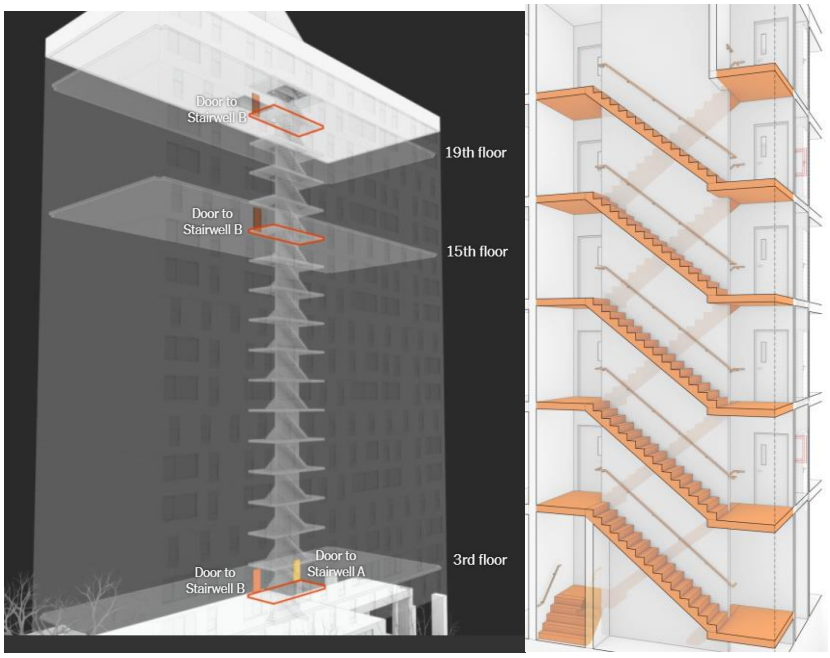

Figure 2: Scissor Stairwell Layout (Source: NYT and Speckert, nd.)

The Bronx Apartment consisted of a centrally located scissor stairwell, as shown in Figure 2. Scissor stairs are composed of two different flights of stairs providing two separate paths of climbing or descending located within one stairwell enclosure. The 1964 Uniform Building Code was the applicable code for the Bronx Apartment building and was able to provide assumptions of dimensions on stair and door widths which were not provided by the New York Times.

2.2. Consolidated Fire and Smoke Transport (CFAST)

Consolidated Fire and Smoke Transport (CFAST) is a two-zone fire and smoke model developed by the National Institute of Standards and Technology (NIST). CFAST has the capability to predict the distribution of smoke, fire gases, and thermal conditions created by a fire within a compartmentalized structure. Computational fire and smoke models are commonly used by engineers for performance-based design and forensic investigators to study the effects of a fire. These computational fire models such as CFAST are constantly updated and maintained as computing power and our knowledge of fire phenomena continues to progress. CFAST has undergone verification and validation assessment for various scenarios in accordance with ASTM 1355, the Standard Guide for Evaluating the Predictive Capability of Deterministic Fire Models. However, the successful assessment of one group of scenarios in a computation model does not extend to all possible scenarios. There is limited available data regarding the verification and validation of reduced-scale experiments in CFAST. One such experiment is the NIST Vent Study conducted by Farzana and Schovanec in 2017, but the only available data is recorded in Section 4.14 of the CFAST Verification and Validation Guide.

2.2.1. Zone Model

Zone models solve the conservation equations for energy and mass in control volumes as functions of time. Fires are represented as a source of energy and mass is represented as a plume, which acts as a pump for the mass from the lower layer to the upper layer through entrainment. These control volumes represent the rooms or compartments being modeled and are further broken into two separate control volumes where one accounts for the hotter upper layer and the other represents the colder lower layer. In order for zone models to function multiple assumptions are often required and can be found in the SFPE Handbook Chapter 29 of for Compartment Fire Modeling. Perhaps the most relevant assumption to this study is that the upper and lower layers are assumed to be spatially uniform, meaning that all points in a respective layer will have identical temperature, species concentration, and other property values. Additionally, in models where there are multiple rooms or compartments connected to each other the model can account for the flow between these spaces with vents.

2.2.2. Inputs and Outputs

CFAST requires users to input characteristics of the compartment(s), fire, and define a length of time to run the simulation such as dimensions, ambient conditions, parameters of the fire such as heat release rate, and define a length of time to run the simulation. The inputs can be found in each tab on the top of the program window. Parameters such as ambient conditions, thermal properties of surface materials, and the location and size coordinates of ceilings/walls/floors are all required for compartments. Wall vents & ceiling/floor vents are used to simulate doors, windows, or any penetration through a wall or ceiling/floor. These vents need to be user defined by location, size, and opening fraction. HVAC and forced flows can also be simulated by inputting mechanical ventilation.

Input parameters of the fire include location, size, growth curve, chemical composition, peak heat release rate, heat of combustion, and radiative fraction. Users can select to use a pre-set t^2 fire growth curve or make a custom fire curve with points defined by HRR at specified timestamps. CFAST also can detect the time an object takes to heat up via radiative or convective heat transfer. This object, a target, can be used to emulate a sprinkler or fire alarm. To define a target the location, material, and internal target temperature is needed. CFAST can also model sprinkler systems and smoke detectors if given the intended location, activation temperature and obscuration, response time index, and spray density. Heat transfer can also be accounted for between compartments by adding connections. Like other computation fire models, slices can be added to visualize various effects of the fire. 2D Slices can display temperature plane gradients that are more detailed than CFASTs default visual outputs. These can be specified by adding a position, axis and compartment of where the user wants the slice to be. To ensure the CFAST model is as accurate as possible, it is vital to fill in the maximum number of inputs with accurate information.

After the user inputs all the necessary information into CFAST and runs the simulation, the calculated outputs are exported into spreadsheets. The output data includes calculations for temperature, mass flow rate through vents, pressure, mole percentages and mass fractions of the products of combustion, optical density and more. These measurements are divided into upper-

and lower- gas layers and also include the layer height. Devices can also be utilized in CFAST to calculate the sensor obscuration, sensor activation, surrounding gas temperature, and surrounding gas velocity.

After a simulation is run, Smokeview can be accessed for smoke and temperature 2-D slice visualizations as seen in Figure 3. The user can place specific 2-D slices into compartments in the X, Y or Z orientation to see a more detailed view of the temperature gradient rather than the default two-zone layer output. Smokeview also visualizes smoke movement at different points in time.

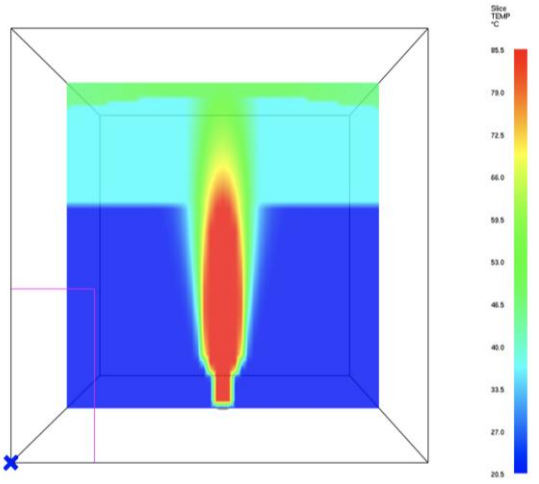

Figure 3: 2-D Slice visualization of gas temperature from CFAST User Guide

2.2.3. Limitations of CFAST

CFAST offers various tools to help quantify and visualize fire zone effects. Despite this, there are still limitations within computational zone models. This section discusses the limitations of CFAST which are applicable to this experiment. The topics presented within this section are derived from the CFAST Technical Reference Guide, and the team's past experience with the program. One commonly encountered obstacle in CFAST is the inability to model ramps, stairs, or any sloped components. To address this, vents were placed to replicate stair openings on the floors and ceilings of stacked compartments.

As previously mentioned, CFAST is capable of modeling multiple rooms or compartments connected to each other. However, CFAST is better optimized to compute a single room and adjacent rooms rather than a series of connected rooms, as more compartments may allow for the greater potential for errors to occur found in CFAST Validation Guide 2.2.2. As the hot gas flows from compartment A to B, there is some uncertainty in the mass flow rate through the door and in heat losses to the walls. As the hot gases progress to other compartments, the uncertainties become greater.

Additionally, ventilation and surface connections between compartments need to be carefully configured because errors within these features may prevent the simulation from running.

Another limitation of CFAST is the sensitivity regarding pressure. Simulation run time depends heavily on the ventilation and pressure of the connecting compartments. Without proper ventilation, the program will recognize the compartment failing because the pressure is expanding beyond data computation. This was a particular challenge faced when modeling the upper 3N compartment connecting to the hallway, and from the hallway to the stair shaft which presented the biggest challenge of pressure. Many compartments studied in the CFAST Validation Guide are conducted at a full-scale with a transient fire growth rate. Reduced-scale modeling is less common due to these pressure errors encountered mainly in the stair shaft.

2.3. Key Factors in Compartment Fires

2.3.1. Smoke Generation Techniques

Smoke modeling involves complex numerical tools used to simulate fire behavior, smoke dynamics, air quality, and to ascertain the impacts of fires. To adequately simulate smoke production throughout an experiment, several smoke generation techniques were considered. The purpose of the use of smoke in our experiments is to realistically model smoke from a fire. Key components of applicable smoke generation techniques involve its scalability, visibility, repeatability, and controllability of smoke production rates. Other considerations for applicable techniques include the smoke's buoyancy, soot production, temperature effects, path of smoke spread, and its ability to be compared to CFAST. Table 1 in Appendix A shows the comparison of the various smoke generation techniques, dichotomized into smoke and smoke-like methods.

Smoke is composed of solid particles released during combustion. Hot smoke methods involve the use of a heat source, often a flame, to produce smoke. Three techniques evaluated include pool fire, crib fires, and burners. A pool fire is defined as a turbulent diffusion fire burning of evaporating material from a layer of liquid at the base of the fire. The most significant drawback to pool fires is the inability to have a continuous flow into the pan, which may limit the duration of experiments. Additionally, the heat release rates, and plume height are determined from the surface area of the pan and the depth of the fuel, once ignited, if the flame height exceeds predetermined calculations, this risks the integrity of the enclosure. A crib fire is a stack of square cross-sectional sticks in an array where the burning spread rates are governed by the processes internal to the crib. The largest drawbacks to crib fires is its size, and the inability to control the heat release rate. Another fire-based method is a burner fire. A burner fire involves a device that contains gaseous or liquid fuels, which is lit to produce a flame. In an everyday setting, burners can be seen on stovetops and grills. In a laboratory setting, different types of burners include Bunsen, Meker, and Tirrill. Common fuels used in burners consist of natural gases (eg. methane) and liquid petroleum (eg. propane). For experimental purposes, a pipe burner is considered as a smoke source in an enclosure. The pipe burner would consist of steel or copper piping, with holes cut uniformly along the top. The most advantageous aspect of burners for experiments is the ability to control the flow rate of gas to the burner. This can allow the heat

release rate and flame height to be controlled and known throughout the experiments, which in turn, allows for repeatability.

Smoke-like, or artificial smoke methods typically involve mechanical devices which employ liquid or gas droplets to create fog or haze. The purpose of artificial smoke in some experiments may be for repeatability purposes or the lack of a laboratory environment to test with real smoke. Theatrical "Smoke" and Fog Machines typically involve helium, carbon dioxide, or dry ice to produce fog. According to smoke movement studies, pure helium can be used to generate a cold buoyant plume as the surrogate of fire smoke. Theatrical smoke is commonly used to test smoke detectors and smoke control design features in aircraft. In contrast to hot smoke plumes from burning materials, theatrical smoke generators provide smoke plumes at relatively low temperatures which means they are not very buoyant. Furthermore, theatrical smoke plumes themselves cannot simulate the volumetric gas expansion effects associated with combustion. Other research into alternative smoke methods include smoke machines and saltwater modeling, with repeatability being the advantageous aspect. The majority of these methods resulted in non-buoyant plumes with significant uncertainties in regard to scaling principles.

2.3.2. Fire Dynamic Principles

Fire dynamics is the study of how fires start, spread, and develop. This area of study is composed of chemical, fire science, material science, fluid mechanics, and heat transfer principles, to determine their influence on the behavior of fire. The main principles of fire dynamics in a compartment fire are the control volume, conservation of mass, and conservation of energy.

Fire plumes are defined as the buoyant stream of heated gases and combustion products rising above a fire. Fire plumes are typically buoyancy driven, which means that the increase in temperature or correlated decrease in density of the heated gases surrounding the fire allow for the gases to flow upwards. Buoyancy driven plumes often create that hot upper layer, which fills the surface area of the ceiling and then descends. Vertical movement of the buoyant gases in the fire plume from the surrounding atmosphere is known as air entrainment. Air entrainment causes pressure differentials, which create flow. These changes in pressure will influence the hot gas layer and the flow path in an enclosure. When flows are not driven by temperature, they may be driven by a turbulent force, also known as a jet plume. In these situations, an upper layer would not form, rather, the jet plume would direct the flow of gases.

Heat release rate is defined by Babrauskas in Chapter 26 of the SFPE Handbook by the size of the fire. The heat release rate determines the size of the fire because it is also the rate at which the combustion reactions produce heat. Therefore, a larger HRR value indicates a faster rate of combustion reaction and a bigger fire. It is also a vital characteristic of the fire and is required for most other critical calculations that can categorize the fire's behavior.

Mass flow rate is directly related to the heat release rate and the heat of combustion of the chemical being burned as seen in Equation 1. The heat of combustion is unique to the chemical unlike the mass flow rate and heat release. Often the chemical being used is known, therefore either the heat release rate or mass flow rate is needed to solve for the other. After obtaining a

desired heat release rate, the mass flow rate could be calculated in Equation 1 (Drysdale, 2011).

$$\dot{m} = Q/\Delta H_c \qquad \textit{(Equation 1)}$$

2.3.3. Scale Modeling Principles

Scale modeling for fire does not simply mean conducting experiments at a reduced physical scale. Reducing the linear dimensions and characteristics of a physical fire situation and conducting experiments with the reduced-scale model is not sufficient. In addition to geometric scaling, it is necessary to maintain mechanical, thermal, and chemical similarity in the reduced-scale model. The scaling laws are derived from the dimensional analysis and fundamental equations describing the physical/chemical phenomena. A commonly used physical scaling law in fire is known as Froude scaling displayed in Equations 2-4, which are applicable to buoyant flows associated with fires but do not fully encompass all aspects of scaling. For our model, the characteristic length (l) was determined to be 96 in / 8 in. The law of scaling is based upon the Froude Number, which can be expressed in terms of the rate of heat release (Cote et al., 2008).

Froude Number: $F_r \sim Q^{2/5}/D \sim V\sqrt{D}$ *(Equation 2)*

Heat Release Rate Scaling: $Q^* \sim \frac{Q}{p_\infty c_p T \sqrt{g} l^{5/2}}$ *(Equation 3)*

Time Scaling: $t^* \sim \sqrt{\frac{l}{g}}$ *(Equation 4)*

Scale modeling using Froude scaling laws has been successful in addressing smoke movement issues. However, because different fire phenomena scale differently, it is generally difficult to study complex fires on a small scale. These differences in scale limit the use of scale modeling principles. It is notably difficult to scale convective flows and radiation at the same time. Thus, Froude modeling cannot be applied readily to fire problems where radiation is important, for instance (FPH, 2008).

3. Project Scope and Methods

3.1 Mission Statement

To physically and numerically reconstruct and test a scaled model of an actual fire event, evaluate the results, and investigate the effect certain building elements have on fire spread.

3.2 Objectives of Fire Test and Simulations

To accomplish the project mission, our team utilized the following objectives:

- Research Bronx Fire Case Study
- Identify Key Areas for Replication
- Formulate Building Details
- Calculate Reduced-Scale Model Dimensions
- Design and Construct the Test Apparatus
- Configure the Building in CFAST
- Develop Fire Size and Growth Parameters
- Conduct Preliminary Bench Tests
- Develop Data Acquisition Software and Program Codes
- Install and Test the Instrumentation on the Test Apparatus
- Develop the Testing Procedure
- Run Fire Tests and Simulations
- Evaluate the Experimental and CFAST Results

4. Physical Model for Lab Tests

To accomplish the objectives of our laboratory testing, we developed a set of building assumptions to reconstruct a fire testing apparatus modeled after the Bronx Fire incident. We pinpointed the critical regions for our reconstruction and crafted a design plan, procured materials, and constructed the testing apparatus. We then identified the areas where data collection was essential and selected the most appropriate and beneficial trials to meet our project goals. We installed, tested, and programmed instrumentation for data collected and determined the best methods for data analysis. Additionally, we created testing procedures for each test trial and conducted preliminary testing.

4.1. Experimental Model Design

4.1.1. Scale-Model Dimensions

The conceptualization of our reduced scale fire model before the construction phase was imperative in ensuring efficient use of our construction time. The methods we utilized to design our model involved esingstimating dimensions, sketching it out, and drafting a Solidworks model. The building dimensions and layout was obtained from the New York Times article and Dr. Muthu Selvaraj, who had conducted previous research on this building. There were some dimensions which we could not obtain from the article, including stairwell and door width, so the remaining dimensions were estimated from the 1964 NYC Building Code. However, the intent of this project was not to exactly replicate the Twin Parks North West building, so not all aspects of our model are similar.

Drafting our model before building also helped us prevent incorrect cutting, editing and fabrication of our limited materials. Although we had original design plans, construction challenges arose leading to multiple modifications and iterations of our model. The dimensions of the scaled model can be found in Appendix D Figure 4 below displays the virtual Solidworks model of our test apparatus.

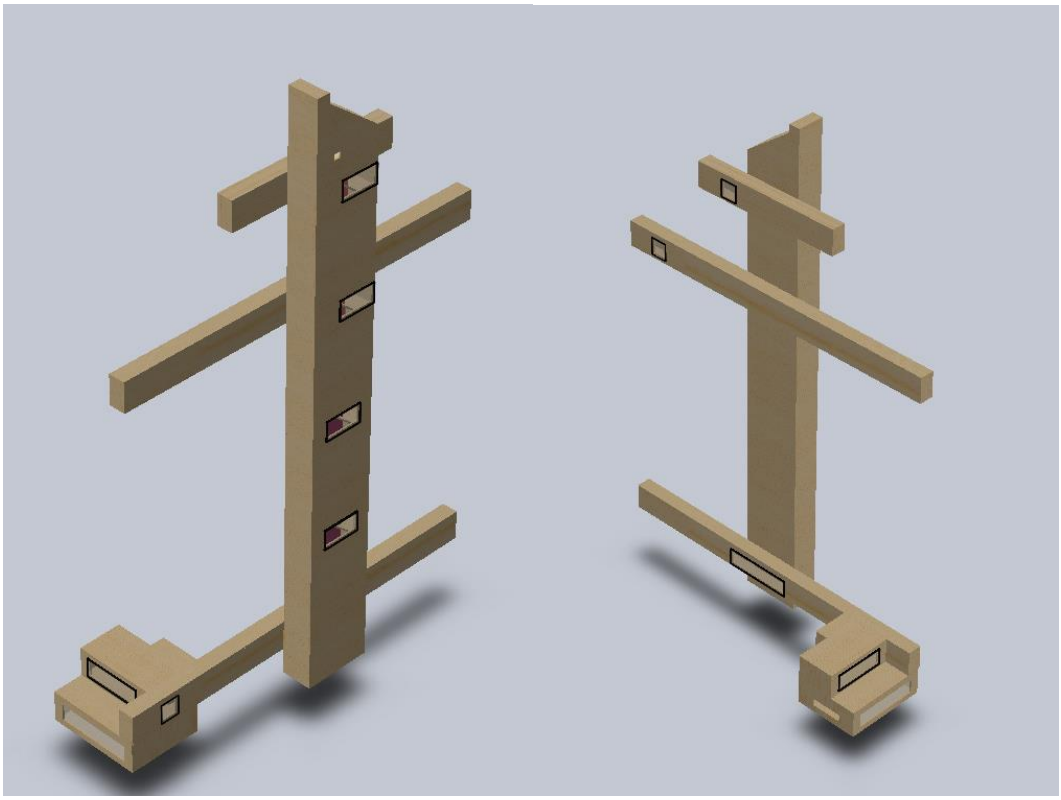

Figure 4: Experimental fire test building in Solidworks, front and back view.

We had preliminary designs to anticipate potential restrictions with resources and size limitations. Initially, we had to decide on a scale to convert the full-sized high-rise Bronx Apartment dimensions that would be feasible for this experiment. Our group decided on a 1:12 scale meaning the constructed model we used to test was $1/12^{th}$ of the size of the Bronx Apartments. Because we used the Imperial system for measurement, one foot of the Bronx Apartments was one inch in our experimental model. The reasoning behind utilizing a 1:12 scale was primarily because of the height restriction in the lab. We wanted to maximize the height of our physical model to to obtain the largest feasible reduced scale. We estimated the height of the Bronx Apartment to be approximately 15 feet including the penthouse roof, which is a feasible reconstruction height.

Another construction decision that was made was to omit the first floor because the NYT had reported minimal smoke impact. Heat and smoke rise, so it can be assumed that the first floor would not be greatly affected since the fire started on the second floor. Along with the limited time and space in the lab, we also had limited funding and resources, so we opted to only construct key areas that were critically affected by smoke, according to the NYT. By only constructing key areas we diminished our construction time and in turn increased our fire testing time. These key areas, as shown in Figure 5, consisted of the initial fire location in the apartment, the third-floor hallway, the central scissor stairwell where the smoke travelled up, and the 15^{th} and 19^{th} floors where smoke traveled through via the open corridor doors as reported by the NYT.

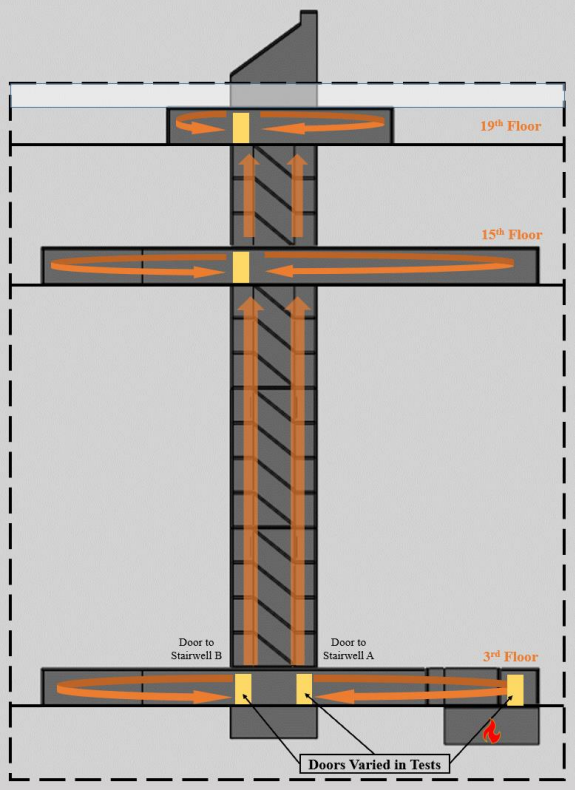

Figure 5: Key areas where smoke spread in the Bronx Apartment building

4.1.2. Physical Construction

To meet the funding and time constraints ½-inch plywood was used for the walls, floors, and ceilings and fastened together with wood glue, screws, and finishing nails. The physical model consisted of the construction of three hallways, one centralized stairwell shaft, the two leveled main burn compartments (apartment 3N), and the penthouse. The three hallways were constructed to represent the 3rd, 15th, and 19th floor and were where smoke spread as a result of failed door latching which resulted in loss of life. The centralized stairwell shaft consisted of a scissor stairwell. The structure was connected in a way that allowed us to disassemble the lower portions of the building (3rd floor hallway and apartment 3N) after each trial to allow for cleaning and cooling. Additionally, we used scaffolding to safely assemble the taller portions of our model and access instrumentation at the top of the building.

Figure 6: Apartment 3N Construction

For the two-story dwelling unit, apartment 3N, we constructed this area into two sections - the upper and lower floor. The lower floor was simplified to not include any interior walls, furniture, or potential obstructions. The lower level of the two-story dwelling unit was the burn area where the mattress had ignited in the actual fire event. For the burn area, we planned to have a pipe burner layout through the floor area with a hole leading to the burner connections, as shown in the front view photo in Figure 6 above. For air supply purposes to keep the fire burning, we cut a rectangular hole along one of the sides of the wall closest to the burner at dimensions 2.5 inches by 11 inches. Along the ceiling of the lower compartment, we applied insulation and metal sheathing so the wood paneling would not catch fire. Connecting the lower floor to the upper we have a square hole, representing where the stair access to the upper floor would be based on the real building. The upper floor also simplified to an open floor plan (no internal walls or furniture), and for visualization purposes, we had polycarbonate sheets along two of the walls (as shown in the side view in Figure 6) to view the burner and smoke flow in the compartments.

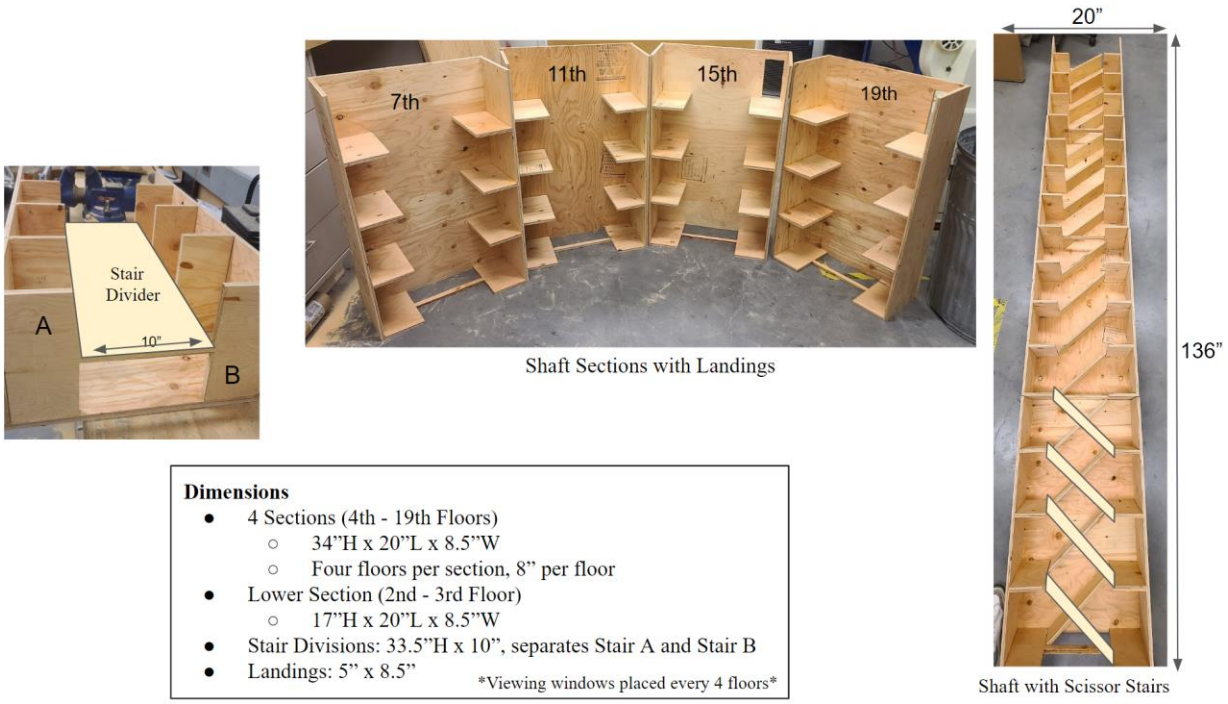

Figure 7: Stairwell Construction

For the stairwell shaft construction, we divided the stairwell shaft into five sections. The first section represented the lower floors (floors 2 and 3), and each of the other four sections represented four floors. The construction of this scaled stairwell was modeled to replicate the actual geometry of the building, with a scissor stair design and holes for doorways intended to demonstrate the open doors within the Bronx fire event. For the stairs, we utilized ramps in place of stair trends to simplify the construction process and save time. Figure 7 above shows the inside construction of the stairwell, the additional wood paneling installed to the backside to fully enclose these stairs, and polycarbonate windows were placed every four floors for smoke visualization. In the stairwell shaft, we added door holes in the locations where the door openings occurred in the actual fire event, this consisted of the corridor doors on the 3^{rd,} 15th, and 19th floor hallways into Stairwell A and B.

Hall-Facing

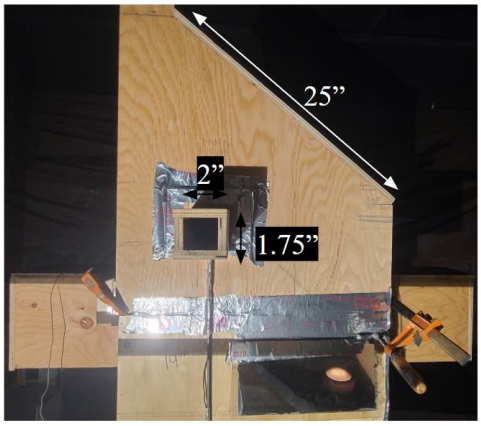

Front View of Penthouse

Window-Facing

Figure 8: Penthouse Construction

The penthouse, pictured in Figure 8, in the scaled model is the highest point that smoke spread, and the only place the smoke should exhaust. This was a simplification for our own testing purposes and does not represent the actual smoke exhaust in the Bronx fire event. The penthouse consists of the final stair landing of Stair B which provided access to the roof and mechanical equipment. In this fire event, there was one window in this roof area in which smoke was able to exhaust. For testing purposes, we constructed a “tunnel” around the window of the penthouse to prevent air flow interference from the hood in the lab.

Figure 9: Construction Assembly

The overall construction consisted of the connection of four main components: the 3N apartment, the hallways, the stairwell, and the penthouse. The construction came out to 15 ft tall, and 10 ft long, with scaffolding needed to assemble and reach the instrumentation along the top of the building, as shown in Figure 9. The structure was connected in a way that allowed us to disassemble after each trial to allow for cleaning and cooling of the lower hallway and 3N compartment.

4.1.3. Fire and Burner Configuration

Another aspect of our experiment that needed to be designed was the fire in the lower floor of the two-story dwelling unit. We needed to establish what kind, size, and type of fire to use. The NYT article stated that investigators determined a mattress was the initial fuel load of the fire, which would have an approximate heat release rate of 1 MW according to Chapter 26 in the 5th Edition of the SFPE Handbook. From this full-scale event, we used Equation 4 to determine a scaled heat release rate of approximately 2.33 kW for our fire test. Originally, we had multiple configurations of our burners to try and reproduce a comparable fire to the Bronx. We considered the quantity of piping, spacing of holes, configurations of the burner, hole sizes, and fuel type. The initial layout consisted of four 12-inch-long pipes with ¼-inch holes spaced 1 inch apart. The second and third configurations reduced the number of pipes to three and then two, respectively. The fourth and final layout that was tested was two 12-inch-long pipes with 1/16-inch holes spaced 1-inch on center.

Figure 10: Second burner trial configuration

As seen in Figure 10, the first three configurations had produced flames that were not uniform because the number of pipes and larger hole sizes caused a greater pressure loss in more remote holes. We had attempted to increase the flow, but this resulted in the flame height reaching the ceiling of our compartment, which put it at risk of burning. Decreasing the number of pipes and the size of the holes in the fourth configuration also decreased the pressure loss and resulted in more uniform flames with a reasonable height. Therefore, we decided that the fourth layout with two 12-inch-long pipes and 1/16th-inch holes would be the best configuration as seen in Figure

11 below. This was determined from the flame height observed during testing and how uniform the flames at each hole burned.

Figure 11: Final Burner Configuration

With this configuration, we tested the maximum flow rate that we could use without becoming too close to the ceiling. The maximum flow rate we felt comfortable testing with on the rotameter was around 29-30 which translates to about 2.3 kW (calculations in Appendix B) which was the desired reduced scale heat release rate to model the 1MW fire. Another factor we had to consider was what type of fire curve we wanted to utilize for our experiments. We ultimately decided to go with a steady-state fire because although it was possible to control and ramp our fire like a t-squared-curve it was more complicated and imposed more uncertainties. Therefore, we determined that a steady-state fire would be easier for replicability and consistency for our results. We also had to decide on the duration of the fire and our experiment. This parameter was estimated from the New York Times article that documented the first 911 call of seeing smoke when the first occupant on the 19th floor saw smoke. We took that time and scaled it to our experimental time with Equation 6 which got us around 5.6 minutes. We decided to use 6 minutes for our experimental run time because we wanted to make sure smoke was visible coming from the top. Before our experimental tests, we had practice trials where our burner ran at 2.3kW steady state for 6 minutes and we saw smoke within the time frame and we concluded this would be long enough for the subsequent tests.

Figure 12: Final Burner Configuration Fire Test

4.2. Measurement Devices

Thermocouples, bi-directional probes, and cameras along with their programming counterparts were utilized to measure and record various values from our fire tests. Appendix E presents the locations of all the devices used in our experiments.

4.2.1. Rotameter

A rotameter (variable area flow meter) is a flow meter that measures the volumetric flow of liquids and gases. This device controls the quantity of propylene flowing into our burner from the propylene bottle. Some of the benefits to rotameters include repeatability, cost effectiveness, low pressure drops, and easy installation and use. The flow of the rotameter was calculated from our desired scaled HRR and the heat of combustion of propylene using Equation 2. The flow rate then needed to be translated to the arbitrary rotameter scale. The desired flow rate was modified (for more details, see Appendix L) using the gas type, temperature, and pressure correlation factors. This actual flow rate was translated by using Appendix L and finding the correlating scale reading from the desired flow rate.

4.2.2. Thermocouples

Thermocouples are devices that measure temperature at a point. They consist of two different types of metals joined together that when exposed to a change in temperature, create a voltage that can be correlated back to temperature. There are two styles of thermocouples; probes and wire, and each style has various combinations of metals with different temperature ratings. The thermocouples chosen for the scope of this project, and perhaps the most common type of thermocouple is K type thermocouple wire. K type thermocouple wire has a temperature range of -200 °C to 1250 °C with standard limits of error of 2.2°C or 0.75% of the measured temperature, whichever is greater. For the temperature ranges observed in this experiment, the applicable standard limit of error will be 2.2°C (Omega, n.d.).

In the experiments conducted as a part of this project, thermocouples were placed along the ceilings of the lower and upper compartments of apartment 3N, the 3rd, 15th, and 19th floor hallways, and adjacent to each bi-directional probe. LabVIEW from National Instruments was used to measure the voltage reading of each thermocouple to the corresponding temperature value. We also utilized various thermocouple extensions and a Data Acquisition system that would work to record temperature in conjunction with LabVIEW. The LabVIEW code (as seen in Figure 13 below), which has a similar interface to an electrical circuit, was provided to us by researchers WPI's Fire Lab.

The "DAQ Assistant" block takes the physical input of the thermocouple connections and makes it into a digital thermocouple reading. The "Write to Measurement File" is how the data is recorded, the type of file the data is written to, and what specific time measurement the program uses. For our program, LabVIEW records the temperature at each designated thermocouple with the date and time of day and creates a spreadsheet from the data collected. The program code we used also live readings from each thermocouple that were all displayed on a time vs temperature graph.

Before setting up the experiment, the thermocouples were tested in two ways to confirm they were working and responsive. Before hooking our thermocouples into the DAQ, we manually tested each thermocouple by plugging them into a laboratory digital thermometer and seeing if the thermocouple would read correct values in ambient conditions and when exposed to a flame.

Once confirmed that the thermocouples were responsive, the thermocouple would be hooked into the DAQ. We would test for responsiveness of the thermocouple like before but with the LabVIEW charts values. This second test was implemented to check that there were no lose or faulty connections and to establish the LabVIEW code was correct.

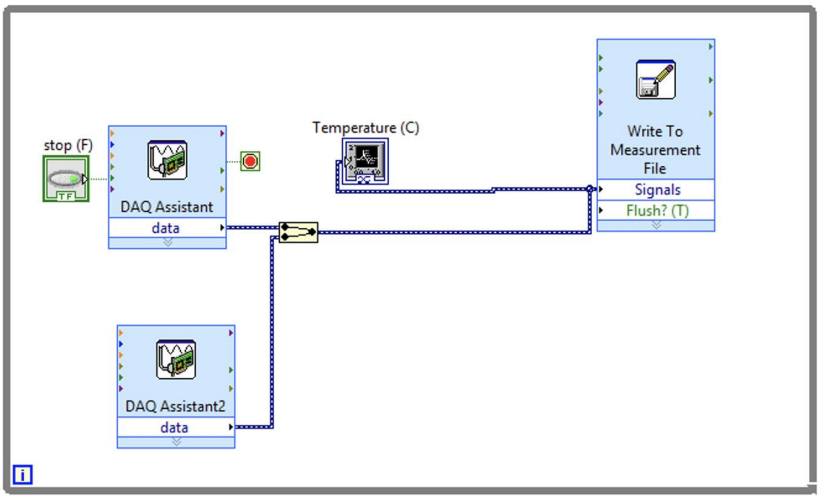

Figure 13: The LabVIEW block diagram for obtaining temperature from our thermocouples.

4.2.3. Bi-directional Probes

Bi-directional probes, seen in Figure 14, are devices which measure the gas flow through an orifice. The device consists of a small cylindrical tube which records the positive flow through one end and the negative flow through the other to determine the pressure differential. These bi-directional probes are placed parallel to the direction of flow, with the positive end facing the direction in which the flow is coming from. The bi-directional probes connect to a pressure sensor which outputs the differential pressures with a supplemental temperature. This allows us to infer the density to solve for the mass flow and velocity of the gas through Bernoulli's Equation. However, this does not account for the extensive tubing connecting the probe to the Raspberry Pi reading these values, which creates a significant pressure loss. The equations in Appendix B.3 are utilized to determine the efficiency (ε) which can then be used to calculate the effective bidirectional pressure in Equation 7. The effective bidirectional pressure can then be used to solve for velocity.

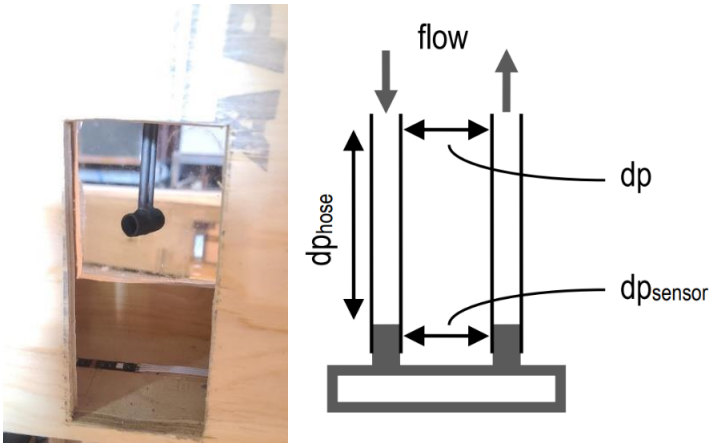

Figure 14: Bi-Directional Probe

$$dp_{eff} = \frac{dp_{sensor}}{1+\varepsilon} \qquad \textit{(Equation 5)}$$

The bidirectional probes are experimentally calibrated to determine the amplification factor. This amplification number is a dimensionless unit and is dependent upon the orifice diameter. The correlation of the amplification factor for a 1 cm diameter was determined from previous laboratory experiments and is as follows:

$$\text{for } dp_{eff} < 0.25 \text{ Pa}, \quad f(x) = ax^4 + bx^3 + cx^2 + dx + e \qquad \textit{(Equation 6)}$$

$$dp_{eff} > 0.25 \text{ Pa}, \quad f(x) = 0.006935(x^{-3.238}) + 1.817$$

where a = -9530.7, b= 5089.9, c=-917.87, d=64.28, and e=0.61. Once the effective bidirectional pressure is calculated, the velocity can then be calculated using the velocity equation for Pitot-tubes, Equation 9. Pitot-tubes use the same correlations as bi-directional probes, which is why this equation can also be used for bi-directional probes, but with different correction factors.

$$v = k\sqrt{\frac{2\Delta P_{eff}}{\rho}} \qquad \textit{(Equation 7)}$$

where dp_{eff} is the effective bidirectional pressure, ρ is the density of air at the correlation temperature, and k is the amplification factor.

According to the study, *The Examination of Bidirectional Velocity Probe used in Flames,* as the flow of the bidirectional probe decreases, the uncertainty of the device's accuracy increases (Gill et al., 2009). Additionally, the digital differential pressure sensor is only precise to 0.1 Pa. Our experiments have minimal flows, so this uncertainty is significant.

A Raspberry Pi was utilized with the bi-directional probes as a simple computer which runs with python code. The code we used was provided to us by researchers in WPI's Fire Lab, however,

we needed to adjust for the number of ports utilized in our tests. We also had to change the time step of how often the bi-directional probe was taking data. Originally the code was recording a value every millisecond, however for our experiment a reading per second was sufficient. Additionally, our digital differential pressure sensor setup only allowed us to read 4 bi-directional probes per Raspberry Pi; therefore, we needed two computers with identical code to run in sync to capture the 5 bi-directional probes readings. Once the fire test was completed the python code produced a long text file of the raw data. This raw data was a single column that needed to be sorted into different columns for time and bi-directional probe readings. A MATLAB code in Appendix F, provided to us by researchers at WPI's Fire Lab, helped us rearrange the raw data to useable data. The data was sorted into a spreadsheet that was then used to make calculations and graphs from.

The bi-directional probes, digital differential pressure sensors, and python code were also tested for responsiveness. The probes connection hoses were initially blown into from the positive side by one group member while the group member was reading the live values from the Raspberry Pi. Implemented to all bidirectional probes, this test was to ensure the pressure transducers were responsive to a pressure change. The value on the Raspberry Pi would max out to a given maximum positive value, to the magnitude of 100,000, meaning it was sensing a pressure change. If a negative value was read, then the bi-directional probe would need to be flipped around, and if there were no reading other troubleshooting methods needed to be implemented. These would entail ensuring the right bi-directional probe was selected on the computer, and confirming the air was going into the right bi-directional probe. Another similar preliminary test had to be run where the process described above was utilized except the flow would be directed into the bi-directional probe rather than through the tube. Similar trouble shooting techniques from above was also done if there were issues.

4.2.4. Cameras

The cameras were used in our experiments to record smoke conditions of various compartments. The building was mostly constructed from plywood, however strategically placed windows were used to see inside the structure. We had five cameras to record through various compartment windows located near the 3N apartment, 3rd floor hallway, 15th floor hallway, 19th floor hallway. Figure 15 is an example of the type and positioning of camera used throughout the experiment. The 3N apartment camera moved between Test 1 and Test 2 with the intention of filming a more critical point in our building. The camera was moved from the outside of the apartment to outside the apartment door to the hallway in hopes of seeing the smoke flow from the apartment to the hallway. The other cameras were located at the same windows for all experiments. Each camera was used to capture the smoke movement for at least three trials of each test. From this footage, we intended to qualitatively analyze the differences of smoke movement between each experimental test and the CFAST simulations.

Figure 15: Example of a Camera Positioning.

5. CFAST Model

To create the CFAST Model, we first had to make modelling assumptions. CFAST has limitations in regard to building and fire designs, which must be accounted for when basing our model off of a realistic fire event. Based off these modeling assumptions and limitations, we were able to configure the CFAST model and develop fire scenarios. Then, we had to determine key locations where we would measure and record temperature, gas flow and smoke visualization. After our model was set up, we ran our simulations with tests varying the door opening fractions and compared the results to our physical tests. Each simulation has the same conditions and characteristics, except the opening percentage of the wall vents that emulate doors. The following sections discuss in further detail the steps taken to achieve our goals.

5.1. Model Assumptions

CFAST is a computational zone model software, and thus modeling assumptions need to be made to have the necessary parameters to run complete calculations. This section describes the necessary assumptions and simplifications we made, in addition to those already made in CFAST in relation to compartment fire dynamics as discussed in Section 2.2.

Assumptions regarding leakage need to be made to balance the pressure and other losses within the model. This was achieved by creating vents in the burner room. While leakage was considered in CFAST, we expect there was significantly more leakage in the lab tests than had been modeled in CFAST.

5.2. CFAST Model Configuration

5.2.1. Model Geometry

Compartments in CFAST are rectangular prisms that utilize cartesian coordinates to configure compartment length, width, and height which can be viewed in Smokeview. The compartments representing the two-story dwelling units were set as two-zone models and all other compartments were set as one-zone models. CFAST allows the user to distinguish one-zone models as shafts or corridors. Without simplifying these compartments to one-zone models the simulations would not run. The material used for wall, ceiling, and floor geometry was Plywood (1/2 in) from the CFAST thermal properties spreadsheet which also can be found in the SFPE Handbook. Input parameters for the CFAST model used in this study are shown in Appendix M below and an isometric view of the entire model is shown in Figure 16.

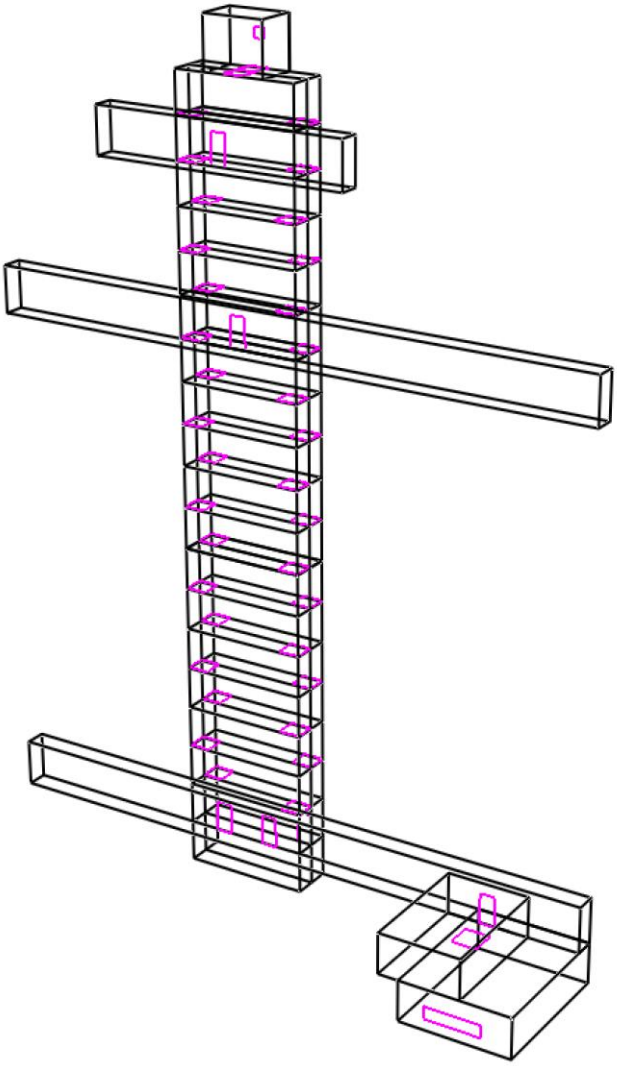

Figure 16: Finalized Compartment Configuration

Doors in the CFAST models were input as wall vents connecting the compartments to each other. Each wall vent dimension is 3” wide and 6” high. As CFAST cannot model door openings as angles, we instead had to use equivalent opening fractions. For the trial of open doors, the opening percentage was set to 1.00, the opening percentage in the trial for 45 degree doors was set to 0.77 and the opening percentage in the trial of 20 degree open doors was set to 0.33. The door opening percentage was determined by taking the ratio of the distance from the edge of the door to the door frame and the full door opening width (3 inches) in the physical fire test model for each door position. This is further explained in Appendix B.2.

Additionally, we had to devise a method to model stairways in CFAST. Each level of Stair A and Stair B was created as a separate compartment yielding two compartments per floor and were set as shaft one-zone models. To model the stair risers, we created ceiling vents on alternating sides

of each compartment as seen in Figure 16. These ceiling vents are 4ft by 4ft which span the width of the compartment. The intention of these vents was to emulate the flow of smoke in a stairwell. Figure 17 below is a visual representation of how these ceiling vents correlate to stair opening where the CFAST ceiling vent are outlined in purple, Stair A is represented by the blue shapes and Stair B is represented by the green shapes.

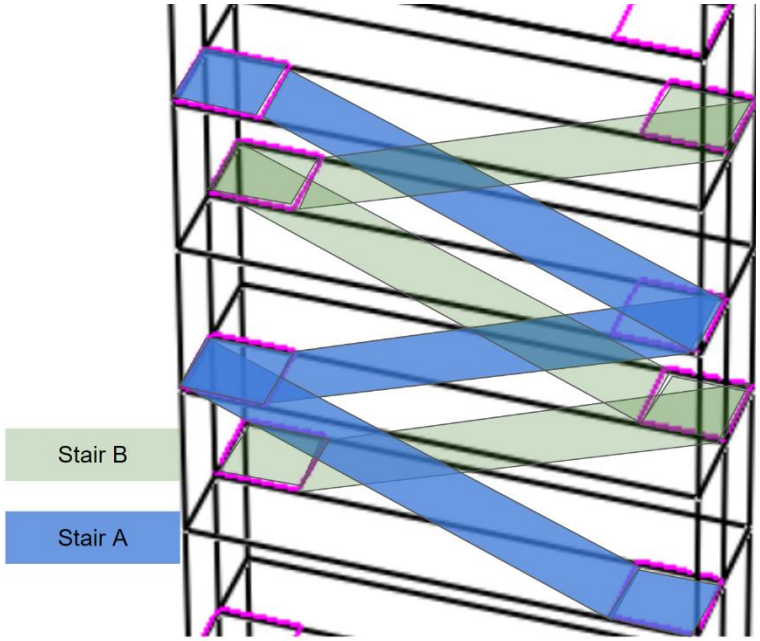

Figure 17:CFAST Vent Layout for Stairwell Configuration

5.2.2. Fire Size & Growth

A steady-state 2.3 kW fire was configured in the lower level of the two-story dwelling unit in the same location our burner was placed in the physical fire tests. The chemical composition of propylene and the heat release rate was entered into CFAST to emulate the lab test fire described in section 4.1.3., which goes more in depth about the fire composition. The fire had a ramp time of 15 seconds and was held at the peak HRR of 2.3 kW for 6 minutes (360 seconds) to align with the physical trials.

The open vent on the side of the lower level of the dwelling unit was used for ventilation in the physical lab test model was also modeled in CFAST to sustain the fire. A vent is required in CFAST for similar reasons to the lab model. If there were no vents, the simulation and experimental fire would have extinguished due to oxygen deprivation.

5.3. CFAST Calculations

For our CFAST runs, no devices were utilized to extract information from our model. CFAST automatically generates output spreadsheet files as mentioned above, with various calculated

values. We used the temperature and mass flow calculation in the compartments and through vents to compare CFAST to our experimental tests.

5.3.1. Gas Temperature

CFAST calculates the average gas temperature in the upper and lower layers of a compartment. The compartments we examined in our simulations were the Lower Compartment of 3N, Upper Compartment of 3N, 3rd floor hallway, 15th floor hallway, and 19th floor hallway. Gas temperature values are calculated for the upper layer by estimating a continuous vertical profile of temperature, according to Appendix A of the CFAST Validation Guide. The upper layer temperatures of each compartment are also necessary to calculate velocity from the mass flow rate. This is a simple relation to the ideal gas law as temperature affects the density of air which in turn affects the velocity.

5.3.2. Vent Mass Flow

In CFAST, the only location mass flow can be measured is through horizontal vents. Mass flow is the total amount of mass moving into one compartment from a second compartment through the total vent area (Peacock et al., 2015). Vent mass flow is another value that CFAST outputs in kilograms per second (kg/s) without the need for additional devices. We took the vent mass flow from the 3N to the hallway wall vent, both 3rd floor hallway wall vents, the 15th floor hallway wall vent, the 19th floor hallway wall vent, and the penthouse exhaust vent that acted as a 'window'. Each of the wall vents represented a 'door', except the window vent in the penthouse. From this, the mass flow rate was used to manually calculate the velocities of gases which was later compared with the velocities from the fire tests. This was done on a separate spreadsheet and was heavily dependent on the change in temperature and mass flow. The mass flow rate equation was rearranged to solve for the velocity of the CFAST output= (as shown in Equation 10).

$$v = \frac{(\dot{m})}{\rho \cdot A} \qquad \textit{(Equation 8)}$$

6. Testing

6.1. Fire Testing

Before we began fire testing, we needed to decide on different conditions we wanted to test. Our main priorities were to focus on how smoke moves, and the different effects door positioning can have in our model. This led to a few variables that could be manipulated for differing results, including behavior of the fire, the possible smoke blockages in our model, and the experimental run time. Our group decided to employ a steady-state fire with the same heat release rate of 2.3 kW, the same simulation time of 6 minutes, but with differing door positions along the 3rd floor. These parameters are also outlined in Table 1 below. As discussed in earlier sections, the heat release rate of the test fire was based on flame height and the feasibility of the fire within our tests. The door positions were varied in each test because of the potential effect it would have on the smoke movement, temperature, and flows. The concept of differing door positions was modeled on the Bronx Apartment Fire case study because the exact status of doors at the time of the fire was unknown. The simulation time was also based on an estimate from the Bronx Apartment Fire. We scaled the approximate time it took for smoke to reach the top during the Bronx Fire (Singhvi et al., 2022) and then scaled it with the equation mentioned above and got slightly under 6 minutes. Three trials were run per test in order for the data to be averaged for each scenario. Many of these parameters were also decided on the fact that we only had two weeks to conduct fire tests.

Table 1: Finalized Physical Testing Trials

Test	Number of Trials	Fire	Degree of Door Opening	Simulation Time
1	3	Steady-state, 2.3 kW	No door	6 minutes
2	3	Steady-state, 2.3 kW	45° open	6 minutes
3	3	Steady-state, 2.3 kW	20° open	6 minutes

6.1.1. Experimental Setup for Physical Tests

The goal of the project was to create an apparatus that allowed for repeatability. This goal was achieved as each of the trials were conducted in the same manner in order to limit the confusion of extra steps. Each group member was assigned to a specific role during the trials which generally continued through the subsequent tests and trials. In Appendix E we listed the series of events in which conducted our trial to ensure repeatability and precision.

A stopwatch was used for each of the trials to best align with the collected data. The group decided this was the best decision to only collect necessary data points as the ambient points were not needed for data comparison. Each of these steps were completed in succession from the top of the testing apparatus down to the initial opening of the propylene tank. These steps were the same for all of the trial conditions and varied door positions. This was done to create the best opportunity for consistent data collection. The group only changed the position of the door to test the affect door positioning had on smoke movement through the building. No other data collection specific testing procedures were changed during the varied door positions. The time between tests varied as we had to allow for the cooling of our compartment to prevent inaccurate temperature readings.

6.2. Overview of Tests: CFAST and Fire Tests

As previously mentioned, we conducted three tests. These tests involved the varying of door openings in the 3rd floor hallway, which included the two doors into the stairwell and the door into apartment 3N. In the lab tests, the three variations of door openings were tested which include fully open, 45 degrees, and 20 degrees. The same door locations were used in CFAST with equivalent door opening fractions of 100%, 77%, and 33%. The door configurations for the lab tests and CFAST are further described in Table 2 and pictured in Figure 18.

Table 2: Door Configurations of Tests

	Test 1	Test 2	Test 3
CFAST (Vent)	100%	77%	33%
Lab (Door)	Open	45 degrees	20 degrees

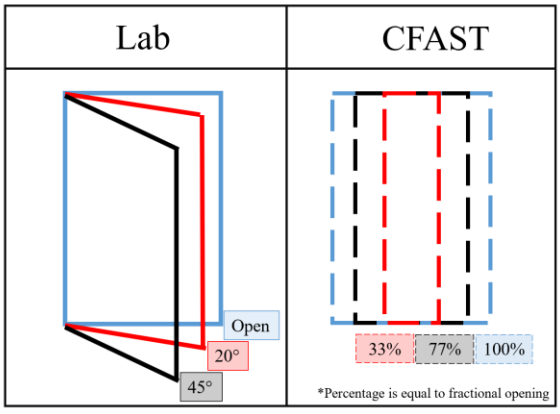

Figure 18: Door Configuration between our lab tests and CFAST tests

7. Results and Analysis

The temperature, velocity, and smoke visualization results from CFAST and the fire tests were analyzed graphically. Graphs were made for each measurement at 3N, 3rd Floor Hallway, 15th Floor Hallway, 19th Floor Hallway, and the Penthouse. Peak temperatures and velocities were utilized to create a graph to track the values as they moved through the testing apparatus. Additionally, calculations were also conducted to determine the percent difference between the CFAST and test results to evaluate the degree to which the results compared. We also compared the timing for smoke to reach the penthouse in CFAST and the lab tests using cameras and Smokeview renderings and analyzed the smoke appearance as it progressed up the building. To compare the results of the smoke visualization, side-by-side photos were placed at time intervals of two minutes.

7.1. Temperature

In this section, the increase in temperature from ambient conditions at selected locations within the building are graphically compared between lab tests and CFAST simulations. The selected locations, in order as they appear, are the Lower Compartment, Upper Compartment, 3rd Floor Hallway, 15th Floor Hallway, and 19th Floor Hallway. The naming convention of each test is displayed in Table 2 above and the location of each thermocouple can be found in Appendix E.

The temperature data from the three trials of each lab test were grouped together based on the location of the thermocouple and door configuration. The test data was aligned with the time of ignition in each trial set as 0 seconds. From this basepoint, the temperature values of the three trials were averaged for each second over the following 360 seconds. In order to align the temperature results with the temperature values calculated in CFAST, the temperature from each thermocouple along the ceiling of each compartment was averaged for each time step.

Additionally, the operation of the hood in WPI Fire Lab causes the ambient temperature to vary from trial-to-trial. Therefore, to determine the ambient temperature for each trial, data collection was started at least 60 seconds before the start of the trial. The temperatures recorded over these first 60 seconds were averaged to determine the ambient temperature for each trial. Then, the ambient temperatures of the three trials for each door configuration were averaged to reflect how the 360 seconds of temperature data mentioned was presented. It was not necessary to calculate the ambient temperature in CFAST, ambient temperature is a user defined value. The ambient temperatures for each test are displayed in Table 3 below.

Table 3: Ambient Temperatures throughout the building

	Lower Compartment	Upper Compartment	Hall 3	Hall 15 & 19
Lab Test 1	18.9 °C	18.9 °C	18.1 °C	18.0 °C
Lab Test 2	24.8 °C	26.4 °C	21.0 °C	17.0 °C
Lab Test 3	22.9 °C	23.1 °C	18.3 °C	17.6 °C
CFAST (All tests)	20 °C	20 °C	20 °C	20 °C

7.1.1. Lower Compartment

The temperature rise results in the upper layer of the Lower Compartment are shown in Figure 19 below for the reduced-scale model. Tests 1 and 2 followed similar trends for both CFAST and the lab test data and appear to overlap since the difference in temperature between them is less than 1 °C. Test 3 was expected to see higher temperatures because the vent opening percentage and door position were the smallest, resulting in more heated air to be retained inside of the compartment. In the CFAST simulations, temperatures in Test 3 were about 5 °C higher than Tests 1 and 2, whereas for the lab tests the temperatures in Test 3 were roughly double the temperatures observed in Tests 1 and 2. This discrepancy is anticipated to be caused by the necessary assumptions CFAST makes for a zone model. However, it should be noted that due to scheduling constraints, less time was given between trials in lab test 3 for the structure to cool leading to a higher ambient temperature and possibly higher temperature rise results.

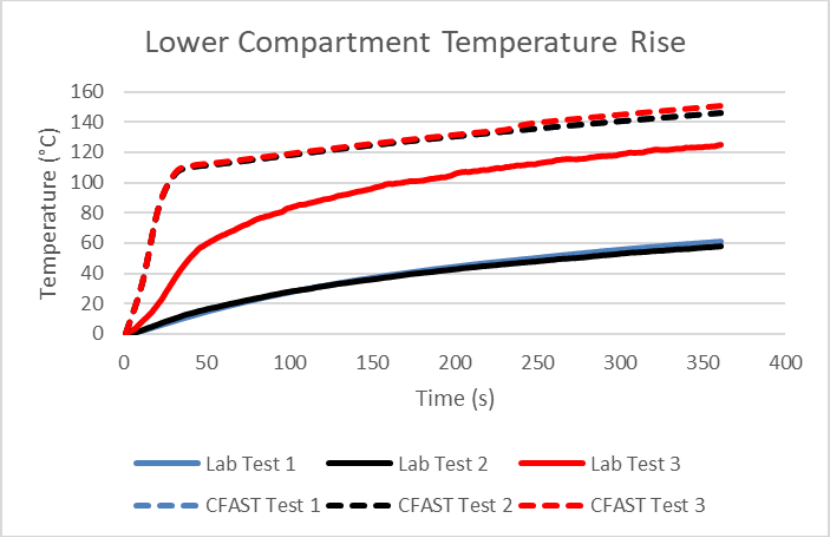

Figure 19: Lower Compartment Temperature Rise

7.1.2. Upper Compartment

The temperature rise results in the upper layer of the Upper Compartment are shown in Figure 20 below for the reduced-scale model. The opening percentage of the vents was expected to have a significant effect on the temperature rise observed in the Upper Compartment since this is where the vent opening was located. This was proven to be true as the temperature rise data showed the greatest difference between tests in the Upper Compartment. However, the order of how much temperature increased in each test did not match what was expected. The temperature increase in CFAST Test 1 was typically 1-2 °C greater than CFAST Test 2, and the temperature rise in CFAST Test 3 was observed to be lower than CFAST Test 2 by at most 10 °C. Since heated air is more buoyant than cool air and will rise to the ceiling, it was expected that CFAST Test 3 would have the highest increase in temperature, CFAST Test 2 the second highest, and CFAST TEST 1 the lowest increase. The same behavior was observed in the lab tests, where lab Tests 1 was roughly 10 °C higher than lab Tests 2, and lab Tests 2 was 2-3 °C higher than lab Test 3.

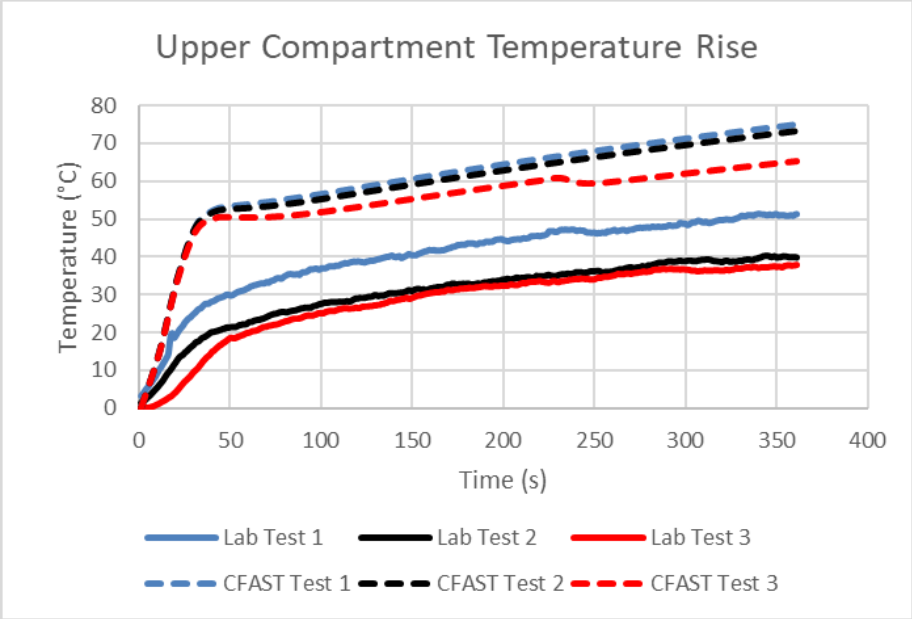

Figure 20: Upper Compartment Temperature Rise

7.1.3. Hall 3

The temperature rise results in the upper layer of Hall 3 are shown in Figure 21 below for the reduced-scale model. Examining the plots of the CFAST tests, the temperature values in CFAST Test 1 are typically 1°C greater than in CFAST Test 2. The temperature observed in CFAST Test 3 was lower than both CFAST Test 1 and Test 2 by approximately 2-3 °C. Since the vent opening percentage was the smallest for CFAST Test 3, it was expected that it would allow the least amount of heated air to flow through and therefore had the lowest increase in temperature. For the lab tests, the temperature plots for Lab Tests 1 and 2 were typically within 2 °C of each other, whereas the temperature in Lab Test 7 was about 7 °C less than Lab Tests 1 and 2. Lab Test 2 had a higher temperature than Lab Test 1 by 2-3 °C. The temperature rises in Test 3 were expected to be the lowest of the three because the smaller openings at the doors would allow less heated gas to flow from the Upper Compartment into Hall 3, and from Hall 3 into the stairwell. Additionally, while Lab Test 1 saw a higher temperature rise than Lab Test 2 in the Upper Compartment, it saw a slightly lower temperature rise in Hall 3. CFAST Test 1 had a higher temperature rise in both the Upper Compartment and in Hall 3 than CFAST Test 2.

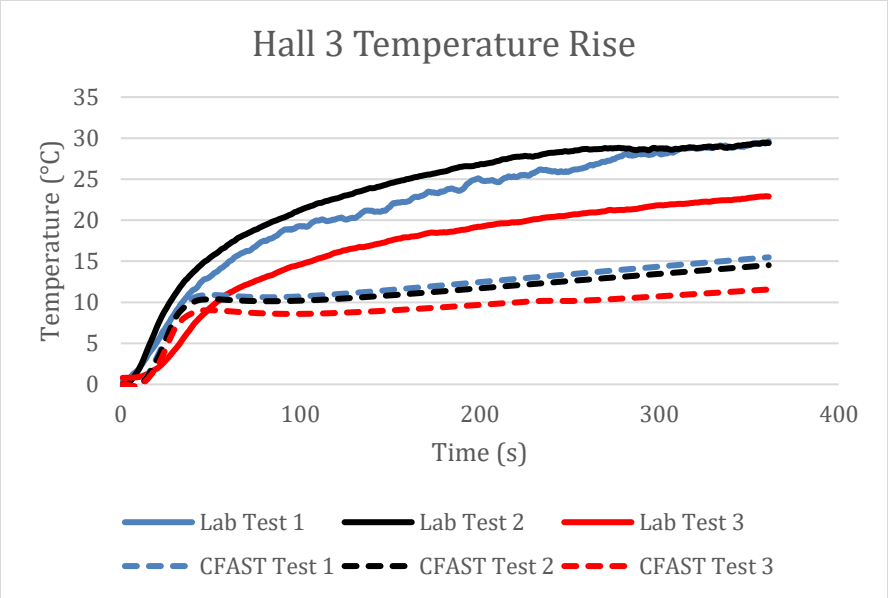

Figure 21: Hall 3 Temperature Rise

7.1.4. Hall 15 & Hall 19

The temperature rise results in the upper layers of Halls 15 and 19 are shown in Figures 22 below for the reduced-scale model. For the entire duration of the tests the temperature rise was observed to be close to 0 °C, which means that the temperatures remained at ambient. Therefore, these temperature rises offer no significant comparison between CFAST and the lab tests, although it is encouraging CFAST's approximations matched the behavior observed in the lab tests. The temperatures in Hall 15 and Hall 19 have implications on the behavior of the smoke, as discussed further in Section 7.3.

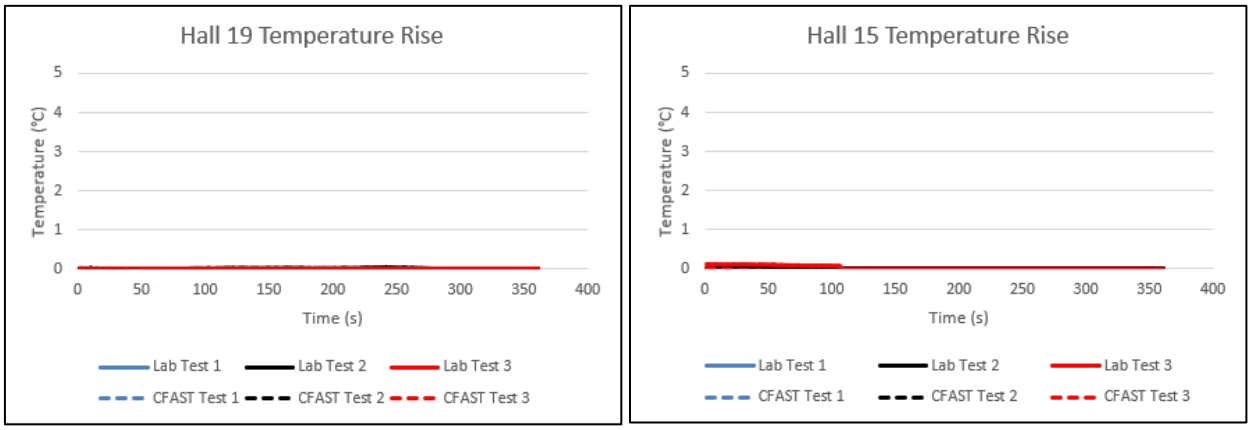

Figure 22: Hall 15 & Hall 19 Temperature Rise

7.1.5. Peak Temperature Rise by Location

Figure 23 below displays the peak temperature rise recorded at each location, for the purpose of observing air temperature rise as the air flows through the model. As expected, the temperature

rise decreased as the heated air moved further away from the fire room through the model. The decrease in temperature rise was more constant for the CFAST simulations than in the lab tests. For each test, the highest value of temperature rise throughout the 360 second test period was plotted as a function of its location.

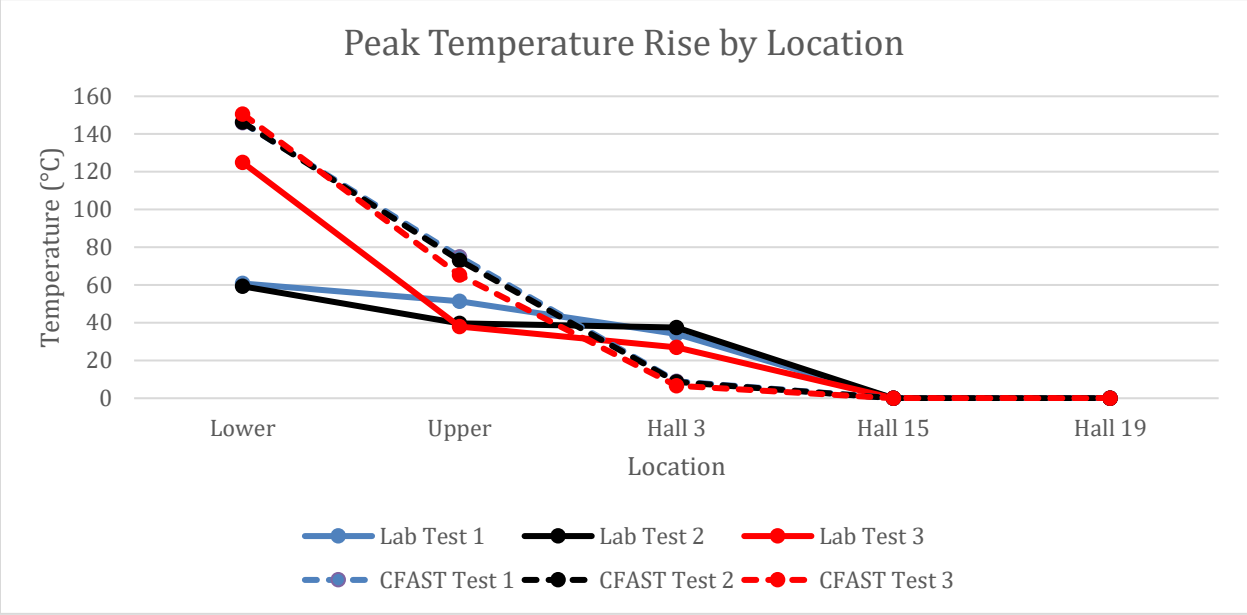

Figure 23: Peak Temperature by Location

7.1.6. Full Scale CFAST Model

When we ran our reduced-scale CFAST simulations, they each returned an error message saying that the dimensions of the compartments were not within typical bounds. The typical bounds for width, depth, and height in CFAST are 0.5 m to 100 m (~1.66 ft to 328 ft). As noted in previous sections of this report, our typical compartment height was 8.5 in (0.2159 m). In an effort to understand how CFAST approximated compartment geometry outside the typical bounds, a CFAST model with full-scale dimensions and a HRR of 917 kW was simulated for each test. Unfortunately, due to time constraints, only the overall trends of the full-scale and reduced-scale tests were analyzed. The results for these full-scale simulations are displayed in Figure 24 below.

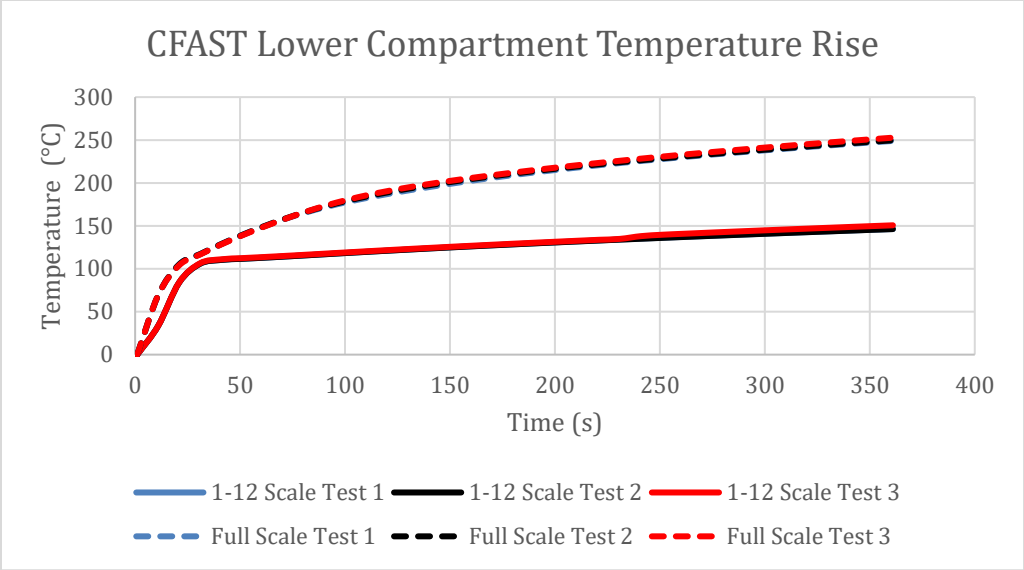

Figure 24: Lower Compartment Temperature Rise for the Full-Scale Model

The magnitude of temperature rise in the full-scale was significantly larger than the reduced-scale, but this was expected to be due to the significantly larger HRR. Both simulations develop similarly over the first 25 seconds, but the slope of the temperature rise plot for reduced-scale simulations plateau harder than the full-scale simulations after the initial 25 seconds. Results for the other four locations can be found in Appendix P.

7.1.7. Temperature Percent Difference

Percent difference is defined as the absolute value of the ratio of the difference between two numbers and their average, expressed as a percentage. The percent difference tells us the error of measurement in an experiment, as this value increases the error increases.

$$\frac{|X_1 - X_2|}{\frac{X_1 + X_2}{2}} x\ 100 = \text{Percent difference} \quad \textit{(Equation 9)}$$

The 3rd Floor Hallway was observed to have the greatest difference, with percent differences over 100%. Additionally, the percent difference for the Lower Compartment in Test 1 and Test 2 was also relatively high, around 80%. The Upper Compartment saw percent differences of less than 60%, and the 15th and 19th Floor Hallways did not see a difference in temperature. Table 4 below displays the percent difference between peak temperatures at each location, for each test. Equation 11 below was used to calculate the percent difference.

Table 4: Percent Differences of Peak Temperatures between CFAST & Lab Tests

Overview of Percent Differences from Peak Temperatures between Tests 1, 2, and 3			
Location	Test 1 (%)	Test 2 (%)	Test 3 (%)
Lower Compartment	82	85	19
Upper Compartment	38	59	53
3rd Floor Hallway	117	125	122
15th Floor Hallway	0	0	0
19th Floor Hallway	0	0	0

7.2. Velocity

To analyze our velocity data, we used quantitative graphical techniques and compared our data at each location. As mentioned in the bi-directional probe section, the outputs from our physical tests produced differential pressures, which were then used to calculate velocity using the correlation equations. The velocity data was recorded from each bi-directional pressure device and categorized into their different locations. Once all of the data was collected, we averaged the data from each trial between tests filtering out the noise and outliers. We also had to offset the velocity to account for the ambient air conditions of the lab. Originally the data was noisy, as there were several fluctuations which made it difficult to observe the trends, so we averaged the data between increments of ten seconds. Then, once the trends became clearer, we plotted the CFAST results on the same graphs. From there, we compared the overall trends and the peak velocities between the physical tests and CFAST tests.

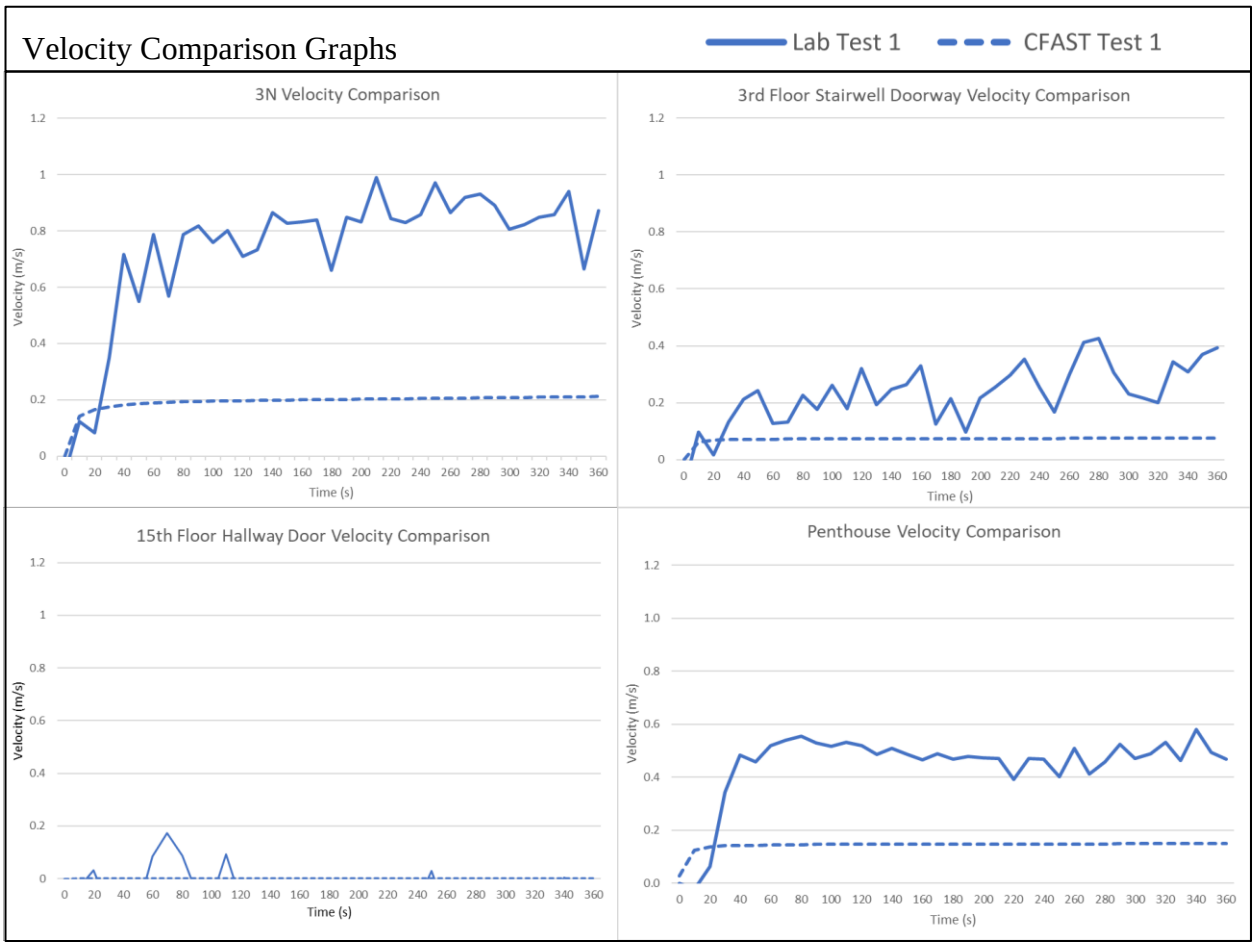

Figure 25: Velocity Comparison for Open Doors Test

The experimental and CFAST velocity results at different locations within the building are shown in Figure 25. The comparison of the CFAST and experimental velocity results yield similar trends. The overall trends of the graphs showed that the locations which experienced the most significant velocities are (in order of greatest to lowest flows): apartment 3N, Penthouse, 3rd Floor Hallway and Stairwell. The velocities within apartment 3N were the most significant, as this was the origin of the fire. The greatest temperatures were also seen in this area, which enabled a buoyant smoke plume to travel up to the upper compartment and through the doorway into the hall. The velocities observed experimentally fluctuated between 0.7 and 0.9 m/s at steady burning conditions. The velocities recorded in CFAST yielded much lower values, at 0.2 m/s. From the apartment, the smoke flows through the 3rd Floor Stairwell, filling the entire volume of the hallway, creating a stratification with a minor upper layer formation, and then flowing into the stairwell. The bi-directional probe located in the doorway connecting to the stairwell on the 3rd Floor correlated velocities fluctuating between 0.1 and 0.4 m/s, appearing to have an upward slope. Within the 15th Hallway door, the flows appeared to yield no velocity for CFAST, and a fluctuation of around zero, with some flows actually moving opposite (showing negative values). The hypothesis within the experimental velocity values is that the smoke is traveling into the 15th floor and filling the hall, and as there is no exhaust in this area, or no significant leakage, the smoke is filling and back flowing into the stairwell. Additionally, at very

low flows, bidirectional probes may not be able to provide consistent or accurate data, which could result in these fluctuations around 0 m/s. Moving up the stairwell, the smoke continued to disperse and become less buoyant-driven, and more flow-driven, which resulted in the majority of the flow being pushed out of the penthouse, the primary exhaust. The results of the CFAST and experimental trials yielded velocities of 0.5 m/s and 0.15 m/s, a difference of 0.35 m/s. Figure 26 below displays the peak velocity recorded at each location, for the purpose of observing velocity as the air flows through the model.

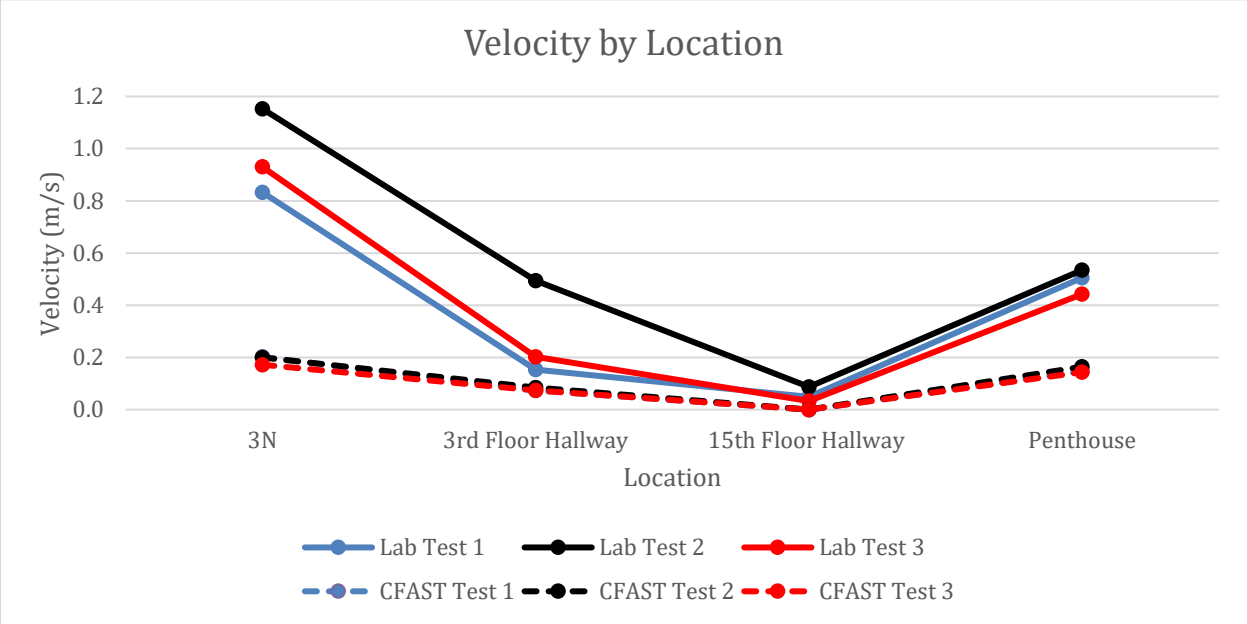

Figure 26: Velocity by Location

Table 5: Percent Differences of Peak Velocities between CFAST and Lab Tests

Overview of Percent Differences from Peak Velocities between Tests 1, 2, and 3			
Location	Test 1 (%)	Test 2 (%)	Test 3 (%)
Apt. 3N Doorway	140	153	151
3rd Floor Doorway	86	89	76
15th Floor Doorway	200	200	200
Penthouse Window	102	110	123

Comparing the CFAST peak velocities to the Lab peak velocities (in Appendix J), we were able to determine the percentage differences at each location. Overall, the results test-to-test yielded similar percentage differences in the same locations, as shown in Table 5. At apartment 3N, the difference ranged from 140% to 151%, this means that our lab tests were quite different from

CFAST. The 3rd Floor doorway yielded the smallest percent difference, which ranged between 76% and 89%. This means that our measurements between the lab tests and CFAST were most closely related in this area. In the 15th floor doorway, all of the results yielded a 200% difference, which makes sense as CFAST recorded values close to zero, while our lab tests ranged between 0.05 to 0.1 m/s. This means that there was the most significant error within the 15th floor doorway between CFAST and the Lab. At the Penthouse window, results concluded a difference which ranged between 102% and 123%. Overall, these velocity results yielded significant errors between CFAST and the lab tests.

7.2.1. Mass Flow

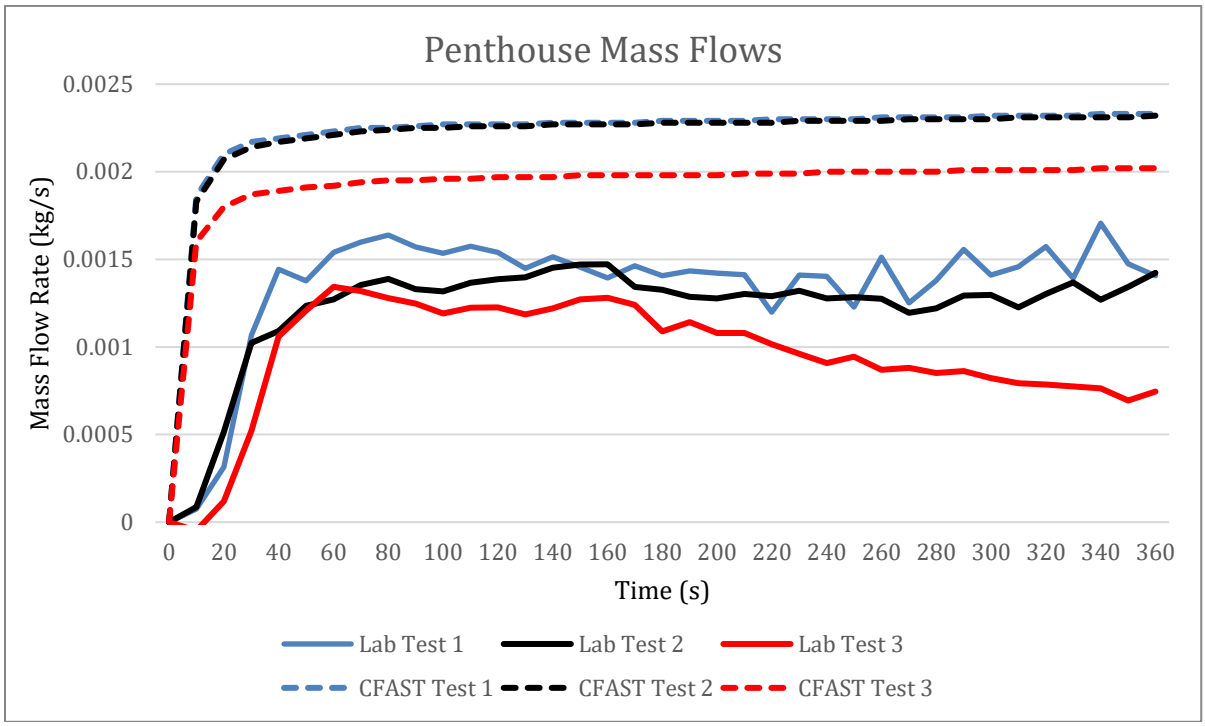

Figure 27: Mass Flow at the Penthouse

Figure 27 above represents the recorded mass flows in the cross-sectional area of the window in the penthouse. The comparison between the CFAST and the Experimental mass flows yield similar trends. The results of the CFAST mass flows in Test 1 and Test 2, with the doors at 100% and 77% open, show nearly the same value, around 0.00225 kg/s. Meanwhile, Test 3 (at 33% open), yields lower mass flows than that of the previous tests, at a peak value 0.002 kg/s. The results of the experimental data show similar trends, at lower mass flow readings. Test 1 shows fluctuations around 0.0015 kg/s, Test 2 shows more steady values around 0.0013 kg/s, and Test 3 shows a down sloping trend, unlike all of the other tests, which peaks around 0.0013 and then decreases to 0.00075 in 6 minutes. The comparisons shown within Figure 27 show similar trends, yet greater mass flow values within the CFAST tests. These differences are likely a result of leakage which was much more observable in the experiments compared to the numerical modeling program, which does not experience leakage unless input. Additionally, it can be noted

the effect of doors played a significant role in the different mass flow recordings, especially in CFAST, where it appears the difference between 77% and 100% wasn't significant enough for different mass flows, however the difference between 77% and 33% was 0.0005 kg/s. Overall, the mass flow graph above can deduce that the air coming into our compartment is very closely related to the air exhausting, when comparing our lab tests and CFAST.

7.3. Smoke Visualization

Along with quantitative results as mentioned above, we also gathered qualitative results. We tried to observe the smoke movement throughout our building by capturing multiple videos of smoke through various windows of our structure. The reason we wanted to observe smoke movement was to potentially compare the 911 calls of reported smoke in the Bronx Fire with our smoke movement results. Although we cannot make any firm conclusions or correlations about the Bronx Fire from our model, it was more used to see if our scaled model was somewhat similar to the Bronx Fire.

We chose to post-process our 20 minute videos to still frame visualizations by taking snap shots of the same points in time across all tests at each location. The first row is at 0 minutes when the fire is just beginning and as you go down the rows the progression in time increases by increments of 2 minutes. Each column, with a label on the x-axis, represents the location of where the footage captured. A single trial was used to represent a test, intending to ensure the smoke movement will be accurately depicted rather than utilizing multiple different trials. The trial videos that were extracted from the camera footage was reliant on which trial videos were the visually clearest. Generally, the difference of the visual data at each location is not readily comparable across Test 1, Test 2, and Test 3.

Figure 28: Test 1 Camera Results

In the open-door trial, as seen in Figure 28, it is clearly seen as time progresses each location becomes visually darker indicating that the room is being filled with smoke. The smoke development can be seen at every location at varying degrees. There are no distinct layers that can be seen in every location. In general, the 3rd floor cameras do not depict the smoke well, regardless of a layer development or not. However, the upper hallways have better visuals that clearly show the lack of layer development. From the visuals, we can assume there is no layer development because the whole room just becomes darker with no distinct upper layer. The penthouse view is from a different trial because the position that was taken in this trial lacked clear visuals of the smoke coming from the penthouse. However, this trial had a very similar time for smoke reaching the top which we decided would be an acceptable representation of the other trial.

The footage from Test 2 and 3, in Appendix K showed similar results to Test 1 where the 3rd floor footage was not clear, but the upper hallways were slightly more clear showing smoke but with no clear layer development. However, a point that was comparable was the footage taken at the Penthouse location. As seen in Figure 29, we could take snap shots from each test and compare the smoke at the Penthouse. The red shapes added onto the photos are to highlight the smoke that came from the penthouse tunnel. Based on this initial comparison, the open and 45° door position had smoke production between 2 and 4 minutes whereas the 20° door position had smoke production between 4 and 6 minutes. This is further discussed in later sections.

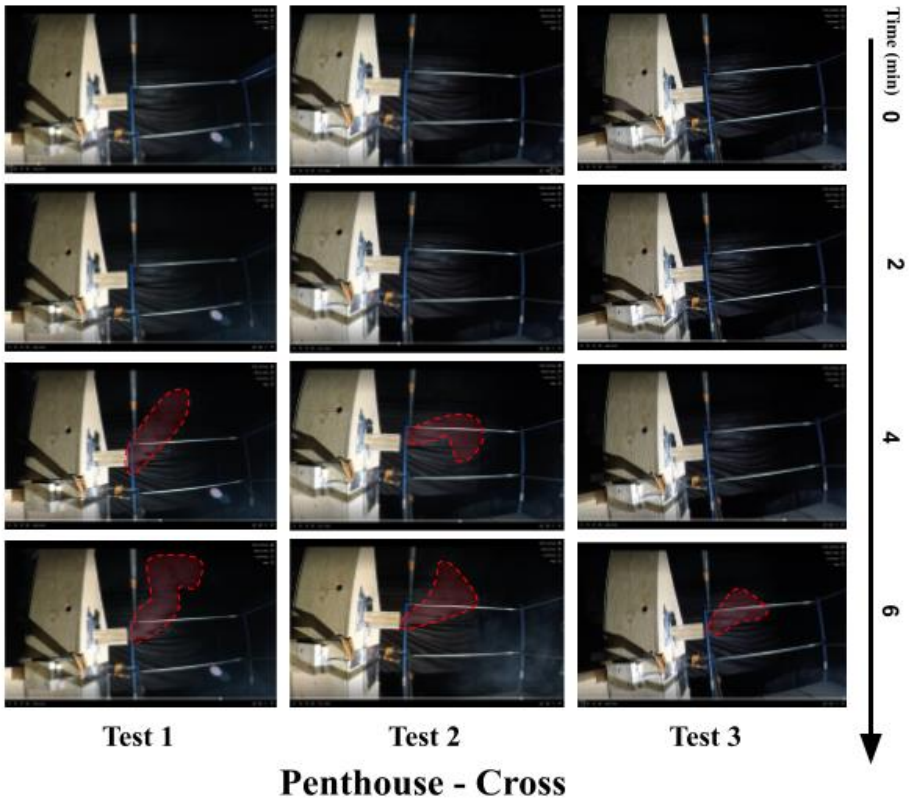

Figure 29: Penthouse Smoke Exhaust Comparison between All Tests

We also wanted to compare the smoke spread up the building in our experimental model to the actual Bronx Apartment fire event. According to the 911 calls in the Bronx Apartment, it was approximated that the actual fire event took 20 minutes to show smoke at the top floors. In this fire, the status of all the doors throughout the building was unknown. The purpose of introducing doors into our physical fire experimental trials was also to compare the effects the doors would have on the time for the smoke to reach the penthouse. At a 1:12 scale, the time for the smoke to reach the top of the scaled apartment was 5.6 minutes (340 seconds). We took the time from each test starting at the fires ignition to when we saw smoke coming from the penthouse. Then, we averaged the trial times to represent the time it took for the smoke to reach the top of the experimental model which is displayed in Table 6. This estimation was only done visually based on the camera footage.

Table 6: Each tests average time for the smoke to reach the penthouse

Time for Smoke to Reach Penthouse				
	Experimental Time	CFAST Model Time	Difference Between Experimental and CFAST Model	Bronx Fire Time
Test 1	2:40	4:10	43%	5:40
Test 2	3:40	4:30	27%	
Test 3	4:30	4:50	7%	

Comparing our fire tests smoke visualization results to the Bronx fire event, the time from Test 3 for smoke to reach to the top of the building was most similar to the actual fire event. It was also determined in Table 4, the fully open test took 2 min 40 seconds, which scales to about half of the real fire event. With doors at 45º, the duration lengthened by 1 minute 20 seconds and closing the doors to 20º open, the smoke slowed by approximately an additional 1 minute. These smoke movement results from our fire tests are vastly different from our CFAST Smokeview smoke movement results. Part of the reason the results might not be similar is because they are not direct comparisons. For our experiment we used camera footage to determine the time it took for smoke to reach the top, whereas with CFAST we could see within the compartments to determine when smoke first reached the top.

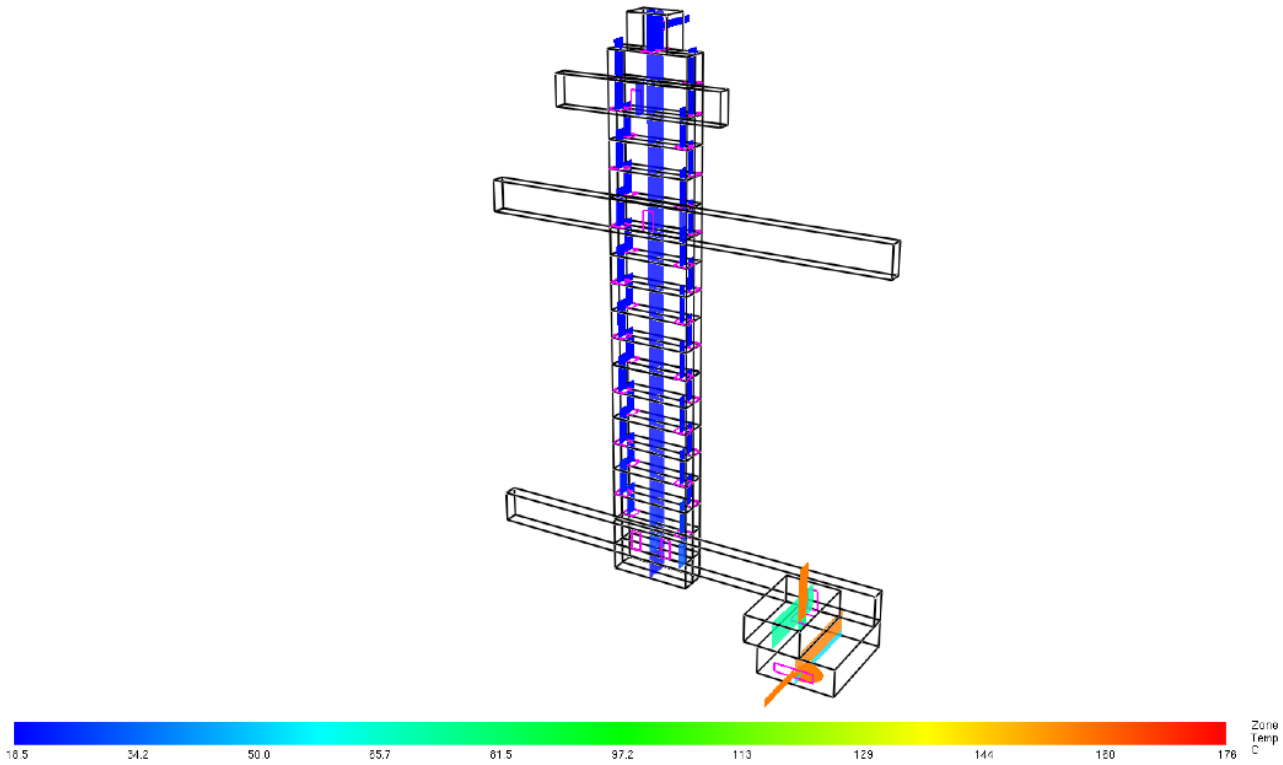

Figure 30: Temperature of Upper/Lower Layer at 240 seconds

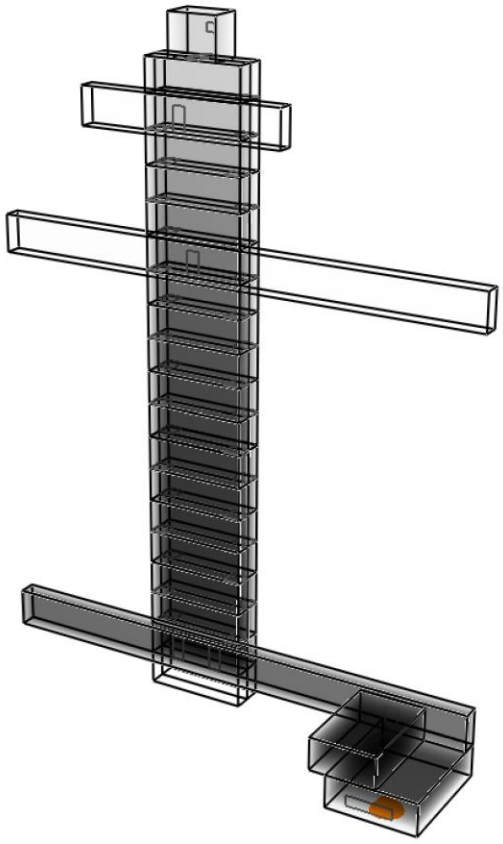

Figure 31: Smokeview of Upper/Lower Layer at 240 seconds

Using Smokeview, we observed the smoke development and flow, as seen in Figure 30, throughout the compartments and flowing out of the penthouse. Each of these times varied for the different door angles. As seen in the above table, the CFAST smoke travel time stamp varied with each door angle. This was determined by when the smoke accumulated in the penthouse. Once the penthouse was a gray color but not black. At this point of smoke obscuration, the time stamp was recorded on the table. Additionally, as mentioned above in our fire tests the doors changed the angle and position whereas the cross sectional was reduced in CFAST.

8. Conclusion

Analysis concluded that at a reduced-scale, CFAST approximated the general trends of the fire test data with reasonable agreement for temperatures but demonstrated a wider range of variability for smoke movement, velocities, and pressure.

Temperature trends observed in CFAST simulations and lab tests generally agreed but demonstrated distinguishable differences in magnitude between tests. The main discrepancy that may have resulted in the over approximation of temperature in CFAST compared to the lab tests was leakage. While leakage was accounted for in the CFAST models, it may have not been enough compared to what was experienced in our lab tests. Unfortunately, we did not use any methods to determine the leakage in our lab tests therefore this could not be quantified. There were many other simplifying assumptions made to the CFAST model that may have affected the results. Another difference between CFAST and lab tests is how temperature and other values are recorded. In CFAST, the temperature output value is the average temperature in the gas layer, whereas our measurements in lab tests are at specific points using thermocouples.

Values for velocity and mass flow rate were successfully calculated from the raw pressure differential measurements of the bi-directional probes. However, because the bi-directional probes were not positioned directly in the cross-sectional areas of the doorways the data could not be directly compared with CFAST. While there was a clear difference in the results between door configurations, it was difficult to determine clear trends from the velocity data and compare it to CFAST for all of our trials. Of those measurements that were able to be made within doors or windows, the most significant was that at the penthouse window where the test and computer simulation had a percent difference of 102% for Test 1, 110% for Test 2, and 124% for Test 3. It should also be noted that the flows observed throughout the lab tests were very low, which resulted in greater uncertainties within the bi-directional probe's accuracy. This was evident in the fluctuations of the graphs for the lab tests and was the source of difficulty when trying to determine trends. Additionally, we did not record velocity and mass flow rate in our lab tests using the same methods that CFAST does. We calculated velocity and mass flow by using the pressure differentials recorded by the bi-directional probes. In CFAST, values for mass flow rate are only available at vents which significantly limits the flexibility and freedom of these measurements. Velocity through a vent in CFAST must also be manually calculated from the calculated values of mass flow rate.

We also compared the timing for the smoke to reach the penthouse to see the impact of the door positions on smoke spread. Our results indicated that as the doors closed, it took longer for the smoke to reach the penthouse. The time for smoke to spread to the penthouse varied between CFAST and our lab tests with the changing of door positions. The calculated and measured times had a percent difference of 43% for Test 1, 27% for Test 2, and 7% for Test 3. Both CFAST and our fire Test 3 yielded results that most closely compared the smoke spread scaled timing for the Bronx Event. The discrepancies within these times may be a result of the different methodologies used to record smoke spread. To assess the smoke timing, we reviewed the footage of the camera facing the penthouse and used stopwatches to record time in our trials, both of which could have been subject to human error. Overall, there was a limited amount of quality smoke visualization footage from our lab tests to directly compare with CFAST, which

made determining trends and comparing the two difficult. The lab was dark, the camera footage wasn't as clear as we had anticipated, and there may have been smoke exhausting from the penthouse not visible to us at the base of the model. In CFAST, we reviewed the Smokeview simulations and used markers to determine when the smoke reached the penthouse.

Our experiments were successful in generating a signification amount of smoke and seeing smoke layers develop in the upper layers of the Lower and Upper Compartment. However, the temperature of the smoke decreased as it progressed through the structure which eventually reached ambient temperature around the 15th floor. This caused the flow of smoke to be convectively forced instead of buoyancy driven and resulted in the distribution of smoke within the upper portions of our building. Where the temperature of the smoke was ambient it appeared as a dark fog as opposed to developing in the upper layer as is typical in compartment fires. This demonstrated that in the upper floors of a high-rise it is not temperature that is the biggest threat, but the harmful chemicals within smoke and the other gaseous byproducts of fire.

The door positions in the fire tests and CFAST simulations influenced the results. A difference in temperature rise can be seen between each test for both CFAST and fire tests, although in CFAST it was less prominent. As the doors closed, the delay of smoke exhausting from the penthouse window increased in the experimental trials. This influence of the doors closing also resulted in higher temperatures near the immediate fire area (lower level of apartment 3N), and slightly slower velocities throughout the building. The rest of the building generally experienced lower temperatures as the doors closed, due to the reduction in gas flows. In the upper level of the third-floor apartment, the highest temperatures were recorded within Test 1, which correlates with CFAST, however, we struggled to interpret the data gathered, and further investigation is suggested to gain a better understanding of the results. In CFAST, the temperature results between door positions also correlate with the results of our lab experiments.

9. Recommendations For Future Testing

The recommendations below include strategies for improving future laboratory work, additional research that could be done to expand this study, and improved correlation with computer modeling output.

Refined Testing Strategies

In the future, to conduct these experiments with increased accuracy and frequency for data collection we recommend constructing the test apparatus with a transparent, detachable backing to allow for easy viewing of the insides of the compartments and smoke spread. This would also allow for physical access to the compartments to be cleaned and ensure repeatability within each test. To reduce the leakage within the test apparatus, we suggest the application of fire caulking, silicon, and foil tape. We were able to use these methods to prevent excessive smoke leakage and fire spread, and they were also used to secure instrumentation. Additionally, once construction is complete, we recommend the use of a calibrated fan to determine the mass flow input at one end and the output at another. This would be beneficial to adequately assess the leakage throughout the building so leakage can be properly modeled within the computational model. These methods are best utilized for better observation and measurement of smoke movement throughout a testing apparatus.

To better evaluate velocity, we recommend using different devices than bi-directional probes to measure velocity at lower magnitudes and that may be easier to work with, such as flowmeters. We did not have access or available funding to use devices other than the bi-directional probes. Alternatively, positioning the bi-directional probes directly in the cross-sectional area of any vents or doorways, parallel to the flow. Position and orientation are essential when comparing these values to those in CFAST, since it only collects gas flow data through the vents along a plane and averages the respective values across the entire plane. Additionally, we recommend placing more thermocouples across the ceilings of relevant compartments, since the upper layer temperature output from CFAST is an average of the calculated upper layer temperatures. When using other computational models, it is imperative to understand how the program calculates to ensure replicability in a physical fire test.

For smoke visualization, we recommend making objects with marked measurements to place in relevant compartments to quantify the development of a smoke layer that can easily be replaced. Further research into lighting techniques may also be beneficial, as our lights had trouble showing the smoke and became discolored after repetitive testing. Additionally, using cameras placed inside the compartments that can be controlled by a remote and synchronize with other cameras would allow video recordings to all start at the same time stamp. We spent approximately five minutes before tests starting each camera individually, and then had to edit each recording and trim the videos to all start at the same time in order to cross-compare them with each other.

Methods to Better Correlate CFAST Experiments with Fire Tests

We are proposing methods to better ensure the experiments in the computational model and the lab can be compared. Before the lab tests are constructed, it would be beneficial to first create the CFAST model and run a simulation to determine potential fire behavior and design limitations.

We also recommend utilizing measurement inputs which can be directly replicated in the laboratory. To improve CFAST tests, the simulations should be run with different zone types defined in the compartment geometry. This is better to gauge the sensitivity of different zone configurations and effects it has on the calculations to better align with the fire tests. CFAST can better expand its computational analysis by adding a stair geometry option during the compartment input phase of modeling, but this is not possible within the context of a two-zone model.

Future Testing Possibilities

In the future, we hope this study can lead to further developments in reduced-scale high-rise fire tests. Some ideas for future work include the variation of the heat release rates, alternative burner techniques, different and more accurate instrumentation, a variation of the scale and a wider arrangement of door configurations. Additionally, it may be beneficial to expand the scope of this research to include other computational models, such as FDS. Ideally, future testing will also include scaling of more than just the heat release rate. These ideas can lead to feasible and reliable alternatives to full-scale tests and may also lead to the use of reduced-scale fire tests to validate computational fire models.

Bibliography

Cote, A. E., Grant, C. C., Hall, J. R., Solomon, R. E., & Powell, P. A. (2008). *Fire Protection Handbook.* National Fire Protection Association.

Gill, W., Donaldson, A. B., Hogan, B., Bocanegra, H., & Yilmaz, N. (2009, April 1). Examination of the bidirectional velocity probe used in flames. *Examination Of The Bidirectional Velocity Probe Used In Flames*. (Conference) | OSTI.GOV. Retrieved April 20, 2023, from https://www.osti.gov/servlets/purl/1142602

Hurley et al. (Eds.). (2016). *SFPE Handbook of Fire Protection Engineering*. Springer. https://doi.org/10.1007/978-1-4939-2565-0

Peacock, R. D., Reneke, P. A., and Forney, G. P. (2015). *CFAST – Consolidated Fire And Smoke Transport (Version 7) Volume 3: Verification and Validation Guide* (NIST TN 1889v3; p. NIST TN 1889v2). National Institute of Standards and Technology. https://doi.org/10.6028/NIST.TN.1889v2

Peacock, R. D., Reneke, P. A., and Forney, G. P. (2015). CFAST – *Consolidated Model of Fire Growth and Smoke Transport* (Version 7) Volume 2: User's Guide (NIST TN 1889v2; p. NIST TN 1889v2). National Institute of Standards and Technology. https://doi.org/10.6028/NIST.TN.1889v2

Singhvi, A., Glanz, J., Cai, W., Grothjan, E., & Gröndahl, M. (2022, July 8). *The Chain of Failures That Left 17 Dead in a Bronx Apartment Fire*. The New York Times. https://www.nytimes.com/interactive/2022/07/08/nyregion/bronx-fire-nyc.html

Speckert, C. (n.d.). *The Second Egress:Building a Code Change*. The Second Egress: Building a Code Change. Retrieved April 26, 2023, from https://secondegress.ca/Scissor-v-Single

Thermocouple Guide: *Everything You Need To Know*. (n.d.). Https://www.Omega.Com/En-Us/. Retrieved April 19, 2023, from https://www.omega.com/en-us/resources/thermocouple-hub

Appendix A: Smoke Generation Techniques

	Smoke Source	Pros	Cons	Design Considerations
Fire-Based Smoke	**Pool Fire** -Diesel -Plastic Beads -Pellets	-Able to be on a small scale -Creates real smoke -Visualization with sooty smoke	-Might not create enough smoke due to limited fuel -Cannot control the heat release rate	-Open flame, involves wrapping in foil which introduces re-radiation -May need to pump in diesel continuously)
	Crib Fire	-Scaling research available -Visualization with sooty smoke	-Too large for compartment	-Open flame, involves wrapping in foil which introduces re-radiation
	Pipe Burner -Methane (cleaner) -Propane (cleaner) -Toluene (denser) - Propylene (denser)	- Able to control fire size/height - Able to control smoke production - Propylene and Toluene have sootier smoke from burns	- Methane and Propane may burn clean; smoke production needs to be added	-Smaller open flame, need to measure smoke mass to mass of fuel used -Open floor burner underneath -Burner can extend through pipe along room wall, with holes drilled for flows -May need to injected dyes for visualization
Artificial Smoke	**Theatrical Smoke and Fog Machines** (Helium and Air)	-Buoyancy can be mimicked -Visualization -Cold smoke doesn't risk structure of compartment	- May be difficult to scale - Temperatures will present differently than that of fire-based smoke - Less buoyant, low-lying fog	- More difficult to compare with CFAST
	Smoke Machine (Glycol and Water Mixture)	- Able to control smoke production volume - May be able to be on a small scale -Visualization of smoke - No structural risk because there isn't a flame - More buoyant than fog machines	-Temperatures will present differently than that of fire-based smoke - Less buoyant than fire-based smoke	- More difficult to compare with CFAST
	Salt Water	-Visualization with dyes	- May be difficult to inject dyes	- More difficult to compare with CFAST

Appendix B: Calculations

Appendix B.1 Flow Calculations

In the laboratory experiments propylene was used which has the heat of combustion of 48,895 kJ/kg (Hurley et al., 2016). Utilizing the mass flow rate from Equation 1 which represents the relationship between the heat release rate and the heat of combustion we can determine the expected flow rate:

$$\dot{m}_{propylene} = \frac{2.33\ kW}{48{,}895\ kJ/kg} = 4.8 \text{ x } 10^{-5} \text{ kg/s}$$

The mass flow rate would have to be around 0.000048 kg/s to achieve the desired heat release rate. This calculation was a preliminary to the actual flow needed through the mass rotameter. The calculations for the actual flow through the mass rotameter can be seen in Appendix L.

Appendix B.2 Scaling Calculations

Heat Release Rate Scaling
The full-scale high-rise fire was modeled at 1MW. The fire power is set after several trial cases to produce enough smoke to match with the events in the real scenario. According to the SFPE Handbook, numerous tests were conducted on mattresses with a bench-scale heat release rate and generally led to room fires on the order of 1 MW.

To determine the scaled heat release rate for the model:

1 MW Bronx Apartment Fire:

$l_1 = 8\ ft.\ (2.4384\ m),\ l_2 = 8\ in.\ (0.2032\ m),\ Q_1 = 1\ MW\ (1000kW)$

$$\frac{Q_1}{\rho_\infty c_p T\sqrt{g}l^{5/2}} = \frac{Q_2}{\rho_\infty c_p T\sqrt{g}l^{5/2}} \Rightarrow \frac{1000}{Q_2} = \left(\frac{2.4384m}{0.2032m}\right)^{5/2},\ Q_2 = 2.33 \text{ kW}$$

Time Scaling
According to the detailed publication in the New York Times, the fire event was able to be modeled from retracing the 911 calls to determine where and at which time smoke was observed from tenants. Calls were made from more than 40 of the 120 apartments. The fire alarms went on at 10.35 am. 10 minutes before the first 911 call at 10:54 am that reported seeing smoke on the 3rd floor, and 11:37am when the last call came in, for a total burn time of 53 minutes. Within 20 minutes of the start of the fire, smoke shot up the stairwells, entering hallways on higher floors. Within 10 minutes of the first 911 call, smoke was already reported on the 16th floor.

To determine the time for smoke to reach the top of the building in the 1:12 scaled enclosure, the initial assumption is that in the actual fire event it took approximately 20 minutes, based on 911 calls.

$l_1 = 8\ ft\ or\ 2.4384\ m,\ l_2 = 8\ inch\ or\ .2032\ m,\ g = constant,\ \ t_1 = 1200\ seconds$

$$\frac{1200}{\sqrt{2.4384/g}} = \frac{t}{\sqrt{.2032/g}}$$

$$t = \frac{1200}{\sqrt{2.4384}} * \sqrt{.2032}$$

$t = 336.12\ s\ (5.6\ min)$

To determine the duration of the whole fire event, the assumption is that the fire was controlled within an hour, so t_1 would be 3600s.

$$\frac{3600}{\sqrt{2.4384/g}} = \frac{t}{\sqrt{0.2032/g}}$$

$$t = \frac{3600}{\sqrt{2.4384}} * \sqrt{0.2032}$$

$t = 1{,}039s\ (17.3\ min)$

This means that with the fire modeled on a 1:12 scale from the actual fire event, the duration of the experiment would be approximately 17 minutes long. This would account for the initial fire growth period, the flashover within the compartment, and then the firefighters eventually reaching the building and the fire decay period.

Appendix B.3 Door Percentage Calculation for CFAST Correlations

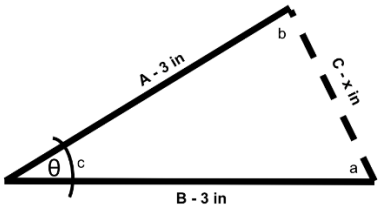

The door percentage input into CFAST was calculated at each different degree opening by taking the ratio of C to B. We used the law of sines to calculate the third side (C).

Appendix B.4 Bidirectional Pressure to Velocity Calculations

$$\varepsilon = -\frac{64}{\pi}\frac{L}{D^4}\frac{\eta_{air}}{\rho_{air}}\frac{m_c}{\Delta p_{sensor}}\left(\sqrt{1+\frac{8\Delta p_{sensor}}{\Delta p_c}}-1\right)$$

$$\eta_{air} = \left(18.205 + 0.0484 \times \left(T[°\mathrm{C}] - 20\right)\right) \times 10^{-6}\,\frac{\mathrm{Pa}}{\mathrm{s}}$$

$$\rho_{air} = \left(1.1885 \times p_{abs}[\mathrm{bar}]\right) \times \frac{293.15}{\left(273.15 + T[°\mathrm{C}]\right)}\,\frac{\mathrm{kg}}{\mathrm{m}^3}$$

$$m_c = 6.17 \times 10^{-7}\,\frac{\mathrm{kg}}{\mathrm{s}}$$

$$\Delta p_c = 62\mathrm{Pa}$$

L = length of hose (sum of hose length to and from sensor) in meter [m]

D = diameter of the tube in meter [m]

η_{air} = viscosity of air at temperature T in Celsius [°C]

ρ_{air} = density of air at temperature T in [°C]

Δp_{sensor} = dp reading of sensor in Pascal [Pa]

p_{abs} = absolute air pressure in hose in bar

m_c, Δp_c = massflow and dp sensor constants where the linear and quadratic contribution to the dp vs. flow relationship of the SDP800 sensor are equal

Appendix C: Materials List

Item	Quantity
2x4x8's Wood	2
Polycarbonate Sheets (12"x24"x3/32")	4
Standard-Wall Steel Pipe Nipple	4
304 Stainless Steel Threaded Pipe Fitting	2
1008-1010 Carbon Steel Shim Stock	1
Nashua Tape	1
CNS Lumber (19/32 in. x 4 ft. x 8ft.)	12
2" star head screws 1 lb.	1
Propane Hose	1
½” Pipe Cap	4
Flare Fitting	1
Fire Caulk	3
Silicone Caulk	2
Various Fittings	-
Propylene (59LB)	1
Closet Lights x 6	1
2x4 12 ft	8
12ft Strip Lights	1

Appendix D: Model Dimensions & Drawing Sheets

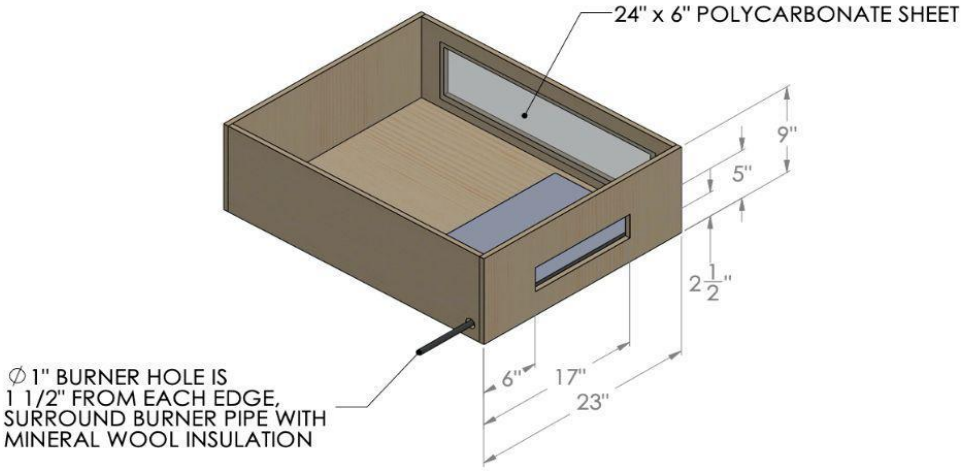

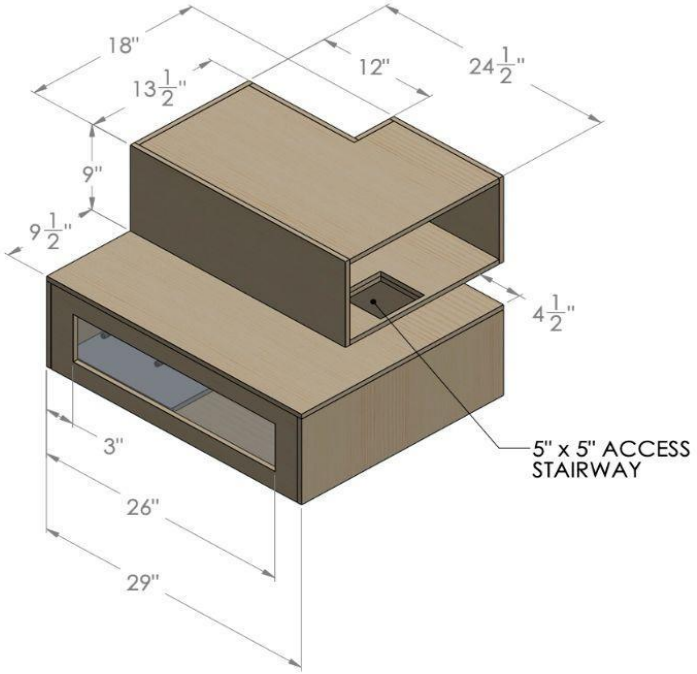

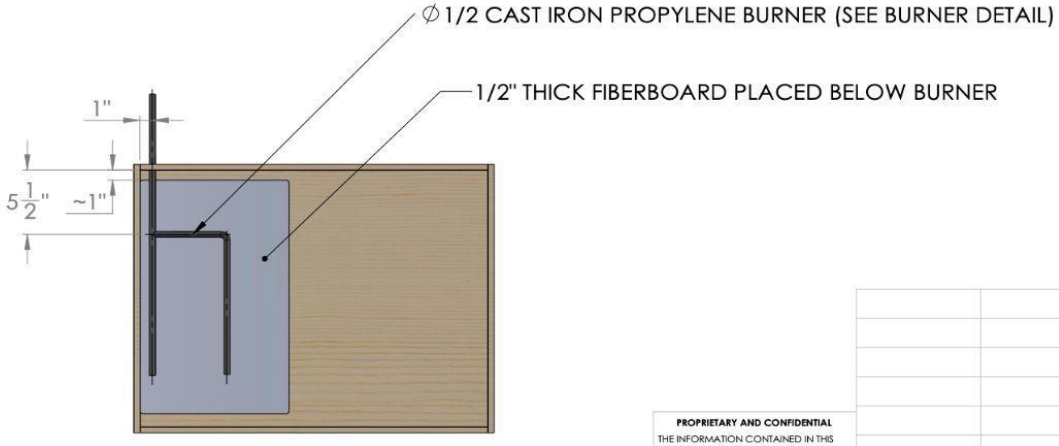

GENERAL NOTE: ALL PLYWOOD IS 1/2" THICK

		UNLESS OTHERWISE SPECIFIED:		NAME	DATE
		DIMENSIONS ARE IN INCHES TOLERANCES: FRACTIONAL ± ANGULAR: MACH ± BEND ± TWO PLACE DECIMAL ± THREE PLACE DECIMAL ±	DRAWN	PMG	2/8/23
			CHECKED		
			ENG APPR.		
			MFG APPR.		
		INTERPRET GEOMETRIC TOLERANCING PER:	Q.A.		
		MATERIAL	COMMENTS:		
		FINISH			
NEXT ASSY	USED ON				
APPLICATION		DO NOT SCALE DRAWING			

TITLE: APARTMENT 3N

SIZE	DWG. NO.	REV
B	3N-01	
SCALE: 1:10	WEIGHT:	SHEET 1 OF 1

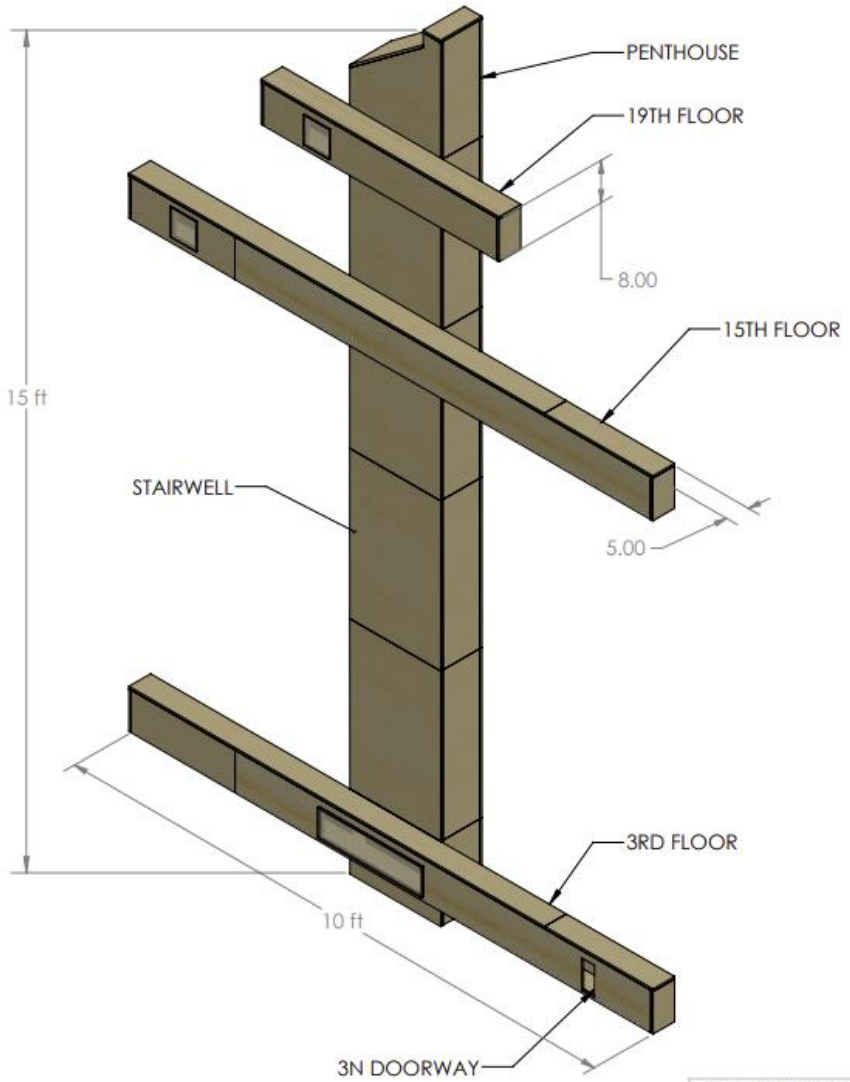

		UNLESS OTHERWISE SPECIFIED:		NAME	DATE
		DIMENSIONS ARE IN INCHES TOLERANCES: FRACTIONAL ± ANGULAR: MACH ± BEND ± TWO PLACE DECIMAL ± THREE PLACE DECIMAL ±	DRAWN		
			CHECKED		
			ENG APPR.		
			MFG APPR.		
		INTERPRET GEOMETRIC TOLERANCING PER:	Q.A.		
		MATERIAL	COMMENTS:		
NEXT ASSY	USED ON	FINISH			
APPLICATION		DO NOT SCALE DRAWING			

TITLE:
SCALE MODEL STAIRS AND HALLWAYS

SIZE	DWG. NO.	REV
B	02	
NTS	WEIGHT:	SHEET 1 OF 1

Appendix E: Instrumentation Layout

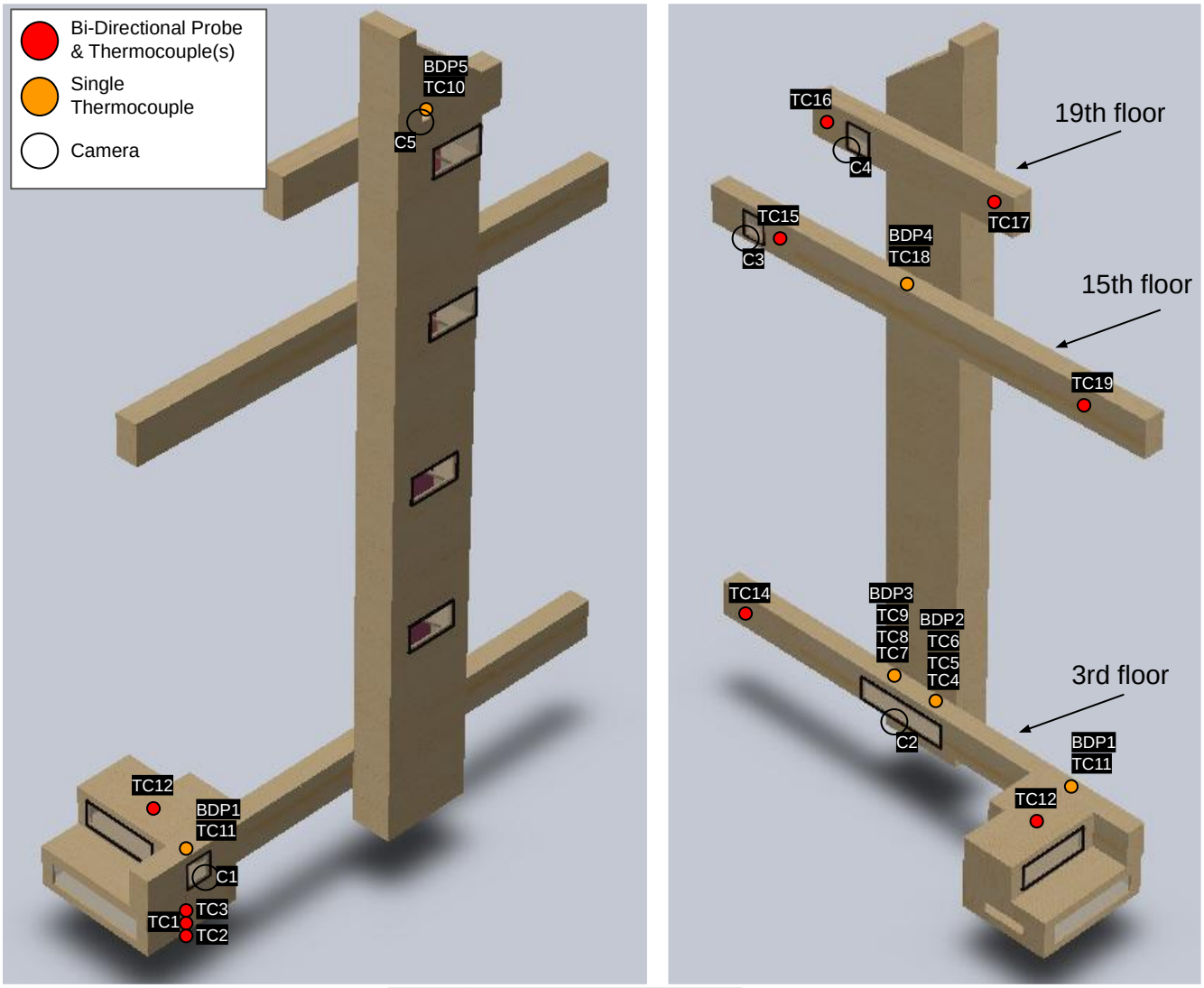

TC	Thermocouple
BDP	Bi-directional Probe
C	Camera

Appendix F: Instrumentation Identification

Figure name	Label	Port	Device	General Area	Relative Location	Additional Information
BDP1	1	RasPI lower - 1	Bi-Directional Probe	Third Floor Hallway, Doorway 3N	Centered in Doorway, at 4" Height	Length of Hose = 48inch
BDP2	2	RasPI lower - 2	Bi-Directional Probe	Third Floor Hallway, Stair Doorway A (farthest)	Centered in Doorway, at 4" Height	Length of Hose = 105 inch
BDP 3	3	RasPI lower - 3	Bi-Directional Probe	Third Floor Hallway, Stair Doorway B (closest)	Centered in Doorway, at 4" Height	Length of Hose = 98inch
BDP4	4	RasPI upper - 1	Bi-Directional Probe	15th Floor Hallway, Stair Doorway B	Centered in Doorway, at 4" Height	Length of Hose = 98 inch
BDP5	5	RasPI upper - 2	Bi-Directional Probe	Roof Penthouse, Window	Centered in Window, at	Length of Hose = 81inch
TC1	0-1	DAQ - A0	Thermocouple	Lower Compartment, Middle Layer	11" Along Wall Opposite Burner, at 0.75" Offset (4.5" Height)	
TC2	0-2	DAQ - A1	Thermocouple	Lower Compartment, Lower Layer	11" Along Wall Opposite Burner, at 0.75" Offset (1" Height)	
TC3	0-3	DAQ - A2	Thermocouple	Lower Compartment, Upper Layer	11" Along Wall Opposite Burner, at 0.75" Offset (8" Height)	
TC4	0-4	DAQ - A3	Thermocouple	Third Floor Hallway, Stair B Lower Layer		
TC5	0-5	DAQ - A4	Thermocouple	Third Floor Hallway, Stair B Middle Layer		
TC6	I-1	DAQ - A10	Thermocouple	Third Floor Hallway, Stair B Upper Layer	Was 0-6 but on the snake doesn't work	
TC7	0-7	DAQ - A6	Thermocouple	Third Floor Hallway, Stair A Lower Layer	Centered in Doorway, at 4" Height	
TC8	0-8	DAQ - A7	Thermocouple	Third Floor Hallway, Stair A Middle Layer	Centered in Doorway, at 4" Height	
TC9	0-10	DAQ - A9	Thermocouple	Third Floor Hallway, Stair A Upper Layer	Centered in Doorway, at 4" Height	
TC10	I-2	DAQ - A11	Thermocouple	Roof penthouse window)	Centered in Doorway, at 4" Height	
TC11	I-3	DAQ - A12	Thermocouple	3N Hallway with Probe		
TC12	I-4	DAQ - A13	Thermocouple	Upper Compartment Upper Layer		
TC13	pipe thermocoup	DAQ - A14	Pipe Thermocouple	In the burner pipe	-	
TC14	F-1	DAQ2 - A0	Thermocouple	3 hallway furthest away		
TC15	F-6	DAQ2 - A6	Thermocouple	15th hallway furthest away		
TC16	F-3	DAQ2 - A2	Thermocouple	Pent far		
TC17	F-4	DAQ2 - A3	Thermocouple	Penthouse close	checked	
TC18	F-5	DAQ2 - A4	Thermocouple	15th floor hallway BDP		
TC19	f-8	DAQ2 - A5	Thermocouple	15th floor closest (.1)		
	N/A	N/A	Smoke Detector	Upper Compartment, Floor	Centered on Floor	
	Cam1	N/A	Camera	Upper Compartment	On Ceiling Outside of Upper Compartment Window	
	Cam2	N/A	Camera	3rd Floor Hallway	On Perch Outside of 3rd Floor Window Facing Door A to Shaft	
	Cam3	N/A	Camera	3rd Floor Hallway	On Perch Outside of 3rd Floor Window Facing Door B to Shaft	
	Cam4	N/A	Camera	15th Floor Hallway	On Perch Outside of 15th Floor Window Facing Door to Shaft	
	Cam5	N/A	Camera	19th Floor Hallway	On Perch Outside of 15th Floor Window Facing Door to Shaft	

Appendix G: Test Procedure

Start of Trial		
Person 2	Verbalize “Start of Trial X”.	
Person 1/4	Turn off all lab lights.	
Person 3	Open the propylene bottle.	
Person 3	Gradually increase the rotameter, checking with Person 1 until ignition. Once the rotameter is flowing gas, yell “propylene”.	
Person 1	Hold the ignited lighter over the burner and ask for propylene. Once the burner has ignited yell “ignition” and remove the lighter.	
Person 2	Record ignition time (lap 9).	
Person 3	Increase the rotameter slowly until the ball reaches the 28 mark. Once the rotameter is at 28 yell “full flow”.	
Person 2	Record time of full flow (lap 10).	
Person 2	Record time when smoke first spews from penthouse (lap 11).	
Person 2	Record activation time of smoke detector (lap 12).	
Person 1	Close propylene bottle 6 minutes after ignition. Verbalize “End of Trial X”.	
Person 2	Stop the stopwatch and record the final time.	
End of Trial		
Person 1/4	Stop GoPros.	
Person 3/4	Turn off LED lights.	
Person 1	Close rotameter (cw = closed).	
ALL	Wait 30 minutes for the structure to vent.	
ALL	Clean 3N compartment and windows.	

Appendix H: Thermocouple Code

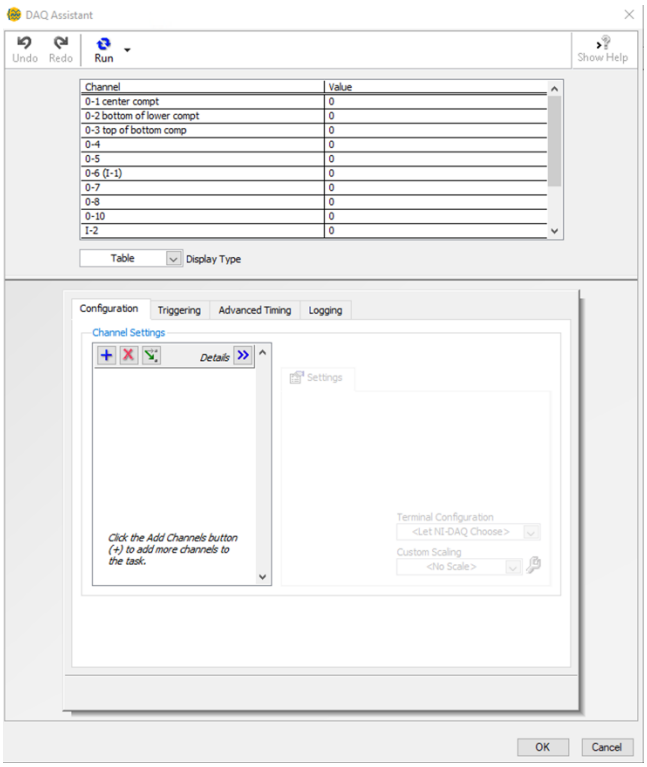

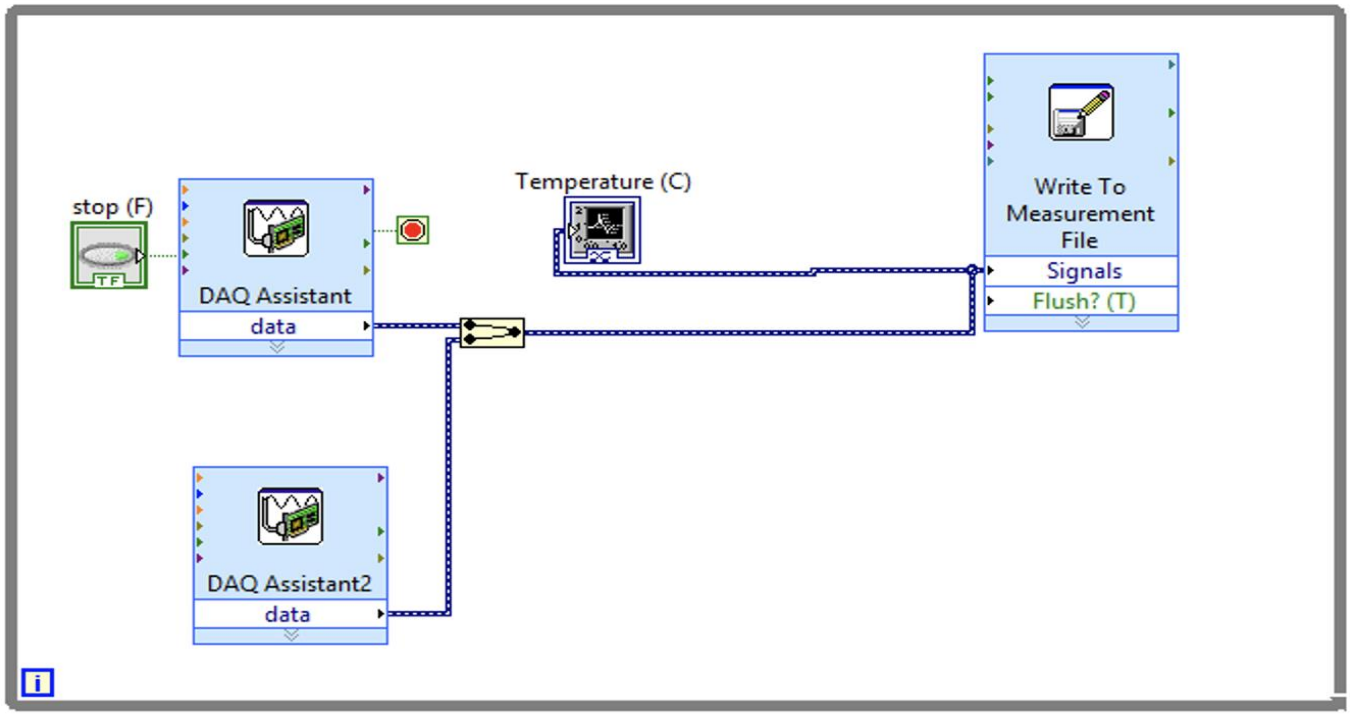

Appendix I: Python & MATLAB Code for Bi-directionial Probe Fire Tests

```
import time
import math
import numpy as np
from Sen_test import SDP8x
from TCA_class import I2C_SW
from datetime import datetime
from time import sleep

# create an empty list of SDP8x devices
test_sensor=[]

# create an instance of the multiplexer class (I2C at address 0x70)
SW=I2C_SW(0X70, 1)
# pause briefly (may not be necessary)
# time.sleep(.1)Closed_PL1_15cm_45Hz

datafile = open("test9000.txt","w")
#when writing to a txt file there is no seperation of which
m = 0
n = 1 #number of sensors
x = 1
f = 2 #Hz
t = 1/f

# the steps below will initialize each device, by toggling relevant multiplexer channel
for i in range(m,n):
    # toggle channel
    SW.chn(i)
    # initialize sensor on that channel
    tmp=SDP8x()
    # append sensor to the list of all sensors
    test_sensor.append(tmp)

# this loop will then display readings for each sensor
#print('Location 61cm away from bed',file=datafile)
j = 0
d = []

while 1:
    time.sleep(1)
    dt = datetime.now()
    d += [dt.strftime("%M")]
    d += [dt.strftime("%S")]
    d += [dt.strftime("%f")]

    for i in range(m,n):
```

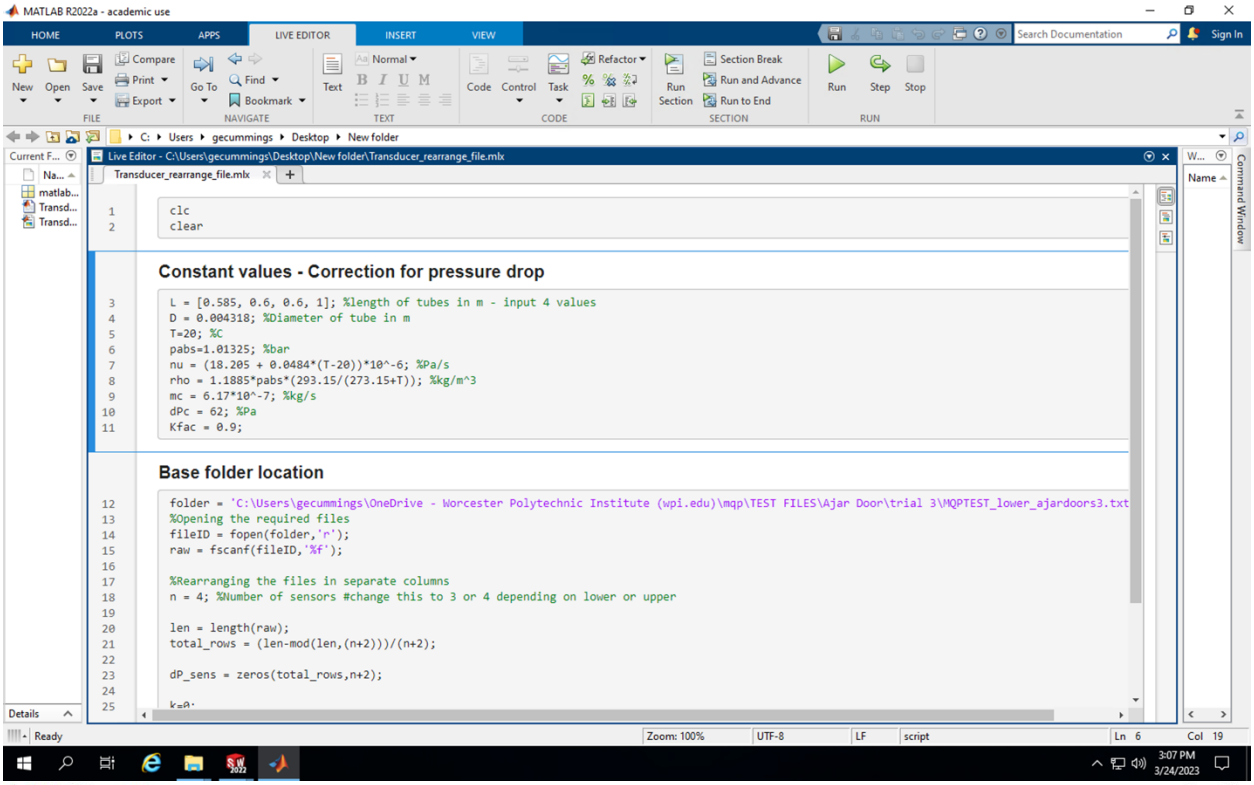
MATLAB R2022a - academic use
Live Editor - C:\Users\gecummings\Desktop\New folder\Transducer_rearrange_file.mlx
Transducer_rearrange_file.mlx
clc
clear
Constant values - Correction for pressure drop
L = [0.585, 0.6, 0.6, 1]; %length of tubes in m - input 4 values
D = 0.004318; %Diameter of tube in m
T=20; %C
pabs=1.01325; %bar
nu = (18.205 + 0.0484*(T-20))*10^-6; %Pa/s
rho = 1.1885*pabs*(293.15/(273.15+T)); %kg/m^3
mc = 6.17*10^-7; %kg/s
dPc = 62; %Pa
Kfac = 0.9;
Base folder location
folder = 'C:\Users\gecummings\OneDrive - Worcester Polytechnic Institute (wpi.edu)\mqp\TEST FILES\Ajar Door\trial 3\MQPTEST_lower_ajardoors3.txt
%Opening the required files
fileID = fopen(folder,'r');
raw = fscanf(fileID,'%f');
%Rearranging the files in separate columns
n = 4; %Number of sensors #change this to 3 or 4 depending on lower or upper
len = length(raw);
total_rows = (len-mod(len,(n+2)))/(n+2);
dP_sens = zeros(total_rows,n+2);
Ready
Zoom: 100%
UTF-8
LF
script
Ln 6
Col 19
3:07 PM
3/24/2023

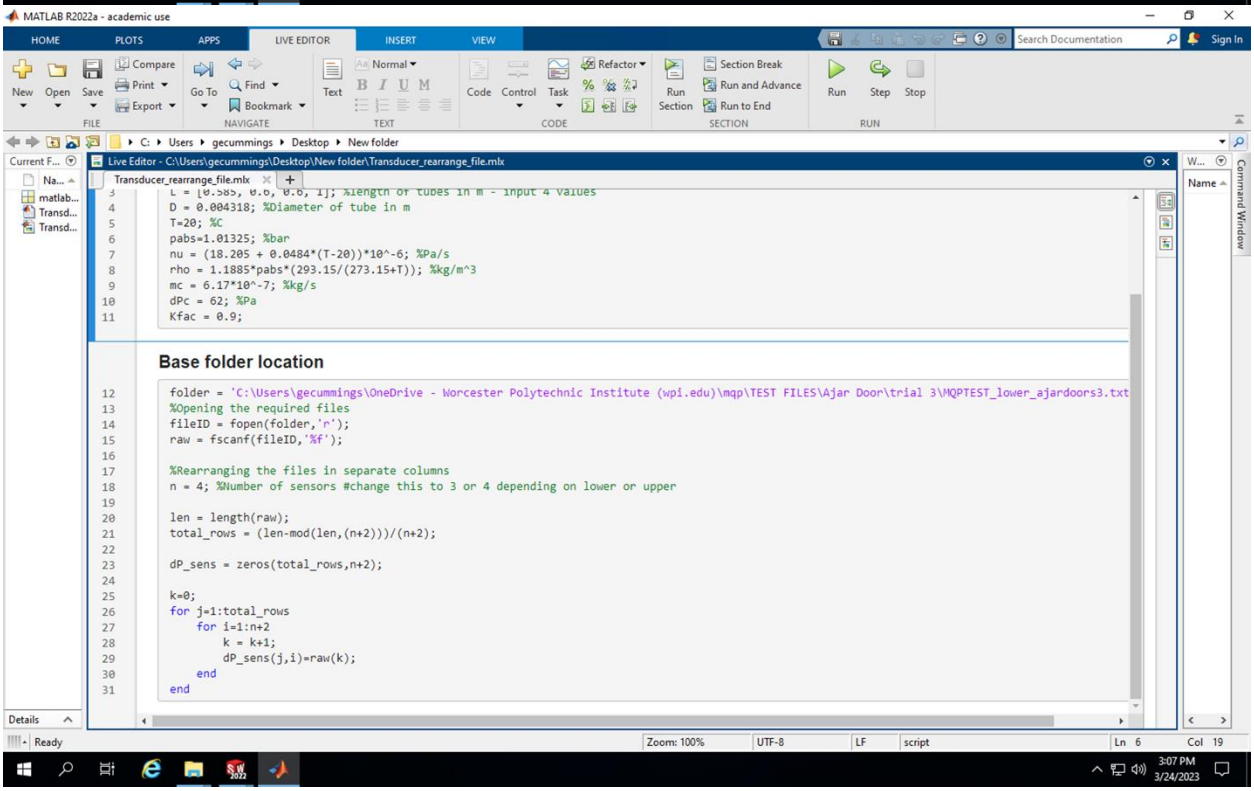
MATLAB R2022a - academic use
Live Editor - C:\Users\gecummings\Desktop\New folder\Transducer_rearrange_file.mlx
Transducer_rearrange_file.mlx
D = 0.004318; %Diameter of tube in m
T=20; %C
pabs=1.01325; %bar
nu = (18.205 + 0.0484*(T-20))*10^-6; %Pa/s
rho = 1.1885*pabs*(293.15/(273.15+T)); %kg/m^3
mc = 6.17*10^-7; %kg/s
dPc = 62; %Pa
Kfac = 0.9;
Base folder location
folder = 'C:\Users\gecummings\OneDrive - Worcester Polytechnic Institute (wpi.edu)\mqp\TEST FILES\Ajar Door\trial 3\MQPTEST_lower_ajardoors3.txt
%Opening the required files
fileID = fopen(folder,'r');
raw = fscanf(fileID,'%f');
%Rearranging the files in separate columns
n = 4; %Number of sensors #change this to 3 or 4 depending on lower or upper
len = length(raw);
total_rows = (len-mod(len,(n+2)))/(n+2);
dP_sens = zeros(total_rows,n+2);
k=0;
for j=1:total_rows
for i=1:n+2
k = k+1;
dP_sens(j,i)=raw(k);
end
end
Ready
Zoom: 100%
UTF-8
LF
script
Ln 6
Col 19
3:07 PM
3/24/2023

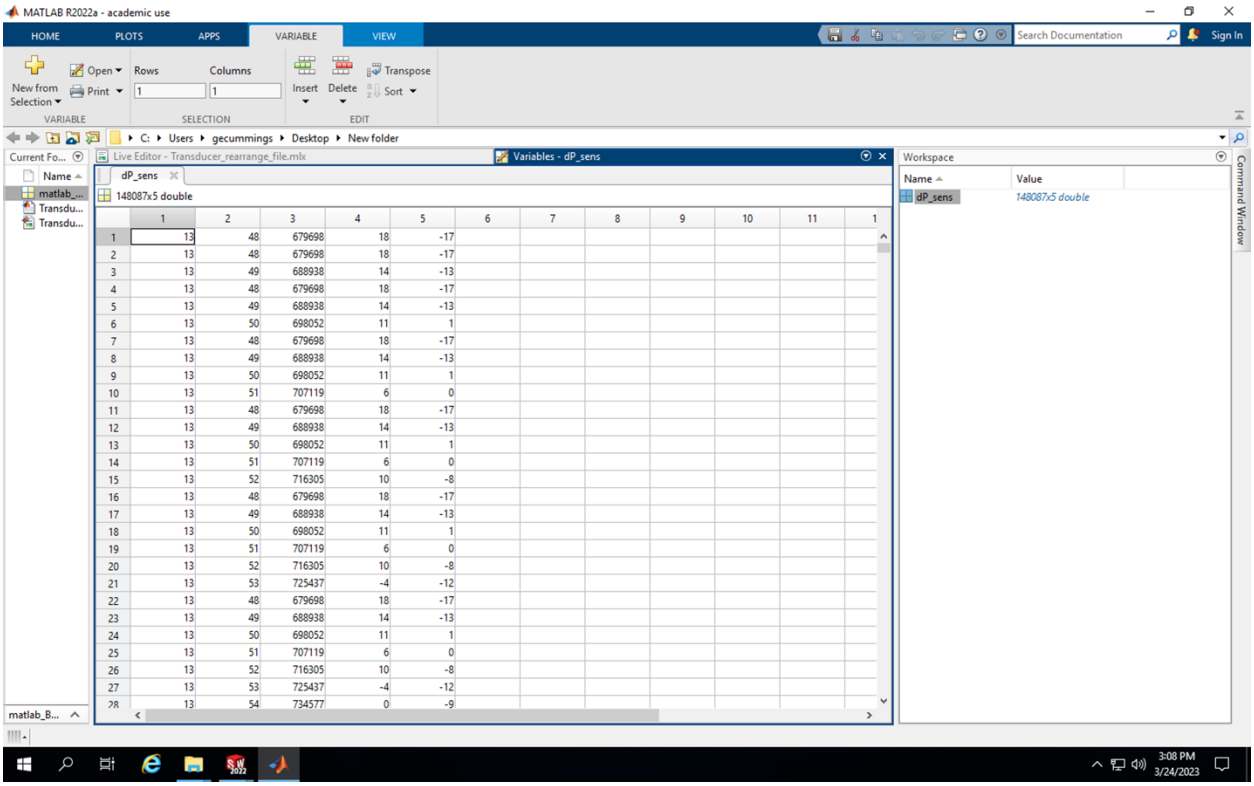

	1	2	3	4	5	6	7	8	9	10	11	1
1	13	48	679698	18	-17							
2	13	48	679698	18	-17							
3	13	49	688938	14	-13							
4	13	48	679698	18	-17							
5	13	49	688938	14	-13							
6	13	50	698052	11	1							
7	13	48	679698	18	-17							
8	13	49	688938	14	-13							
9	13	50	698052	11	1							
10	13	51	707119	6	0							
11	13	48	679698	18	-17							
12	13	49	688938	14	-13							
13	13	50	698052	11	1							
14	13	51	707119	6	0							
15	13	52	716305	10	-8							
16	13	48	679698	18	-17							
17	13	49	688938	14	-13							
18	13	50	698052	11	1							
19	13	51	707119	6	0							
20	13	52	716305	10	-8							
21	13	53	725437	-4	-12							
22	13	48	679698	18	-17							
23	13	49	688938	14	-13							
24	13	50	698052	11	1							
25	13	51	707119	6	0							
26	13	52	716305	10	-8							
27	13	53	725437	-4	-12							
28	13	54	734577	0	-9							

Appendix J: Locational Velocity Graphs and Tables

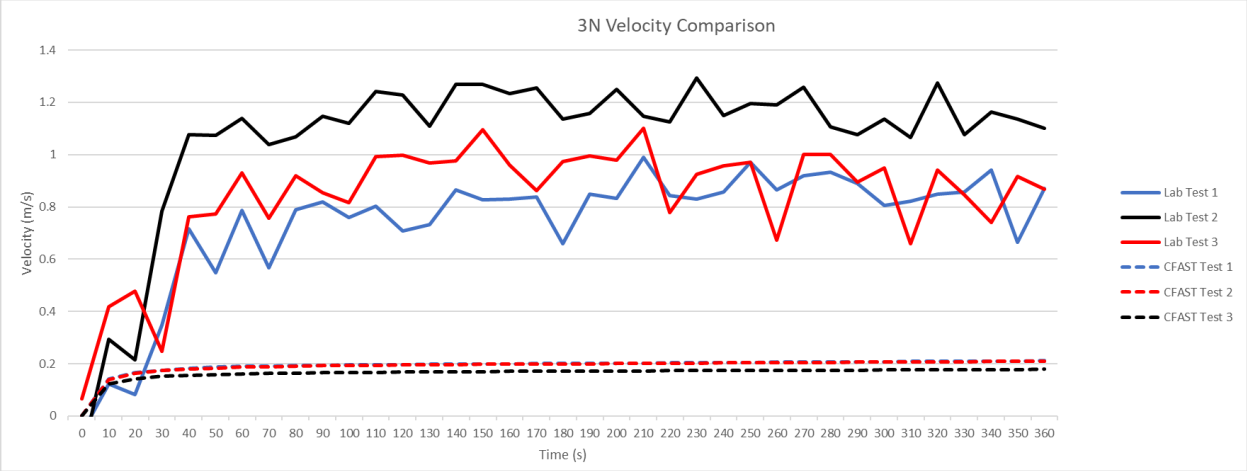

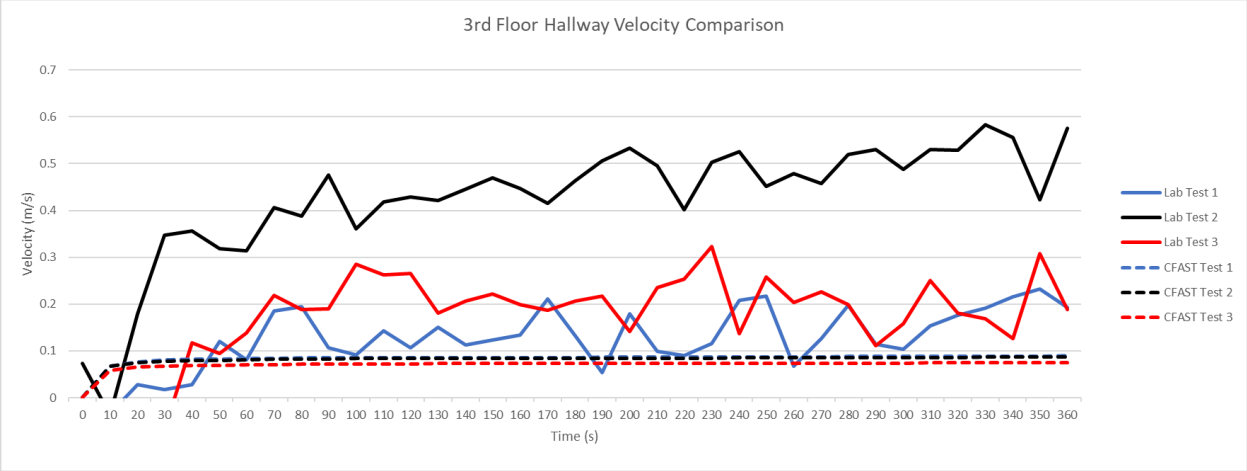

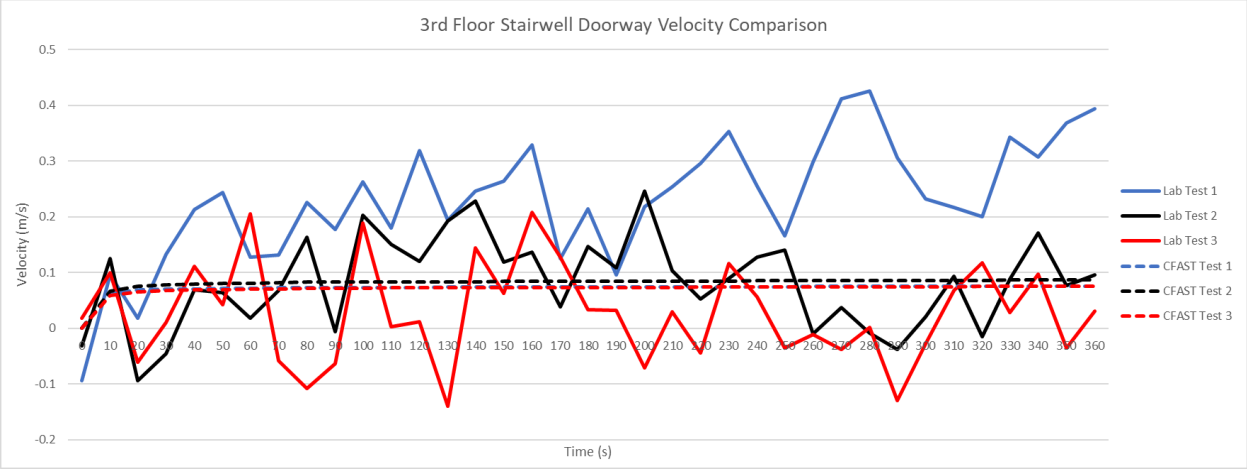

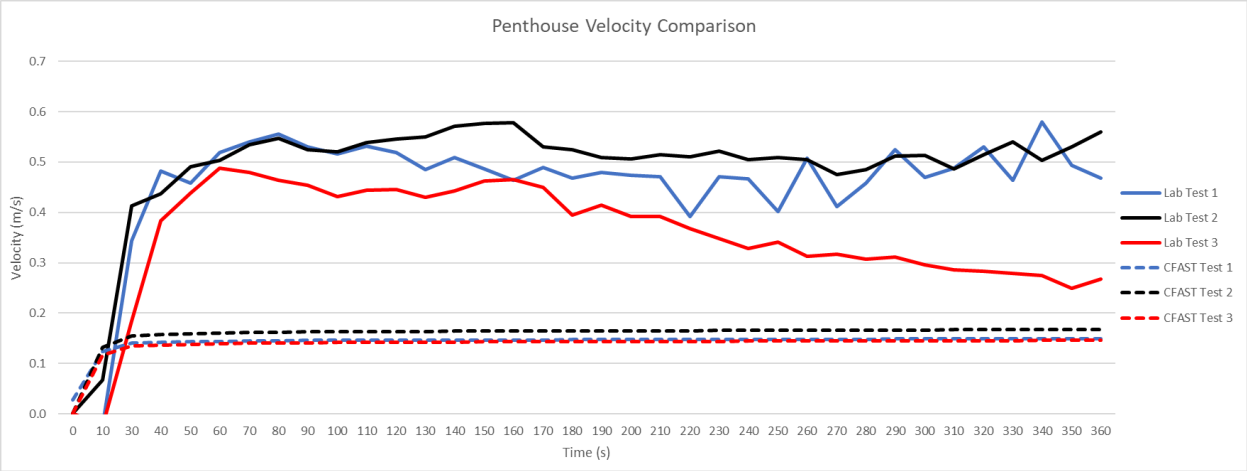

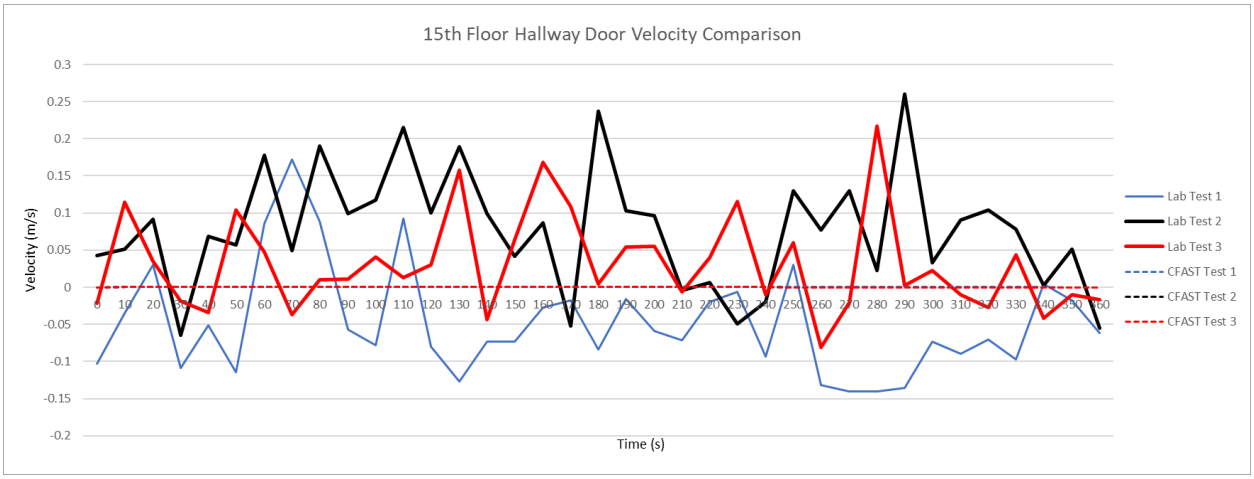

Peak Velocity for Test 1: Fully Open			
Location	Lab Test 1: No Door (m/s)	CFAST Test 1: 100% Open (m/s)	Percent Difference (%)
Apt. 3N Doorway	1.140	0.200	140
3rd Floor Doorway	0.216	0.086	86
15th Floor Doorway	0.071	0.00003	199.8
Penthouse Window	0.508	0.1656	101.6

Peak Velocity for Test 2: Halfway Open Doors			
Location	Lab Test 2: (45 Degrees) (m/s)	CFAST Test 2: 77% Open (m/s)	Percent Difference (%)
Apt. 3N Doorway	1.487	0.1989	152.8
3rd Floor Doorway	0.219	0.0844	88.7
15th Floor Doorway	0.168	0.00003	199.9
Penthouse Window	0.571	0.165	110.3

Peak Velocity for Test 3: Ajar Doors			
Location	Lab Test 3: (20 Degrees) (m/s)	CFAST Test 3: 33% Open (m/s)	Percent Difference (%)
Apt. 3N Doorway	1.241	0.1715	151.4
3rd Floor Doorway	0.033	0.0731	75.6
15th Floor Doorway	0.059	0.00003	199.8
Penthouse Window	0.605	0.143	123.5

Appendix K: Locational Smoke Movement Visuals

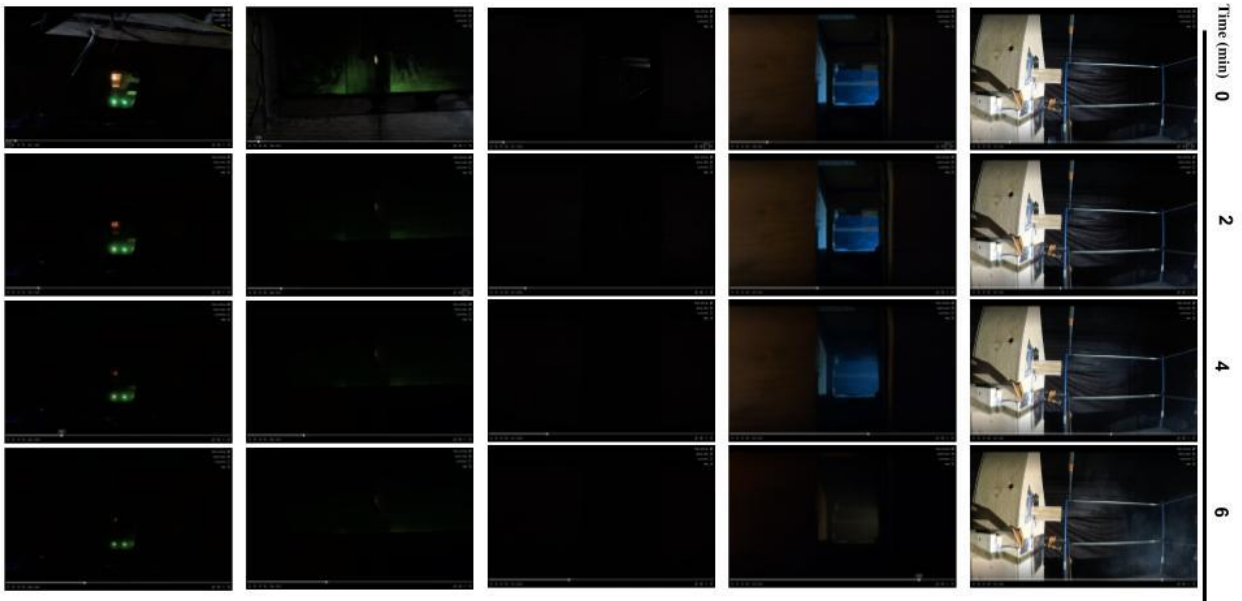

Test 2 - 45° doors

Test 3 - 20° door

Appendix L: Rotameter Calculations & Correlations

Desired HRR (kW)	Correction Factor	
2.33	Gas	0.822
	Temperature	1.009
Expected Flow Rate (L/min)	Pressure	1.066
1.42	Gas Properties	
Rotameter Value	Heat of combustion (kJ/kg)	48895
~29-30	Density (kg/m^3)	1.7855
	Conversion Factors	
	m^3 to L	1000
	s to min	60

Figure 32: Simplified calculations to solve for expected flow rate.

The desired HRR is calculated from Appendix B to scale a 1MW fire to a 1:12 scale. The correction factors are based off measurements that were taken during the experimental fire tests provided in the tables below. The gas correction factor was determined based on our gas we used for the fire in the table below.

HRR = Desired HRR
H_C= Heat of Combustion
CF_L= Conversion factor for cubic meters to liters
CF_m= Conversion factor for seconds to minutes
C_G= Correction Factor of Gas
C_T= Correction Factor of Temperature
C_P= Correction Factor of Pressure
EFR = Expected flow rate

$$EFR = \frac{HRR}{H_C} * CF_L * CF_m * C_G * C_T * C_P$$

$$EFR = \frac{2.3}{48895} * 1000 * 60 * 0.822 * 1.009 * 1.066 = 1.40 \text{ L/min}$$

Appendix M: Rotometer Correction Factors

Matheson®

166 Keystone Drive, Montgomeryville, PA 18936 • Phone (800) 828-4313

NOTE: The factors given below are primarily for flowmeter sizing only. For Flowmeters calibrated for AIR. For more accurate results, the tube should be calibrated for the specific gas.

Gas Being Used	Factor	Gas Being Used	Factor	Gas Being Used	Factor
Acetylene	1.049	Halocarbon-13	0.526	Monomethylamine	0.962
Air	1.000	Halocarbon-13B1	0.434	Neon	1.199
Ammonia	1.294	Halocarbon-14	0.573	Nitric Oxide	0.982
Argon	0.851	Halocarbon-21	0.529	Nitrogen	1.017
Arsine	0.610	Halocarbon	0.567	Nitrogen Dioxide	0.618
Boron Trichloride	0.493	Halocarbon-23	0.643	Nitrogen Trifluoride	0.638
Boron Trifluoride	0.648	Halocarpon-113	0.393	Nitrous Oxide	0.808
1-3 Butadiene	0.730	Halocarbon-114	0.411	Oxygen	0.951
Butane	0.688	Halocarbon-115	0.425	Ozone	0.776
1-Butene	0.707	Halocarbon-116	0.455	Phosgene	0.536
Carbon Dioxide	0.808	Halocarbon-142B	0.535	Phosphine	0.919
Carbon Monoxide	1.017	Halocarbon-152A	0.662	Propane	0.803
Chlorine	0.636	Helium	2.692	Propylene	0.822
Cracked Ammonia	1.844	Hydrogen	3.793	Silane	0.947
CycloPropane	0.830	Hydrogen Bromide	0.596	Silicon Tetraflouride	0.525
Dichlorosilane	0.533	Hydrogen Chloride	0.888	Sulfur Dioxide	0.665
Difluoroethane	0.662	Hydrogen Fluoride	0.734	Sulfur Hexafluoride	0.442
Dimethyl Ether	0.785	Hydrogen Sulfide	0.917	Trichlorosilane	0.466
Disilane	0.648	Isobutane	0.696	Xenon	0.469
Ethane	0.977	Isobutylene	0.717		
Ethylene	1.013	Krypton	0.588		
Fluorine	0.873	Methane (Natural Gas)	1.342		
Halocarbon-11	0.459	Methyl Fluoride	0.915		
Halocarbon-12	0.488	Monoethylamine	0.788		

Gas being used = air x factor Air = gas being used divided by factor

Example: Air to Gas
The flowmeter is calibrated to air. The gas being used is Methane.
For the approximate flow rate in Methane.
Methane factor = 1.342
sccm-Air x 1.342 = sccm-Methane
If the ball float is at 1500 sccm-air, the flow rate in Methane is:
1500 sccm-Air x 1.342 = 2013 sccm Methane

Example: Air to Gas mixture
The flowmeter is calibrated to air. The gas mixture is 3% Methane balance Nitrogen.
For the approximate flow rate for the gas mixture
Methane factor = 1.342
Nitrogen factor = 1.017
Mix factor = (0.03 x 1.342) + (0.97 x 1.017) = **1.027**
sccm-Air x 1.027 = sccm-(3% methane/nitrogen mix)
If the ball float is at 280 ccm air then the flow rate for the mix is:
280 sccm-Air x 1.027 = 288 sccm-(3% methane/nitrogen mix)

Gas Equipment Technology Group
Matheson Tri-Gas, Inc.
166 Keystone Drive
Montgomeryville, PA 18936

UNITS	SLPM AIR	DATE	FEBRUARY 25, 2015
TUBE NUMBER	604 (E700) TYPICAL	STD CONDITIONS	1 ATM & 70 DEG F
FLOAT NUMBER	005	GAS TEMPERATURE	70 DEG F
FLOAT MATERIAL	GLASS	PRESSURE IN TUBE	0 PSIG

SCALE READING	FLOW RATE	SCALE READING	FLOW RATE	SCALE READING	FLOW RATE	SCALE READING	FLOW RATE
150.0	8.61	110.0	6.32	70.0	3.95	30.0	1.47
149.0	8.55	109.0	6.26	69.0	3.89	29.0	1.40
148.0	8.48	108.0	6.20	68.0	3.83	28.0	1.34
147.0	8.42	107.0	6.14	67.0	3.77	27.0	1.27
146.0	8.36	106.0	6.08	66.0	3.71	26.0	1.21
145.0	8.30	105.0	6.03	65.0	3.65	25.0	1.14
144.0	8.25	104.0	5.97	64.0	3.60	24.0	1.08
143.0	8.19	103.0	5.91	63.0	3.54	23.0	1.01
142.0	8.13	102.0	5.85	62.0	3.48	22.0	0.95
141.0	8.07	101.0	5.79	61.0	3.42	21.0	0.89
140.0	8.02	100.0	5.73	60.0	3.36	20.0	0.82
139.0	7.96	99.0	5.67	59.0	3.30	19.0	0.76
138.0	7.90	98.0	5.61	58.0	3.24	18.0	0.70
137.0	7.85	97.0	5.55	57.0	3.18	17.0	0.64
136.0	7.79	96.0	5.49	56.0	3.12	16.0	0.58
135.0	7.74	95.0	5.43	55.0	3.06	15.0	0.52
134.0	7.68	94.0	5.37	54.0	3.00	14.0	0.47
133.0	7.63	93.0	5.31	53.0	2.93	13.0	0.41
132.0	7.57	92.0	5.25	52.0	2.87	12.0	0.35
131.0	7.52	91.0	5.19	51.0	2.81	11.0	0.30
130.0	7.46	90.0	5.13	50.0	2.75	10.0	0.25
129.0	7.40	89.0	5.07	49.0	2.69	9.0	0.20
128.0	7.35	88.0	5.01	48.0	2.63	8.0	0.15
127.0	7.29	87.0	4.95	47.0	2.56	7.0	0.11
126.0	7.24	86.0	4.90	46.0	2.50	6.0	0.07
125.0	7.18	85.0	4.84	45.0	2.44	5.0	0.02
124.0	7.12	84.0	4.78	44.0	2.38		
123.0	7.07	83.0	4.72	43.0	2.31		
122.0	7.01	82.0	4.66	42.0	2.25		
121.0	6.96	81.0	4.60	41.0	2.18		
120.0	6.90	80.0	4.54	40.0	2.12		
119.0	6.84	79.0	4.48	39.0	2.06		
118.0	6.78	78.0	4.42	38.0	1.99		
117.0	6.73	77.0	4.36	37.0	1.93		
116.0	6.67	76.0	4.30	36.0	1.86		
115.0	6.61	75.0	4.24	35.0	1.80		
114.0	6.55	74.0	4.19	34.0	1.73		
113.0	6.50	73.0	4.13	33.0	1.67		
112.0	6.44	72.0	4.07	32.0	1.60		
111.0	6.38	71.0	4.01	31.0	1.54		

Matheson

ROTAMETER
PRESSURE CORRECTION FACTORS

PRESSURE (PSIG) FOR WHICH ROTAMETER IS CALIBRATED	PRESSURE (PSIG) FOR WHICH CORRECTION IS TO BE MADE																									
	0	2	4	6	8	10	15	20	25	30	35	40	50	60	70	80	90	100	120	140	160	180	200	220	240	260
0 OR 14.7 PSIA	1.000	1.066	1.128	1.187	1.243	1.296	1.421	1.536	1.643	1.744	1.838	1.929	2.098	2.254	2.400	2.538	2.669	2.793	3.027	3.244	3.447	3.639	3.822	3.996	4.163	4.323
2	0.938	1.000	1.058	1.114	1.166	1.217	1.334	1.442	1.542	1.636	1.725	1.810	1.967	2.114	2.251	2.381	2.504	2.621	2.839	3.043	3.234	3.413	3.583	3.749	3.905	4.056
4	0.887	0.945	1.000	1.052	1.102	1.149	1.261	1.362	1.457	1.546	1.631	1.710	1.860	1.999	2.128	2.251	2.366	2.476	2.683	2.876	3.056	3.226	3.387	3.543	3.691	3.833
6	0.843	0.898	0.951	1.000	1.047	1.093	1.198	1.295	1.385	1.469	1.549	1.625	1.767	1.900	2.022	2.138	2.248	2.354	2.550	2.733	2.905	3.066	3.219	3.368	3.508	3.643
8	0.805	0.858	0.908	0.955	1.000	1.043	1.144	1.235	1.323	1.403	1.480	1.552	1.688	1.814	1.932	2.043	2.148	2.247	2.435	2.610	2.774	2.928	3.073	3.215	3.350	3.479
10	0.771	0.822	0.870	0.915	0.958	1.000	1.096	1.185	1.268	1.345	1.418	1.488	1.618	1.739	1.852	1.959	2.059	2.155	2.335	2.502	2.658	2.806	2.946	3.083	3.211	3.335
15	0.704	0.750	0.793	0.835	0.874	0.912	1.000	1.081	1.156	1.227	1.293	1.357	1.476	1.586	1.690	1.786	1.877	1.965	2.129	2.282	2.424	2.559	2.687	2.811	2.928	3.041
20	0.651	0.693	0.734	0.772	0.808	0.844	0.925	1.000	1.070	1.135	1.197	1.255	1.365	1.467	1.562	1.652	1.737	1.818	1.970	2.111	2.243	2.368	2.486	2.601	2.709	2.814
25	0.609	0.649	0.686	0.722	0.756	0.789	0.865	0.935	1.000	1.061	1.119	1.174	1.277	1.371	1.460	1.544	1.623	1.700	1.842	1.974	2.098	2.215	2.323	2.431	2.533	2.630
30	0.573	0.611	0.647	0.681	0.713	0.743	0.815	0.881	0.943	1.000	1.055	1.106	1.204	1.292	1.376	1.455	1.530	1.603	1.736	1.860	1.977	2.087	2.190	2.291	2.387	2.474
35	0.544	0.579	0.613	0.646	0.676	0.705	0.773	0.835	0.894	0.948	1.000	1.049	1.142	1.226	1.305	1.380	1.451	1.520	1.646	1.764	1.874	1.979	2.077	2.173	2.264	2.351
40	0.518	0.552	0.585	0.615	0.644	0.672	0.736	0.797	0.852	0.904	0.953	1.000	1.089	1.168	1.243	1.315	1.383	1.448	1.569	1.682	1.787	1.887	1.980	2.071	2.158	2.241
50	0.477	0.508	0.538	0.566	0.592	0.618	0.678	0.733	0.784	0.831	0.876	0.919	1.000	1.075	1.144	1.210	1.272	1.331	1.443	1.546	1.643	1.735	1.822	1.905	1.984	2.061
60	0.444	0.473	0.500	0.526	0.551	0.575	0.631	0.682	0.729	0.773	0.816	0.856	0.931	1.000	1.065	1.126	1.184	1.239	1.343	1.439	1.529	1.615	1.695	1.773	1.847	1.918
70	0.417	0.444	0.470	0.494	0.518	0.540	0.592	0.640	0.685	0.726	0.766	0.804	0.874	0.939	1.000	1.057	1.112	1.164	1.261	1.351	1.436	1.516	1.591	1.665	1.734	1.801
80	0.394	0.420	0.444	0.468	0.489	0.511	0.560	0.605	0.648	0.687	0.724	0.760	0.826	0.888	0.946	1.000	1.052	1.100	1.192	1.278	1.358	1.434	1.505	1.574	1.640	1.703
90	0.375	0.399	0.423	0.445	0.466	0.486	0.533	0.576	0.616	0.654	0.689	0.723	0.786	0.845	0.899	0.951	1.000	1.046	1.134	1.216	1.292	1.364	1.432	1.497	1.560	1.620
100	0.359	0.382	0.404	0.425	0.445	0.464	0.509	0.550	0.588	0.624	0.658	0.691	0.751	0.807	0.859	0.909	0.956	1.000	1.084	1.161	1.234	1.303	1.368	1.430	1.490	1.548
120	0.330	0.352	0.373	0.392	0.411	0.428	0.470	0.508	0.543	0.576	0.608	0.637	0.693	0.745	0.793	0.839	0.882	0.923	1.000	1.072	1.138	1.202	1.262	1.320	1.375	1.428
140	0.308	0.329	0.348	0.366	0.383	0.400	0.438	0.474	0.507	0.538	0.567	0.594	0.647	0.695	0.740	0.782	0.822	0.861	0.933	1.000	1.063	1.122	1.177	1.232	1.283	1.333
160	0.290	0.309	0.327	0.344	0.360	0.376	0.413	0.446	0.477	0.506	0.534	0.560	0.609	0.654	0.696	0.736	0.774	0.810	0.879	0.941	1.000	1.055	1.108	1.159	1.207	1.254
180	0.275	0.293	0.310	0.326	0.342	0.356	0.391	0.422	0.452	0.479	0.505	0.530	0.576	0.619	0.660	0.697	0.733	0.767	0.832	0.891	0.948	1.000	1.049	1.098	1.144	1.188
200	0.262	0.279	0.295	0.311	0.325	0.339	0.372	0.402	0.430	0.456	0.481	0.505	0.549	0.590	0.629	0.664	0.698	0.731	0.792	0.850	0.903	0.953	1.000	1.046	1.089	1.131
220	0.250	0.267	0.282	0.297	0.311	0.324	0.356	0.385	0.411	0.436	0.460	0.483	0.525	0.564	0.601	0.635	0.668	0.699	0.758	0.812	0.863	0.911	0.957	1.000	1.042	1.083
240	0.240	0.256	0.271	0.285	0.299	0.311	0.342	0.369	0.395	0.419	0.442	0.463	0.504	0.542	0.577	0.610	0.641	0.671	0.727	0.779	0.826	0.874	0.918	0.960	1.000	1.039
260	0.231	0.247	0.261	0.275	0.288	0.300	0.329	0.355	0.380	0.403	0.425	0.446	0.485	0.522	0.555	0.587	0.617	0.646	0.700	0.750	0.798	0.842	0.884	0.924	0.963	1.000

FOR ROTAMETER CALIBRATED IN FREE UNITS: ROTAMETER SCALE READING x FACTOR = CORRECTED FLOW FOR NEW CONDITION

BS 3/8/95

Rev B

FRM-0099

Matheson

ROTAMETER
TEMPERATURE CORRECTION FACTORS

TEMPERATURE (°F) FOR WHICH ROTAMETER IS CALIBRATED	TEMPERATURE (°F) FOR WHICH CORRECTION IS TO BE MADE																									
	0	10	20	30	40	50	60	70	80	90	100	110	120	130	140	150	160	170	180	190	200	210	220	230	240	250
0	1.000	0.990	0.979	0.969	0.959	0.950	0.941	0.932	0.923	0.915	0.907	0.898	0.891	0.883	0.876	0.868	0.861	0.855	0.848	0.842	0.835	0.829	0.822	0.816	0.811	0.805
10	1.010	1.000	0.990	0.979	0.970	0.960	0.951	0.942	0.933	0.924	0.917	0.908	0.900	0.893	0.885	0.878	0.871	0.864	0.857	0.850	0.844	0.838	0.831	0.825	0.820	0.814
20	1.021	1.010	1.000	0.990	0.980	0.970	0.961	0.952	0.943	0.935	0.926	0.918	0.910	0.903	0.894	0.887	0.880	0.873	0.866	0.859	0.853	0.846	0.840	0.834	0.828	0.822
30	1.032	1.021	1.010	1.000	0.990	0.980	0.971	0.962	0.952	0.944	0.935	0.927	0.919	0.912	0.903	0.896	0.889	0.882	0.875	0.868	0.861	0.855	0.849	0.842	0.837	0.831
40	1.042	1.032	1.020	1.010	1.000	0.990	0.980	0.971	0.962	0.953	0.945	0.937	0.929	0.921	0.913	0.905	0.898	0.891	0.884	0.877	0.870	0.864	0.858	0.851	0.845	0.839
50	1.053	1.042	1.031	1.020	1.010	1.000	0.991	0.981	0.972	0.963	0.955	0.946	0.938	0.930	0.923	0.914	0.907	0.900	0.893	0.886	0.879	0.873	0.866	0.860	0.854	0.847
60	1.063	1.052	1.041	1.030	1.020	1.009	1.000	0.991	0.981	0.973	0.964	0.955	0.947	0.939	0.931	0.923	0.916	0.909	0.902	0.894	0.888	0.881	0.875	0.868	0.862	0.856
70 OR ROOM	1.073	1.062	1.051	1.040	1.030	1.019	1.009	1.000	0.991	0.982	0.973	0.964	0.956	0.948	0.940	0.932	0.925	0.917	0.910	0.903	0.896	0.890	0.883	0.876	0.870	0.864
80	1.083	1.072	1.061	1.050	1.039	1.029	1.019	1.009	1.000	0.991	0.982	0.973	0.965	0.957	0.949	0.941	0.934	0.926	0.918	0.912	0.905	0.898	0.891	0.885	0.878	0.872
90	1.093	1.082	1.070	1.059	1.049	1.038	1.028	1.018	1.009	1.000	0.991	0.982	0.974	0.966	0.958	0.950	0.942	0.935	0.927	0.920	0.913	0.906	0.899	0.893	0.886	0.880
100	1.103	1.091	1.080	1.069	1.058	1.047	1.037	1.028	1.018	1.009	1.000	0.991	0.983	0.975	0.966	0.958	0.951	0.943	0.935	0.928	0.921	0.914	0.907	0.901	0.894	0.888
110	1.113	1.101	1.089	1.078	1.068	1.057	1.047	1.037	1.027	1.018	1.009	1.000	0.992	0.983	0.975	0.967	0.959	0.951	0.944	0.936	0.929	0.922	0.916	0.909	0.902	0.896
120	1.122	1.111	1.099	1.088	1.077	1.066	1.056	1.046	1.036	1.027	1.017	1.008	1.000	0.992	0.983	0.975	0.967	0.960	0.952	0.945	0.937	0.930	0.924	0.917	0.910	0.904
130	1.132	1.120	1.108	1.097	1.086	1.075	1.065	1.055	1.045	1.035	1.026	1.017	1.008	1.000	0.992	0.983	0.976	0.968	0.960	0.953	0.945	0.938	0.932	0.925	0.918	0.912
140	1.142	1.130	1.118	1.107	1.095	1.084	1.074	1.064	1.054	1.044	1.035	1.026	1.017	1.008	1.000	0.992	0.984	0.976	0.968	0.961	0.953	0.946	0.940	0.933	0.926	0.919
150	1.152	1.139	1.127	1.116	1.105	1.094	1.083	1.072	1.063	1.053	1.044	1.034	1.025	1.017	1.008	1.000	0.992	0.984	0.976	0.969	0.961	0.954	0.948	0.941	0.934	0.927
160	1.161	1.148	1.138	1.125	1.114	1.102	1.092	1.081	1.071	1.062	1.052	1.043	1.034	1.025	1.016	1.008	1.000	0.992	0.984	0.977	0.969	0.962	0.955	0.948	0.941	0.935
170	1.170	1.158	1.145	1.134	1.122	1.111	1.100	1.090	1.080	1.070	1.061	1.051	1.042	1.033	1.025	1.016	1.008	1.000	0.992	0.984	0.977	0.970	0.962	0.955	0.948	0.942
180	1.179	1.167	1.155	1.143	1.131	1.120	1.109	1.099	1.089	1.079	1.069	1.059	1.050	1.041	1.033	1.024	1.016	1.008	1.000	0.992	0.985	0.978	0.970	0.962	0.956	0.944
190	1.188	1.176	1.164	1.152	1.140	1.129	1.118	1.107	1.097	1.087	1.077	1.068	1.058	1.049	1.041	1.032	1.024	1.016	1.008	1.000	0.992	0.985	0.978	0.970	0.963	0.957
200	1.197	1.185	1.173	1.161	1.149	1.138	1.126	1.116	1.105	1.095	1.085	1.076	1.067	1.057	1.049	1.040	1.032	1.024	1.016	1.008	1.000	0.993	0.985	0.978	0.971	0.964
210	1.207	1.194	1.182	1.170	1.158	1.146	1.135	1.124	1.114	1.104	1.094	1.084	1.075	1.065	1.057	1.048	1.039	1.032	1.023	1.015	1.007	1.000	0.993	0.985	0.978	0.971
220	1.216	1.203	1.190	1.178	1.166	1.155	1.143	1.133	1.122	1.112	1.102	1.092	1.083	1.073	1.064	1.055	1.047	1.039	1.031	1.023	1.015	1.007	1.000	0.993	0.985	0.978
230	1.225	1.212	1.199	1.187	1.175	1.163	1.152	1.141	1.130	1.120	1.111	1.100	1.090	1.081	1.072	1.063	1.055	1.047	1.039	1.031	1.023	1.015	1.007	1.000	0.993	0.986
240	1.233	1.220	1.208	1.195	1.183	1.171	1.160	1.149	1.138	1.128	1.118	1.108	1.098	1.089	1.080	1.071	1.063	1.055	1.046	1.038	1.030	1.022	1.015	1.007	1.000	0.993
250	1.242	1.229	1.216	1.204	1.192	1.180	1.168	1.157	1.147	1.136	1.126	1.116	1.106	1.097	1.088	1.078	1.070	1.062	1.054	1.045	1.037	1.030	1.022	1.014	1.007	1.000

FOR ROTAMETER CALIBRATED IN FREE UNITS: ROTAMETER SCALE READING x FACTOR = CORRECTED FLOW FOR NEW CONDITION

BS 3/8/95

Rev B

FRM-0100

Appendix N: CFAST Graphical User Interface

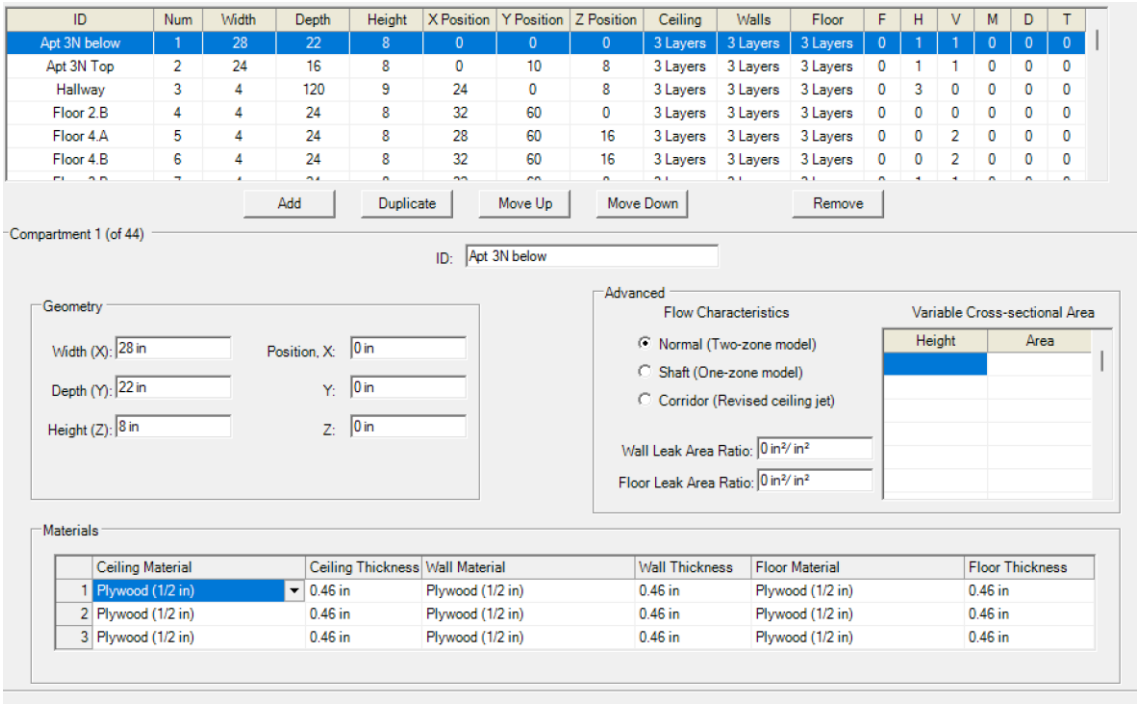

ID	Num	Width	Depth	Height	X Position	Y Position	Z Position	Ceiling	Walls	Floor	F	H	V	M	D	T
Apt 3N below	1	28	22	8	0	0	0	3 Layers	3 Layers	3 Layers	0	1	1	0	0	0
Apt 3N Top	2	24	16	8	0	10	8	3 Layers	3 Layers	3 Layers	0	1	1	0	0	0
Hallway	3	4	120	9	24	0	8	3 Layers	3 Layers	3 Layers	0	3	0	0	0	0
Floor 2.B	4	4	24	8	32	60	0	3 Layers	3 Layers	3 Layers	0	0	0	0	0	0
Floor 4.A	5	4	24	8	28	60	16	3 Layers	3 Layers	3 Layers	0	0	2	0	0	0
Floor 4.B	6	4	24	8	32	60	16	3 Layers	3 Layers	3 Layers	0	0	2	0	0	0

	Ceiling Material	Ceiling Thickness	Wall Material	Wall Thickness	Floor Material	Floor Thickness
1	Plywood (1/2 in)	0.46 in	Plywood (1/2 in)	0.46 in	Plywood (1/2 in)	0.46 in
2	Plywood (1/2 in)	0.46 in	Plywood (1/2 in)	0.46 in	Plywood (1/2 in)	0.46 in
3	Plywood (1/2 in)	0.46 in	Plywood (1/2 in)	0.46 in	Plywood (1/2 in)	0.46 in

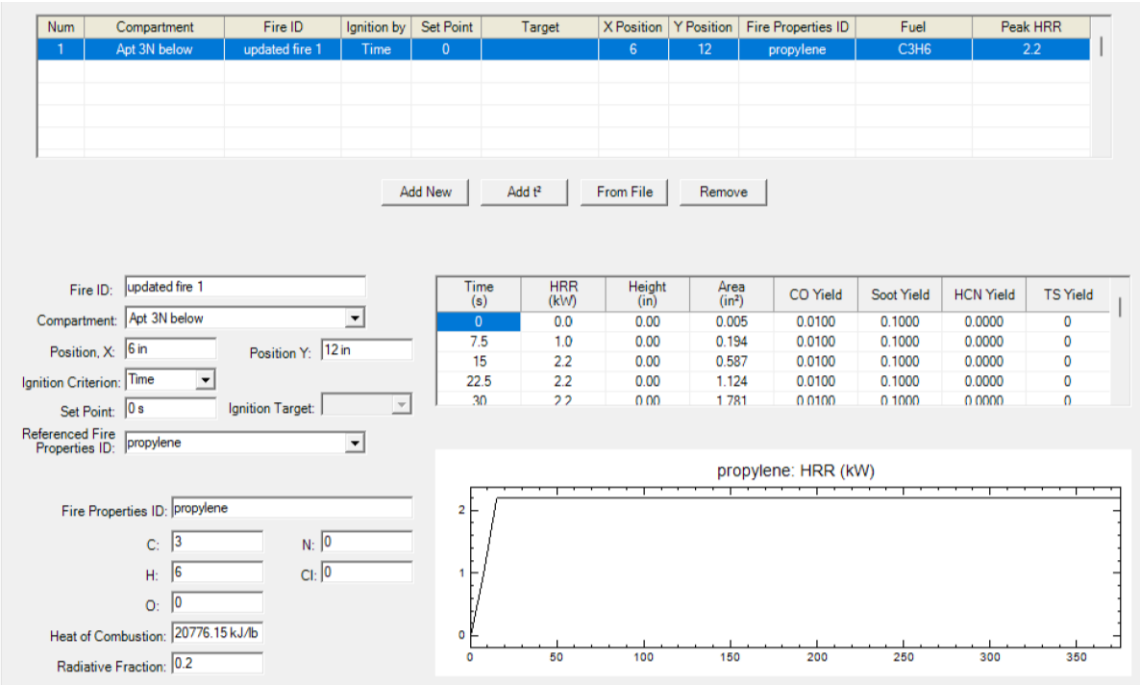

Num	Compartment	Fire ID	Ignition by	Set Point	Target	X Position	Y Position	Fire Properties ID	Fuel	Peak HRR
1	Apt 3N below	updated fire 1	Time	0		6	12	propylene	C3H6	2.2

Time (s)	HRR (kW)	Height (in)	Area (in²)	CO Yield	Soot Yield	HCN Yield	TS Yield
0	0.0	0.00	0.005	0.0100	0.1000	0.0000	0
7.5	1.0	0.00	0.194	0.0100	0.1000	0.0000	0
15	2.2	0.00	0.587	0.0100	0.1000	0.0000	0
22.5	2.2	0.00	1.124	0.0100	0.1000	0.0000	0
30	2.2	0.00	1.781	0.0100	0.1000	0.0000	0

Appendix O: Percentage Difference of Peak Temperature Results

Peak Temperature for Test 1			
Location	Lab Test 1: No Door (°C)	CFAST Test 1: 100% Open (°C)	Percent Difference (%)
Lower Compartment	60.8	146.0	82
Upper Compartment	51.3	75.0	38
3rd Floor Hallway	34.1	9.0	117
15th Floor Hallway	0	0	0
19th Floor Hallway	0	0	0

Peak Temperature for Test 2			
Location	Lab Test 2: (45 Degrees) (°C)	CFAST Test 2: 77% Open (°C)	Percent Difference (%)
Lower Compartment	59.3	146	85
Upper Compartment	39.7	73	59
3rd Floor Hallway	37.4	9	125
15th Floor Hallway	0	0	0
19th Floor Hallway	0	0	0

Peak Temperature for Test 3			
Location	Lab Test 3:	CFAST Test 3: 33% Open (°C)	Percent Difference (%)

	(20 Degrees) (°C)		
Lower Compartment	125.0	151.0	19
Upper Compartment	37.9	65.0	53
3rd Floor Hallway	27.0	7.0	122
15th Floor Hallway	0	0	0
19th Floor Hallway	0	0	0

Appendix P: Full Scale CFAST Results

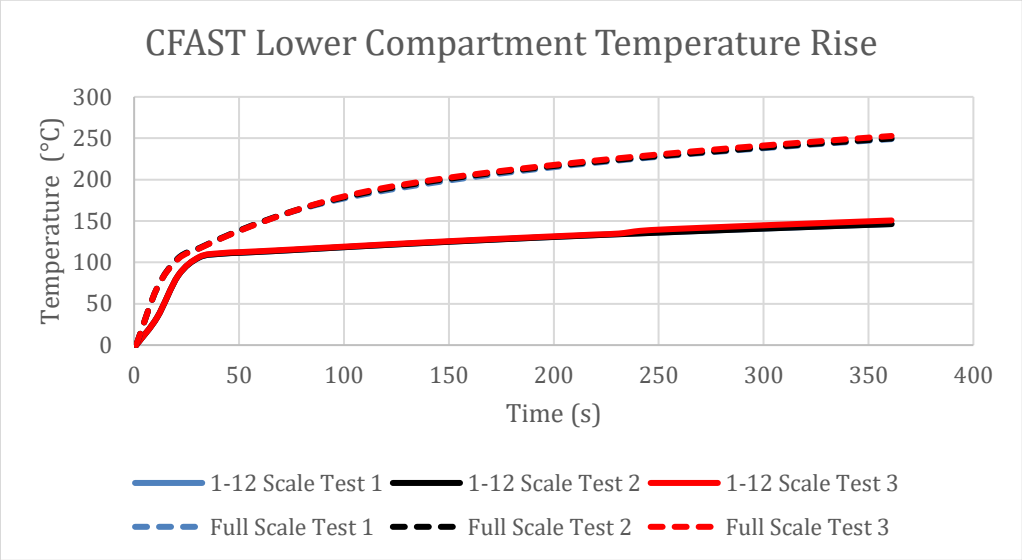

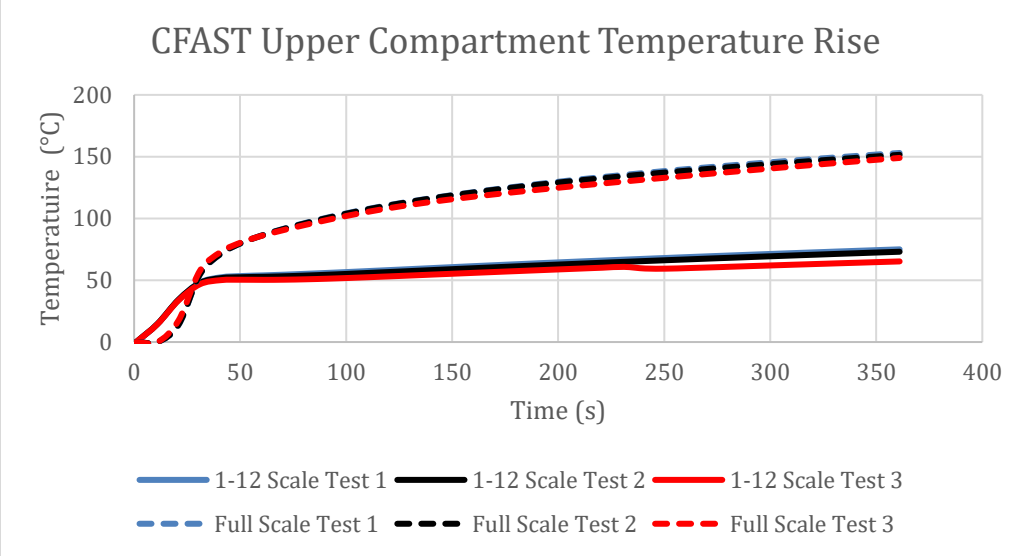

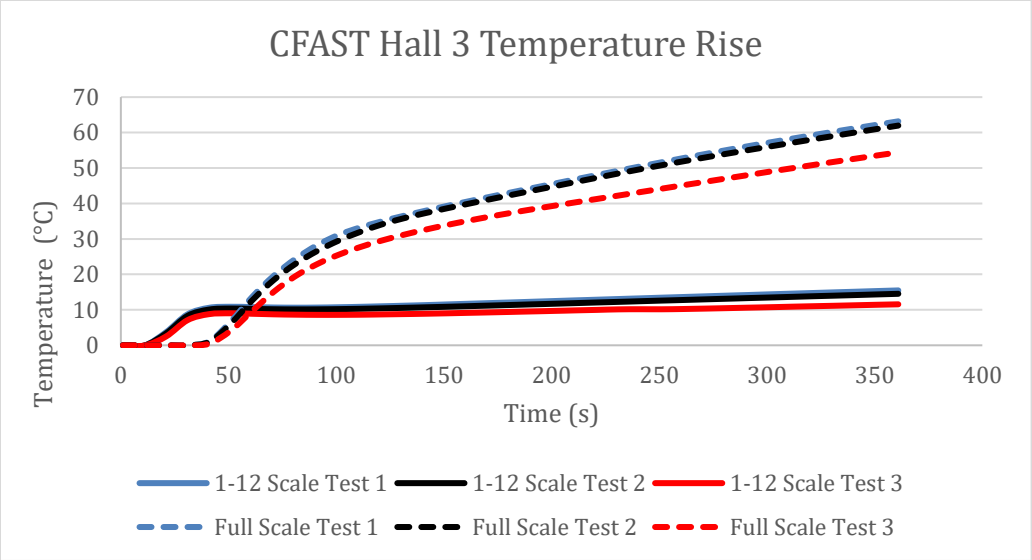
CFAST Hall 3 Temperature Rise
Temperature (°C)
70
60
50
40
30
20
10
0
0
50
100
150
200
250
300
350
400
Time (s)
1-12 Scale Test 1
1-12 Scale Test 2
1-12 Scale Test 3
Full Scale Test 1
Full Scale Test 2
Full Scale Test 3

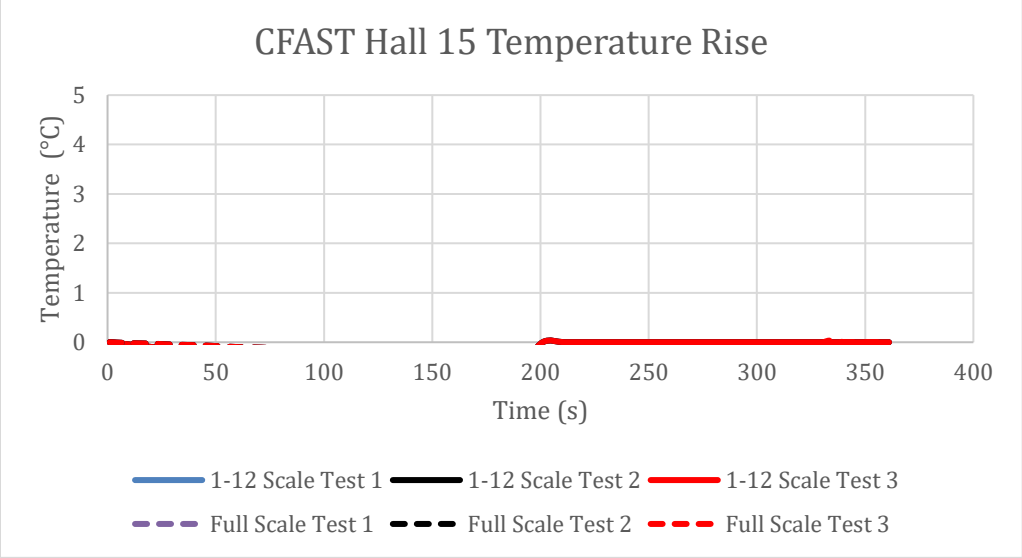
CFAST Hall 15 Temperature Rise
Temperature (°C)
5
4
3
2
1
0
0
50
100
150
200
250
300
350
400
Time (s)
1-12 Scale Test 1
1-12 Scale Test 2
1-12 Scale Test 3
Full Scale Test 1
Full Scale Test 2
Full Scale Test 3

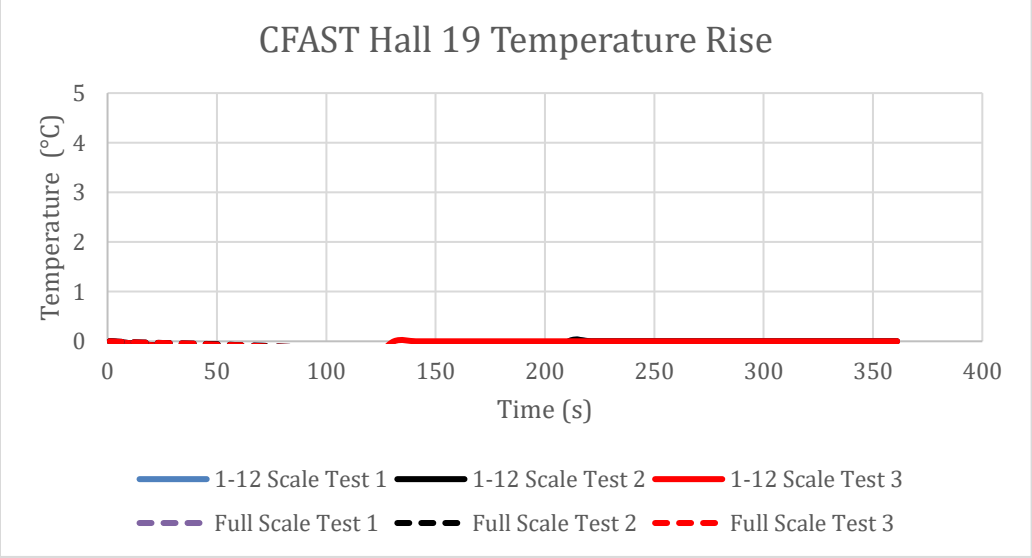
CFAST Hall 19 Temperature Rise
Temperature (°C)
5
4
3
2
1
0
0
50
100
150
200
250
300
350
400
Time (s)
1-12 Scale Test 1
1-12 Scale Test 2
1-12 Scale Test 3
Full Scale Test 1
Full Scale Test 2
Full Scale Test 3